Valdis V. Liepa
Univ. of Michigan
22 December 1978

Interaction Applications Memos

Memo 29

Current and Charge Density Measurements on Scale Model E-3A Aircraft

ABSTRACT

Measured data are presented for the surface current and charge densities induced on scale model E-3A (AWACS) aircraft when illuminated by a plane electromagnetic wave in a simulated free space environment. The measurements were made on 1/150 and 1/100 scale models over the frequency range 225 to 440 MHz, simulating 1.5 to 44.0 MHz full scale. The data are for 15 test points and 3 excitations chosen to complement the full-scale ATHAMAS I/ACHILLES I ground tests made at Kirtland Air Force Base.

CONTENTS

PREFACE

It is a pleasure to acknowledge the assistance of Messrs. M. Tomorski, D. Brown and F. Lenning of The Radiation Laboratory in performing the measurements, data processing and data preparation. The assistance of Mr. Gary Bedrosian of Dikewood Industries, Inc., and Mr. W. Prather of AFWL is also appreciated.

SECTION I

INTRODUCTION

The data presented here were obtained for the Air Force Weapons Laboratory to be used in determining the surface response extrapolation function [1] for the E-3A aircraft. The test points and excitation conditions in the scale model measurements were therefore chosen to conform to those of the full scale measurements made in the ATHAMAS I (Horizontally Polarized Dipole) and ACHILLES I (Vertically Polarized Dipole) simulators at Kirtland AFB.

Surface current and charge data are presented for 15 locations or test points on the aircraft under 3 different excitation conditions. The measured quantities are the axial current component J_a, the circumferential current component J_c, and the normal electric field component E_n. Of the 135 measurement situations possible, 56 were initially picked out, and 43 were finally selected. The resulting data are presented in the form of amplitude and phase plots as a function of the full scale frequency, and have also been furnished to Dikewood Industries, Inc. in digital form on computer cards.

---

1. Carl E. Baum, "Extrapolation Techniques for Interpreting the Results of Tests in EMP Simulators in Terms of EMP Criteria," AFWL Sensor and Simulation Notes, Note 222, 1977.

SECTION II

MODELS, MEASUREMENTS AND DATA

2.1 MODELS

For the measurements two scale models of the E-3A aircraft were acquired, one coming in the form of a plastic kit (Entex No. 8522) 1/100 in scale which was then assembled, and the other as a solid plastic model (MicroWest Inc., Santa Clara, CA) 1/150 in scale. The models were reasonably good replicas of the E-3A in most particulars, but some modifications were necessary to provide adequate (electrical) simulation of the full scale aircraft. These included cutting back the fuselage to station STA:F178 to simulate the removal of the non-metallic radome (the nose of the radome is at STA:130); adding an HF 'probe' to the right wing of the 1/100 scale model (the other model already had it on); and cutting off sections of the rotodome to "remove" the radome. A center section of width 78 inches (full scale) and length equal to the diameter of the rotodome was left to simulate the antenna structure.

After modification in this manner, the models were given at least three coats of silver paint to make them conducting. The lengths and wingspans were then measured to determine the actual scale factors. Because neither model was a precise replica of the E-3A, the factors deduced from the fuselage and wingspan differed slightly, as indicated in Table 1. In converting measured field data to their full scale values, the fuselage

scale factors were used for the case of nose-on and top incidence when the electric vector was parallel to the fuselage, and the wingspan scale factors for top incidence with electric vector perpendicular to the fuselage.

To permit the mounting of the sensors, holes were drilled in the model through which to pass the sensor leads. Figure 1 is a photograph of the two models after modification and painting with holes drilled in the fuselage. When a particular hole was not in use, it was covered with copper tape which shows up as a dark patch in the photograph. As the study progressed, additional holes were drilled in the wings, stabilizers, rotodome and rotodome struts, and the unused ones covered with coper tape.

2.2 MEASUREMENTS

The measurements were made in the Radiation Laboratory's anechoic chamber, a facility specially designed, constructed and instrumented for surface field measurements. A block diagram of the facility is shown in Figure 2. The measurement procedures were similar to those used in previous programs [2, 3, 4], apart from changes resulting from the continued upgrading of the facility and the measurement techniques. In particular,

---

2. Valdis V. Liepa, "Sweep Frequency Surface Field Measurements," University of Michigan Radiation Laboratory Report No. 013378-1-F; Sensor and Simulation Notes, Note 210; 1975.

3. Valdis V. Liepa, "Surface Field Measurements on Scale Model EC-135 Aircraft," University of Michigan Radiation Laboratory Report No. 014182-1-F; Interaction Application Memos, Memo 15; 1978. 1978.

4. Valdis V. Liepa, "Surface Field Measurements on Scale Model E-4 Aircraft," University of Michigan Radiation Laboratory Report No. 014182-2-F; Interaction Application Memos, Memo 17; 1978.

for this program a new broadband transmitting antenna was installed which reduced the lower end of the frequency range from 450 to 225 MHz, thereby providing coverage in the three overlapping frequency ranges 225-1100, 950-2200 and 2000-4400 MHz.

The currents and charges on the models were measured using miniature sensors 2-3 mm in dimension constructed from 0.5 mm diameter semi-rigid coax. Most of the current data were obtained using a surface mounted half-loop probe (SP) whose signal lead was taken from the model at a place remote from the test point and chosen to produce least interaction with the model. A few current measurements were made using an external or free space probe (FSP), but these were confined to situations where the interaction of the model and the probe lead is negligible, as in the case of the measurement of J_c at STA;F510T for top illumination with E parallel to the wings. Only the antisymmetric modes are then excited and these do not couple to the probe lead. For the charge measurements only surface mounted probes were available, and with these the mounting procedures were the same as for the surface mounted current probes. Figures 3 and 4 show the taping required for installing a surface mounted probe on a rotodome strut.

Figure 5 illustrates how the use of more than one scale model can increase the range of full scale frequencies for which data can be obtained. With the measured frequency range 225-4400 MHz (approximately a 20:1 bandwidth), a 1/150 scale model will provide coverage from 1.5 to 29.3 MHz,

and a 1/100 model covers 2.25 to 44.0 MHz, yielding the overall coverage 1.5 to 44.0 MHz, corresponding to a 29:1 bandwidth.

Measurements were made for three different excitations:

Excitation 1 - Top incidence, E parallel to the fuselage

Excitation 2 - Top incidence, E perpendicular to the fuselage

Excitation 3 - Nose-on incidence, E vertical

Figure 6 shows the excitations and the convention used for measurement of the currents. To excite the maximum currents on the rotodome antenna, the array was rotated parallel to the fuselage for excitations 1 and 3, and perpendicular to the fuselage for excitation 2.

2.3 DATA

For each measurement situation the data obtained from the two models over the three frequency bands results in a data set comprising six data files for the transfer function. Due to the different number of sampling points used in each frequency band and the fact that the measurement frequencies were divided by the model scale factors to obtain the full-scale data, the sampling was different in each of the six data files. When the data was recorded, 182 points were used in Band 1 (225 - 1100 MHz), 133 in Band 2 (950 - 2200 MHz), and 144 in Band 3 (2000 - 4400 MHz). However, due to an occasional failure of the network analyzer to properly lock onto the signal at the start of a measurement, a few (perhaps a half dozen) points were sometimes omitted from a data set, resulting in fewer points

than listed above. The exact number of points and the frequency covered in the processed data is given (amongst other information) in line 5 of a data file (See Table 3). For a user of the data, Figure 6 gives the directions of excitation, the polarization relative to the aircraft, and the convention adopted in specifying the circumferential and axial components, J_c and J_a respectively, of the surface current. In all cases the component J_c is perpendicular to J_a. The data presented are normalized relative to the incident field: J/H_o or E_n/E_o for the current and charge amplitudes respectively. The phase reference is that of the incident field at the station where the measurement was made, based on the $e^{i\omega t}$ time convention.

Table 2 summarizes the situations for which data have been obtained, and gives the Figure numbers where the plots for each case can be found. Each Figure number is followed by a letter S (small model, scale 1/150) or L (large model, scale 1/100) specifying the model used in the measurements. The individual (digital) data files are identified with the numbers (filename) in the upper right-hand corner of the plots. Plots of the measured current and charge data are given in the later section.

In addition, the data has been furnished to Dikewood Industries, Inc. in digital form on punched cards. The format used is:

Line	1	FILENAME (4A4)
	2	Comments (18A4)
	3	Comments (18A4)
	4	TITLE used in plotting (18A4)
	5	FMIN, FMAX, AMPMIN, AMPMAX, PHASEMIN, PHASEMAX, NN (4F8.3, 2F8.2, I5)

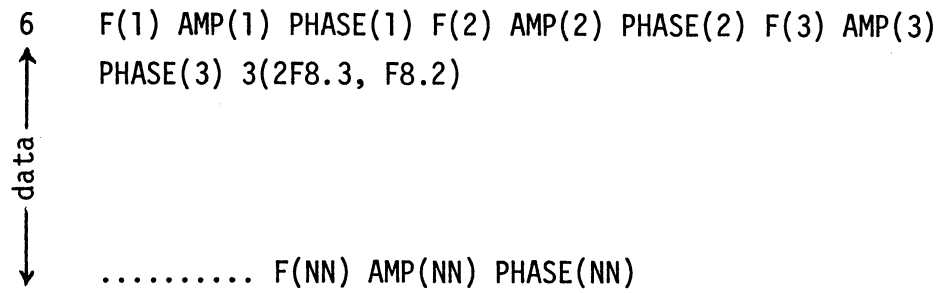

where NN is the number of data points in the set. Table 3 is an example of a typical data file.

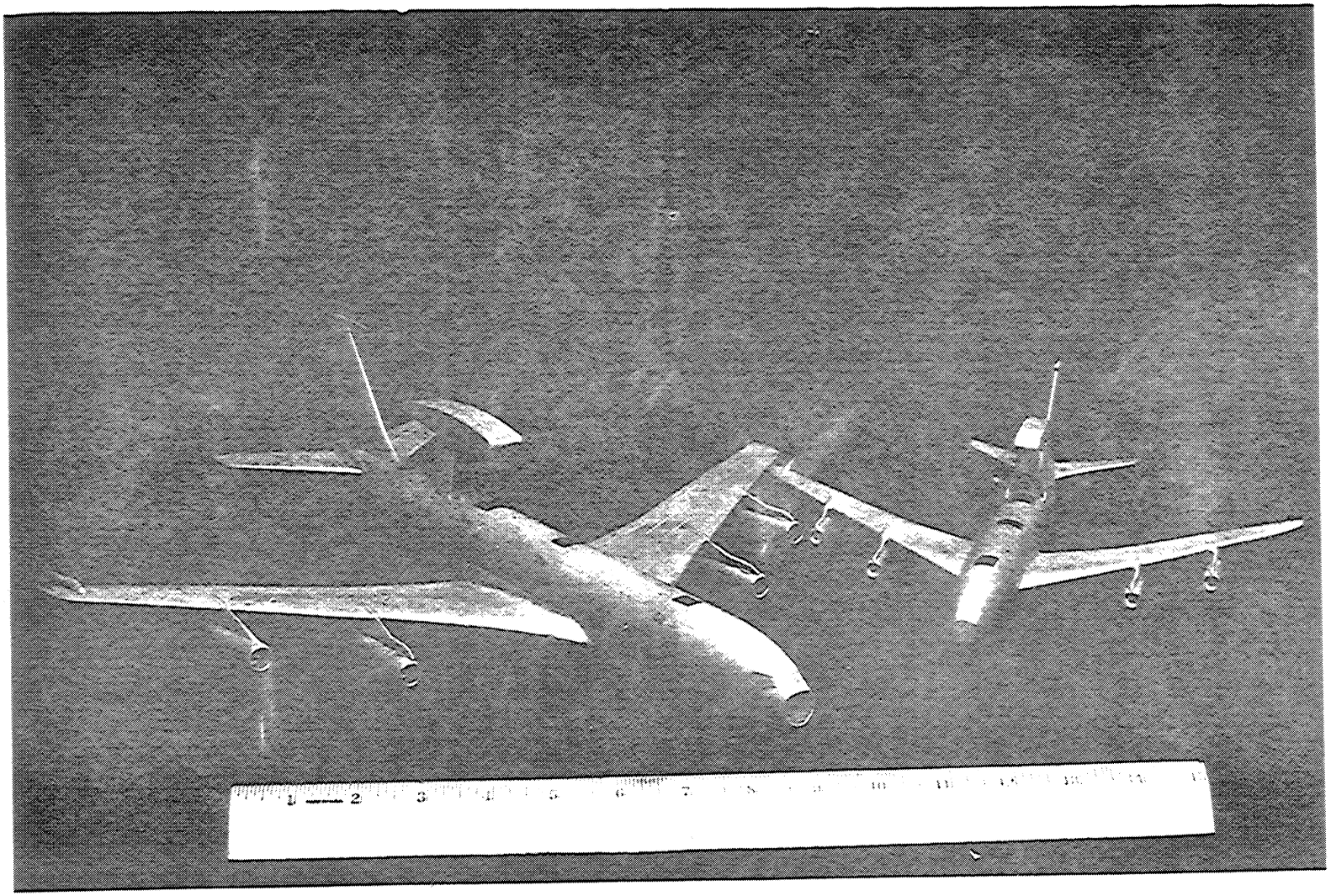

Figure 1. The two models ready for measurement. The antenna structures in this case have been rotated appropriate to excitations 1 and 3.

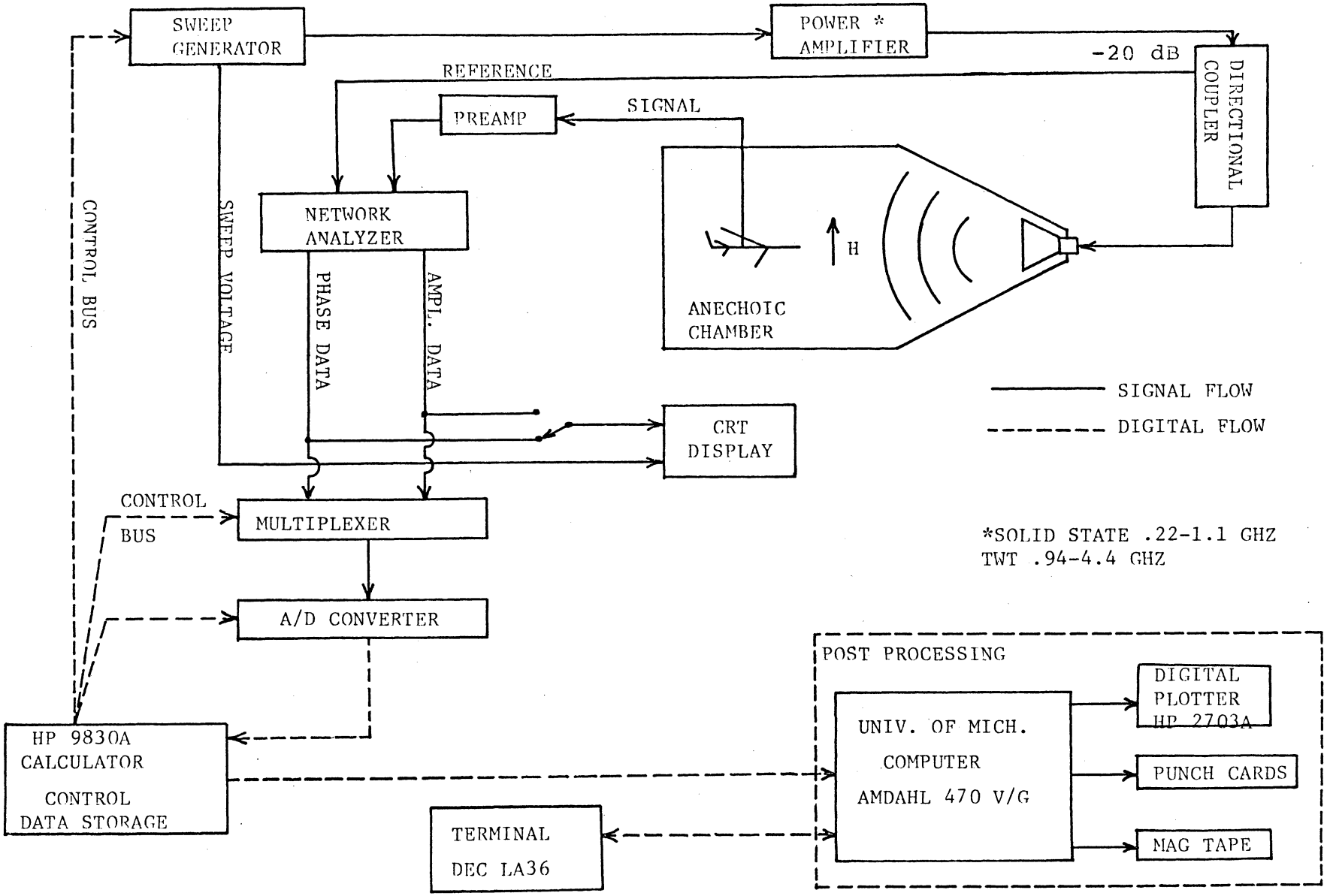

Figure 2. Block diagram of the measurement facility.

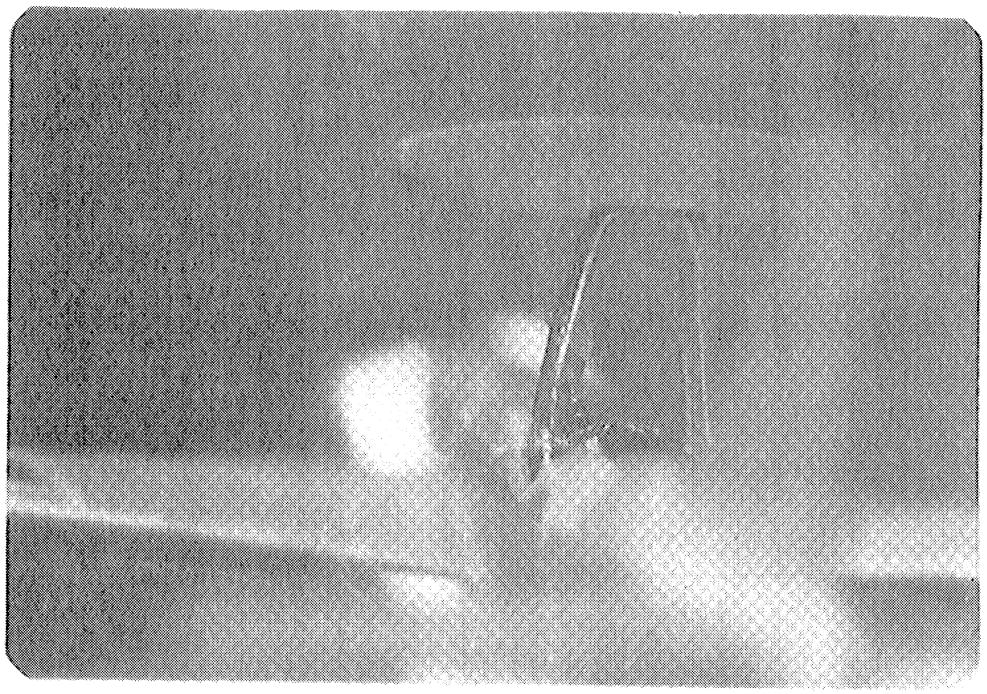

Figure 3. Close-up of the rotodome structure on the 1/150 scale model with a loop probe mounted to measure the current outside the strut. The taping on the inside was necessary to accomodate the lead. The antenna in this case has been rotated for an excitation 2 measurement.

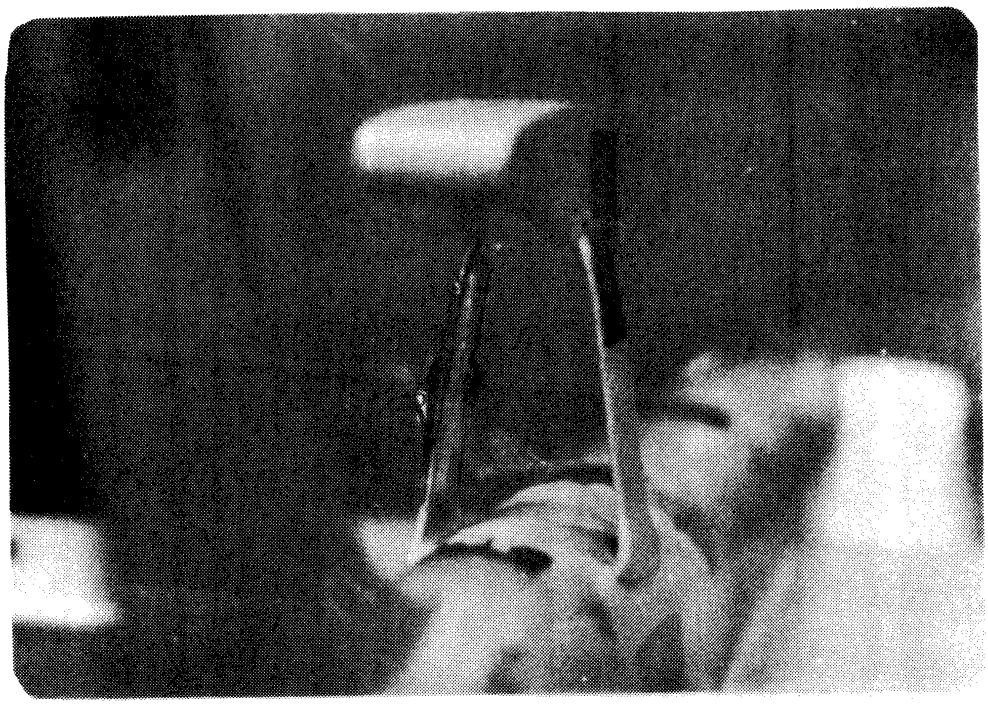

Figure 4. Close-up of the rotodome structure on the 1/150 model with a loop probe mounted to measure the current inside the strut. The taping on the outside was necessary to accomodate the probe lead. The antenna in this case is in a position for excitation 1 and 3 measurements.

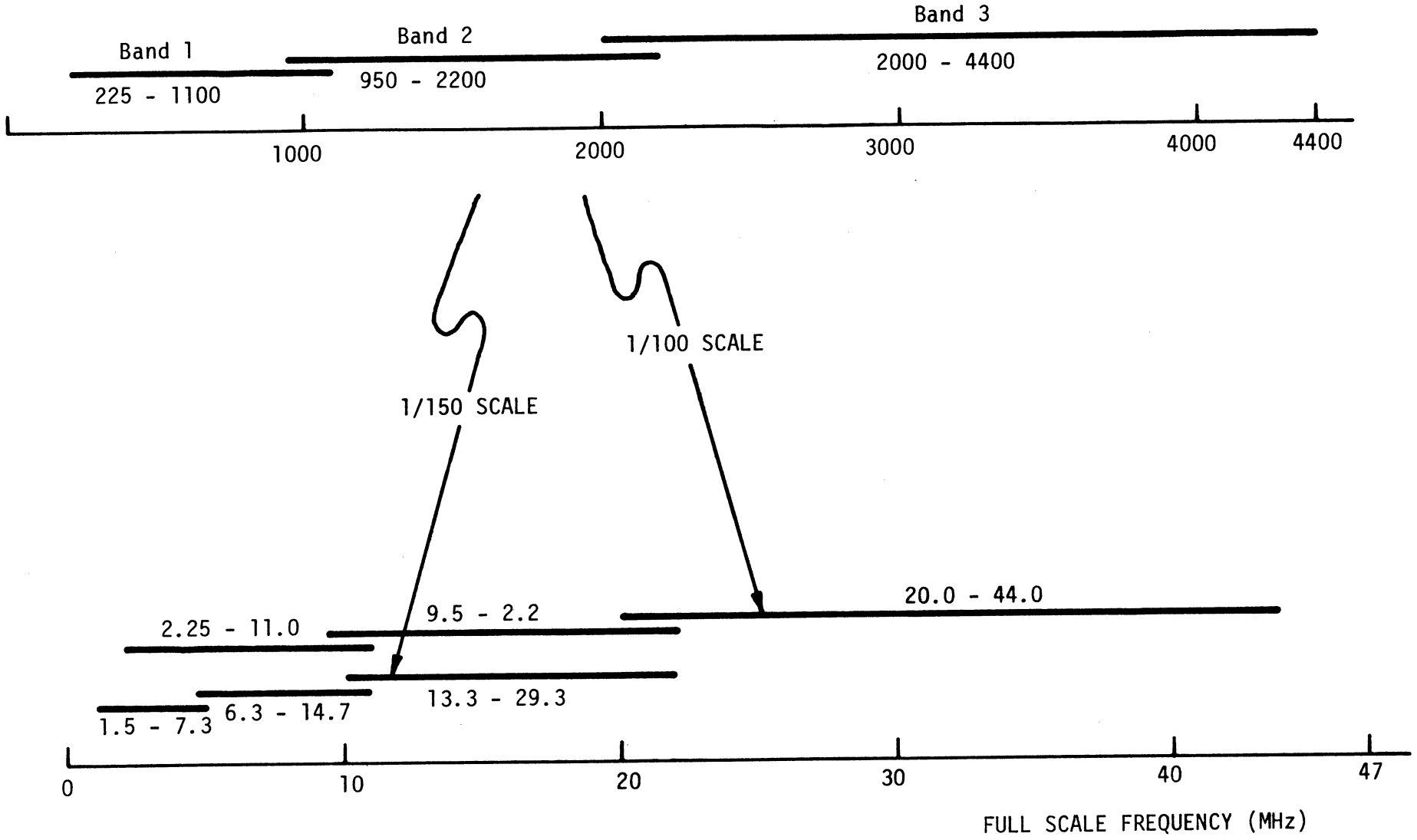

Figure 5. E-3A measurement frequency coverage.

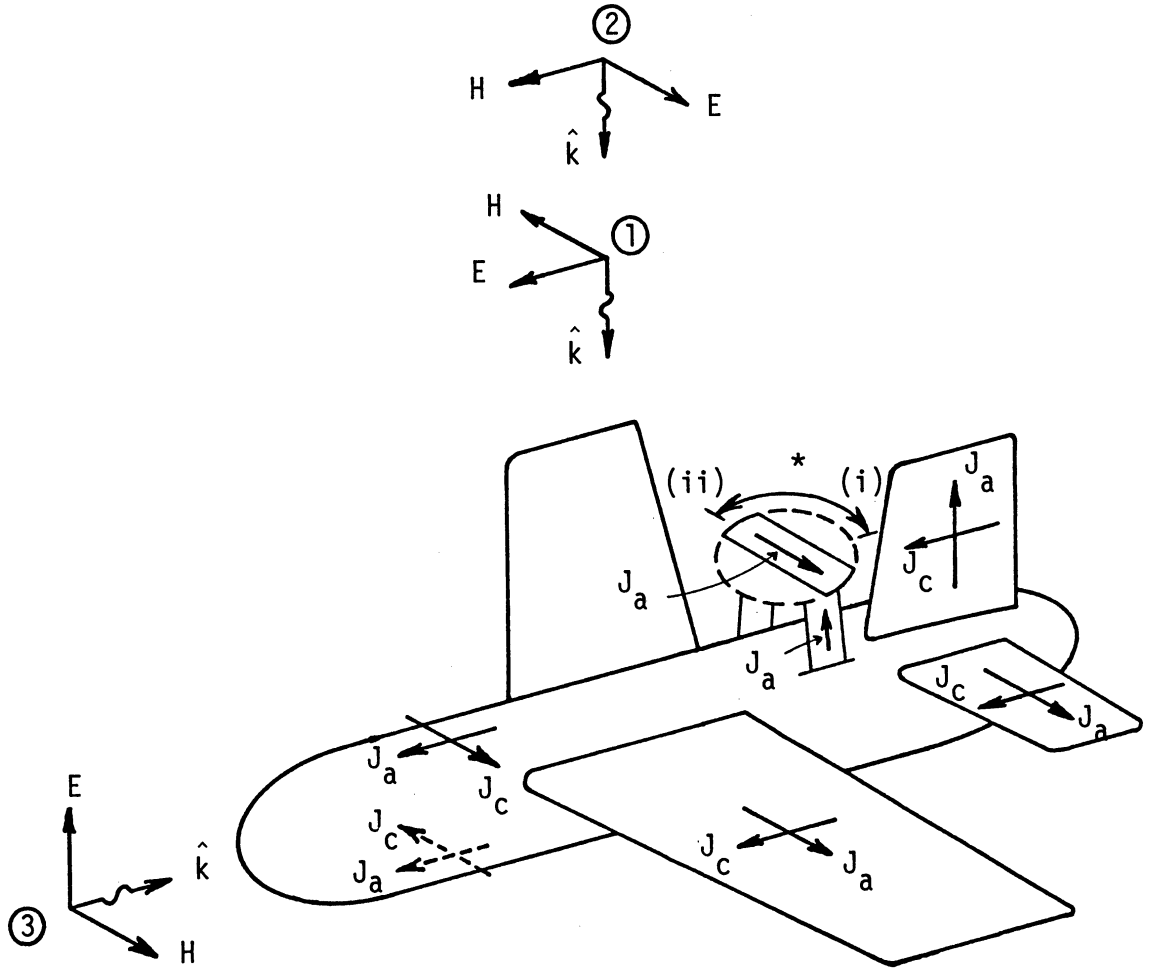

*Positions of Rotodome: Excitations 1 and 3 (i)
Excitation 2 (ii)

Figure 6. Convention for illumination and the measured current components on AWACS.

TABLE 1. MODEL SCALE FACTORS

Model	Length (radome removed) (cm)	Wingspan (cm)	Fuselage scale (radome removed)	Wingspan scale
1/100	44.89	43.97	1/101.12	1/101.03 (1/98.72)*
1/150	30.64	29.73	1/148.15	1/199.95 (1/145.03)*

Full scale length including stabilizers	46.61 m
With radome removed	45.39 m
Full scale wingspan (707-320B)	44.42 m
Full scale wingspan (707-320)	(43.41 m)*

*In determining the scaling factors, the full scale wingspan used was that for the 707-320 version instead of 707-320B, leading to the slightly incorrect scaling factors shown in parentheses in converting measured frequencies to the full scale ones. The data affected are only for excitation 2, and can be corrected by multiplying the frequencies by a factor of 0.977.

TABLE 2. SUMMARY OF DATA MEASURED

STATION	LOCATION	EXCITATION 1 E ‖ Fus.			EXCITATION 2 E ⊥ Fus.			EXCITATION 3 Nose-On		
		J_a	J_c	E_n	J_a	J_c	E_n	J_a	J_c	E_n
F510T	Fwd Fus. Top	01S,L	03S,L	05S,L		04S,L		02S,L		06S,L
F504B	Fwd Fus. Bottom	09S,L	10S,L	08S,L		11S,L				07S,L
W600T	Wg Cent. Top, Left	27S,L			28S,L		25S,L			26S,L
F1000T	RR Fus. Top, Fwd Sts	13S,L								
F1200T	RR Fus. Top, RR Sts	14S,L								
F1070B	RR Fus. Bottom									
F750T	Fus-Wg Jct. Top	15S,L				12S,L		16S,L		43S,L
F670B	Fus-Wg Jct. Bottom	29S,L				39S,L		30S,L		
F178	Fwd Bulkhead			17S,L						18S,L
W970T	Wg Tip Top, Left			19S,L			20S,L			21S,L
VS	Vert. Stab. Side, Left			22S,L			23S,L			24S,L
ROTO	Top of Rotodome			31S,L	40S,L					32S,L
WL372(O)	Strut Center Outside, Left	33S,L			34S,L			35S,L		
WL372(I)	Strut Center Inside, Left	36S,L			37S,L			38S,L		
F1310B,RBL33	RR Fus. Bottom	44S,L				41S,L		45S,L		42S,L

TABLE 3. LISTING OF A TYPICAL DATA FILE

```
>     1    A00S
>     2    E-3A,150,1,Q,Q10,B,8/28/78,DB
>     3    SCALE FACTOR=148.15
>     4    SAMPLE DATA
>     5       1.503   7.343   4.436  13.932 -144.50  167.90  182
>     6       1.503   4.842  98.50    1.535   4.508   94.20   1.568   4.477   89.50
>     7       1.600   4.457  97.80    1.632   4.436   94.60   1.665   4.688   90.60
>     8       1.697   5.140  90.00    1.729   4.645   89.30   1.761   5.117   87.40
>     9       1.794   5.395  90.50    1.826   5.272   92.30   1.858   5.741   90.50
>    10       1.890   6.683  89.70    1.923   7.194   86.10   1.955   7.379   78.20
>    11       1.987   7.516  72.80    2.019   7.691   67.60   2.052   7.464   62.40
>    12       2.084   7.362  57.00    2.116   6.839   53.30   2.149   6.546   55.00
>    13       2.181   6.501  52.40    2.213   6.966   52.20   2.245   7.031   52.60
>    14       2.278   6.950  49.40    2.310   7.194   45.10   2.342   7.379   46.20
>    15       2.374   7.228  40.70    2.407   7.396   36.00   2.439   7.379   36.10
>    16       2.471   6.982  33.90    2.503   7.178   29.10   2.536   7.211   27.90
>    17       2.568   6.592  25.80    2.600   6.442   24.50   2.632   6.546   28.90
>    18       2.665   6.577  28.40    2.697   6.730   27.30   2.729   7.178   27.90
>    19       2.762   7.194  27.00    2.794   7.516   23.90   2.826   7.656   20.80
>    20       2.858   7.745  20.00    2.891   7.691   18.00   2.923   7.980   17.70
>    21       2.955   8.166  14.50    2.987   8.110   11.70   3.020   7.907    7.50
>    22       3.052   7.998   8.20    3.084   8.054    7.70   3.116   8.072    4.30
>    23       3.149   8.054   1.70    3.181   7.852    2.50   3.213   7.816    0.70
>    24       3.246   8.414  -1.40    3.278   8.054   -2.60   3.310   7.780   -5.10
>    25       3.342   7.889  -5.10    3.375   8.166   -3.40   3.407   7.943   -7.10
>    26       3.439   8.356  -8.70    3.471   8.260   -8.10   3.504   8.241   -9.60
>    27       3.536   8.630 -12.40    3.568   8.810  -12.60   3.600   8.241  -16.00
>    28       3.633   8.453 -15.20    3.665   8.790  -13.80   3.697   9.078  -14.50
>    29       3.730   9.441 -18.70    3.762   9.661  -20.10   3.794   9.727  -22.00
>    30       3.826   9.908 -26.20    3.859  10.000  -29.50   3.891   9.683  -33.60
>    31       3.923   9.183 -34.40    3.955   9.204  -37.80   3.988   9.247  -36.70
>    32       4.020   9.141 -37.90    4.052   8.851  -39.90   4.084   9.594  -39.70
>    33       4.117   9.462 -39.80    4.149   9.506  -45.20   4.181   9.572  -48.40
>    34       4.213   9.550 -46.00    4.246   9.141  -49.70   4.278  10.023  -51.20
>    35       4.310   9.908 -53.20    4.343   9.290  -56.20   4.375   9.528  -59.90
>    36       4.407   9.795 -58.00    4.439   9.290  -62.80   4.472   9.311  -67.90
>    37       4.504   9.247 -65.40    4.536   8.892  -66.80   4.568   9.036  -69.30
>    38       4.601   9.204 -71.40    4.633   8.670  -72.10   4.665   8.770  -74.00
>    39       4.697   8.913 -74.20    4.730   9.078  -76.90   4.762   8.414  -80.10
>    40       4.794   8.531 -81.30    4.827   8.472  -80.40   4.859   8.551  -81.30
>    41       4.891   8.298 -85.70    4.923   8.433  -85.20   4.956   8.035  -84.60
>    42       4.988   8.147 -87.20    5.020   8.511  -89.20   5.052   8.395  -89.70
>    43       5.085   7.943 -93.30    5.117   7.816  -92.80   5.149   8.337  -91.00
>    44       5.181   7.925 -97.10    5.214   7.907  -98.10   5.246   8.017  -96.20
>    45       5.278   7.379 -98.70    5.311   8.072 -100.00   5.343   7.691  -99.60
>    46       5.375   7.499 -101.80    5.407   7.586 -101.70   5.440   7.925 -100.70
>    47       5.472   7.656 -103.20    5.504   7.816 -104.70   5.536   7.727 -104.50
>    48       5.569   7.925 -104.70    5.601   7.907 -107.70   5.633   8.017 -109.50
>    49       5.665   7.870 -109.50    5.698   7.889 -109.60   5.730   8.091 -110.30
>    50       5.762   8.511 -111.50    5.794   8.337 -113.10   5.827   8.531 -116.50
>    51       5.859   8.810 -117.10    5.891   8.810 -120.10   5.924   8.590 -124.20
>    52       5.956   8.831 -125.90    5.988   8.298 -126.60   6.020   8.472 -129.40
>    53       6.053   8.531 -130.10    6.085   8.511 -131.20   6.117   8.279 -135.20
>    54       6.149   8.551 -136.20    6.182   8.318 -138.30   6.214   8.279 -143.10
>    55       6.246   7.998 -143.90    6.278   7.762 -144.50   6.311  11.117   44.30
>    56       6.343  13.932  167.90    6.375  13.521  165.70   6.408  13.183  162.40
>    57       6.440  12.882  162.20    6.472  12.735  159.80   6.504  12.359  158.50
>    58       6.537  11.912  156.40    6.569  11.508  156.90   6.601  11.641  157.00
>    59       6.633  11.508  157.30    6.666  11.749  154.50   6.698  11.508  153.80
>    60       6.730  11.350  152.40    6.762  11.246  151.70   6.795  11.455  150.50
>    61       6.827  10.965  149.30    6.859  10.965  148.10   6.892  10.965  149.50
>    62       6.924  11.117  147.70    6.956  11.169  145.40   6.988  10.990  143.40
>    63       7.021  10.520  142.80    7.053  10.839  142.30   7.085  10.765  142.50
>    64       7.117  10.617  139.70    7.150  10.641  140.20   7.182  10.641  140.80
>    65       7.214  10.617  139.40    7.246  11.041  137.50   7.279  10.965  138.10
>    66       7.311  10.814  135.70    7.343  11.324  136.50
*END OF FILE
*
```

- - - DATA - - -

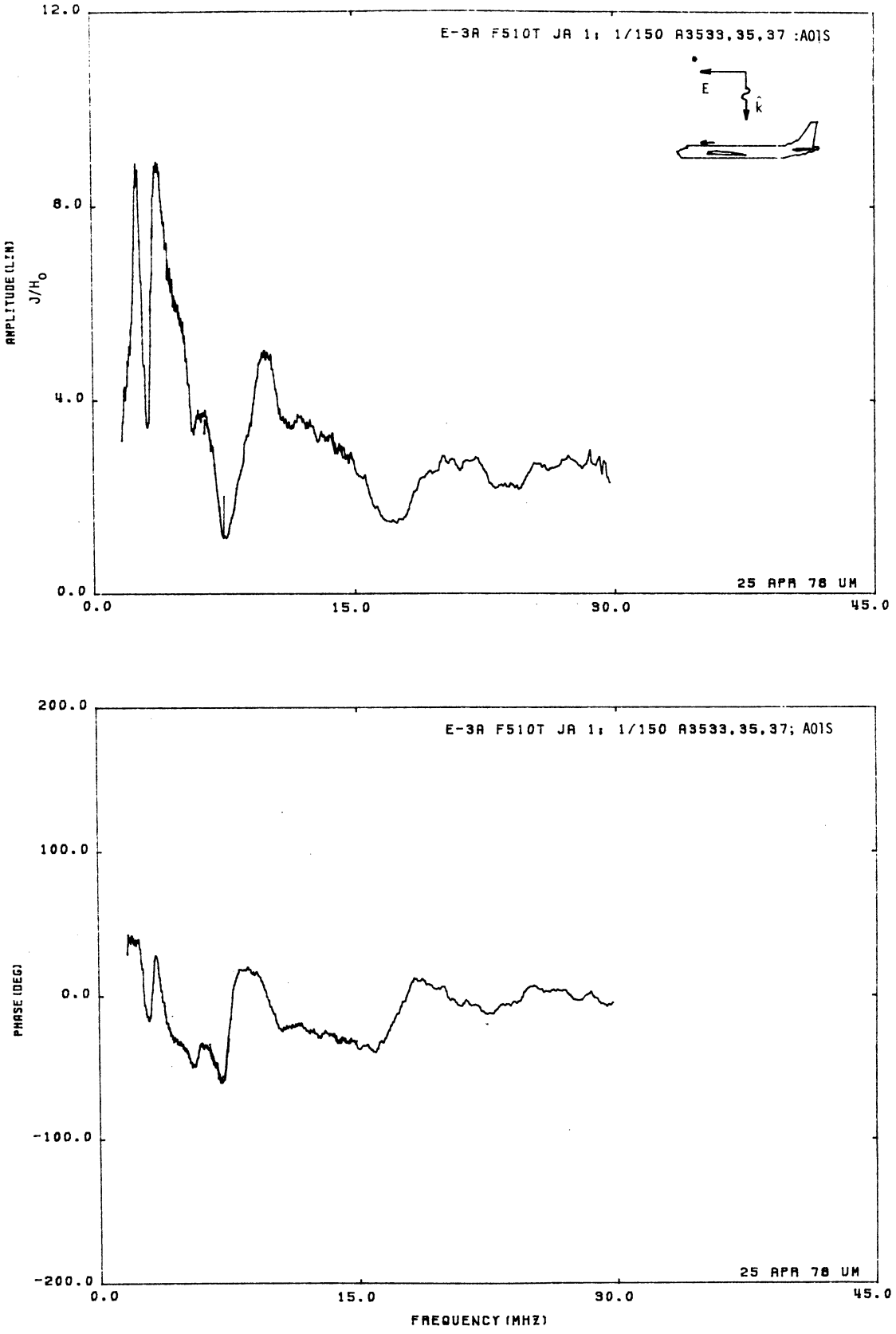

Figure 01S. Axial Current at STA:F510T, Excitation 1, 1/150 Model.

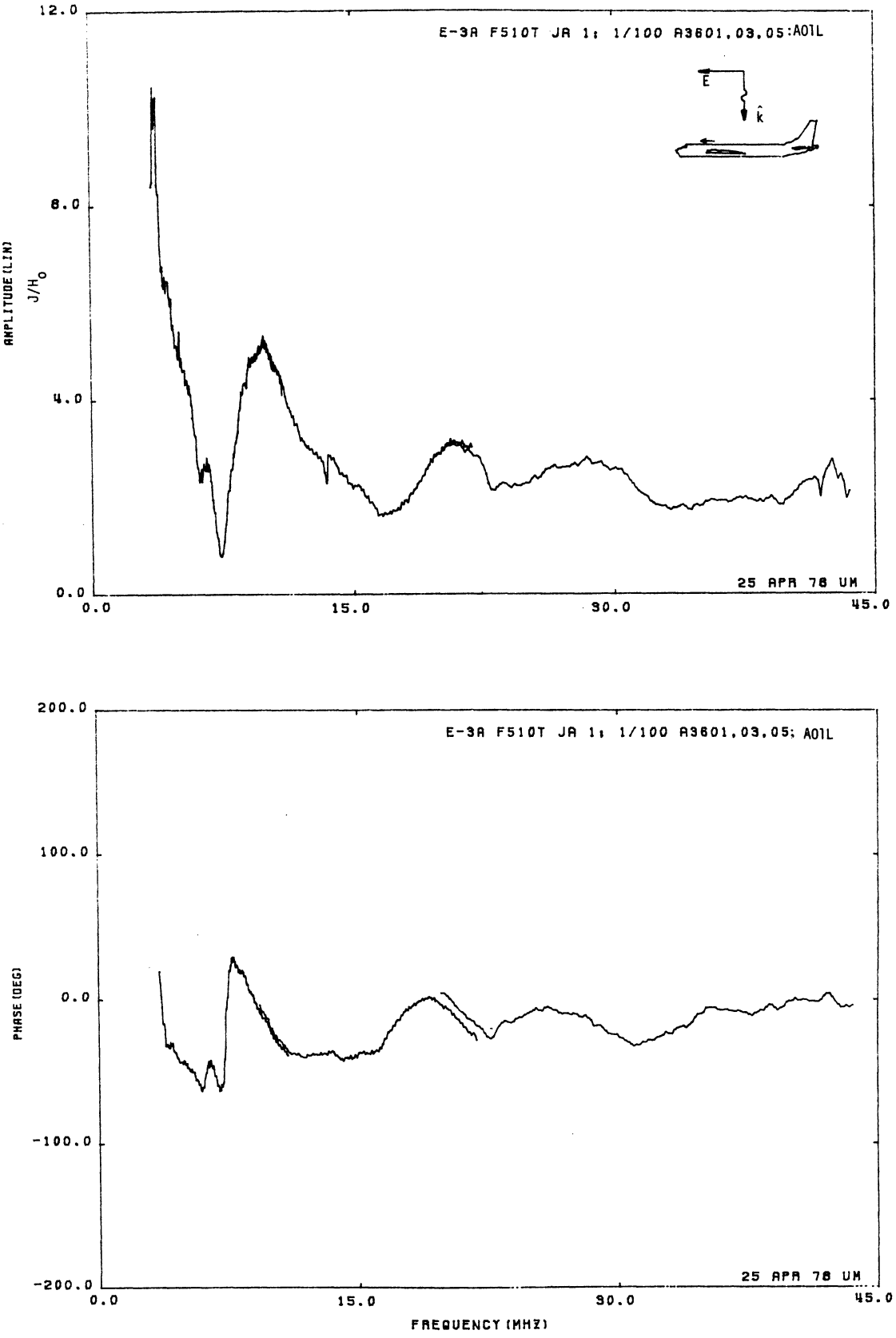

Figure 01L. Axial Current at STA:F510T, Excitation 1, 1/100 Model.

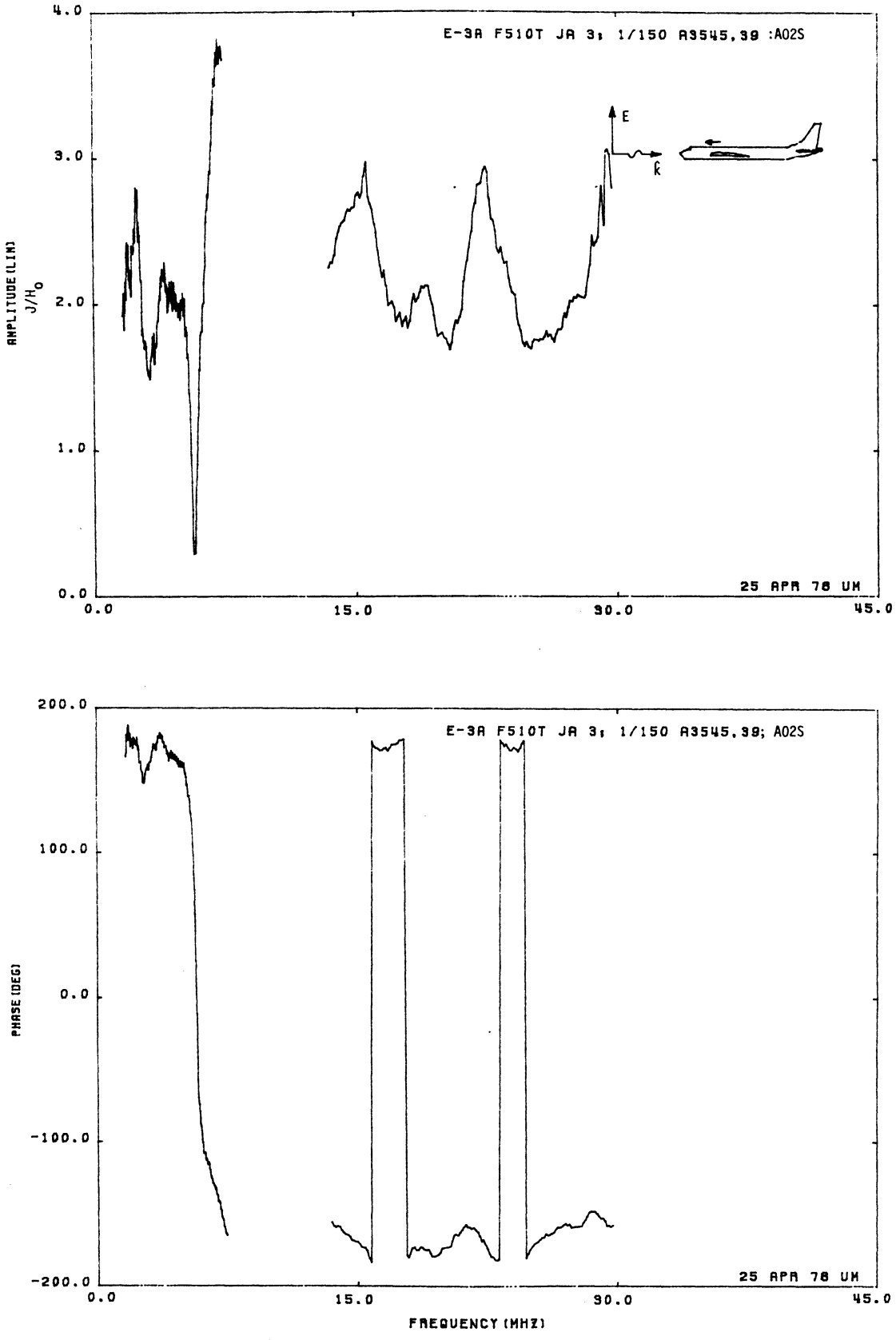

Figure 02S. Axial Current at STA:F510T, Excitation 3, 1/150 Model.

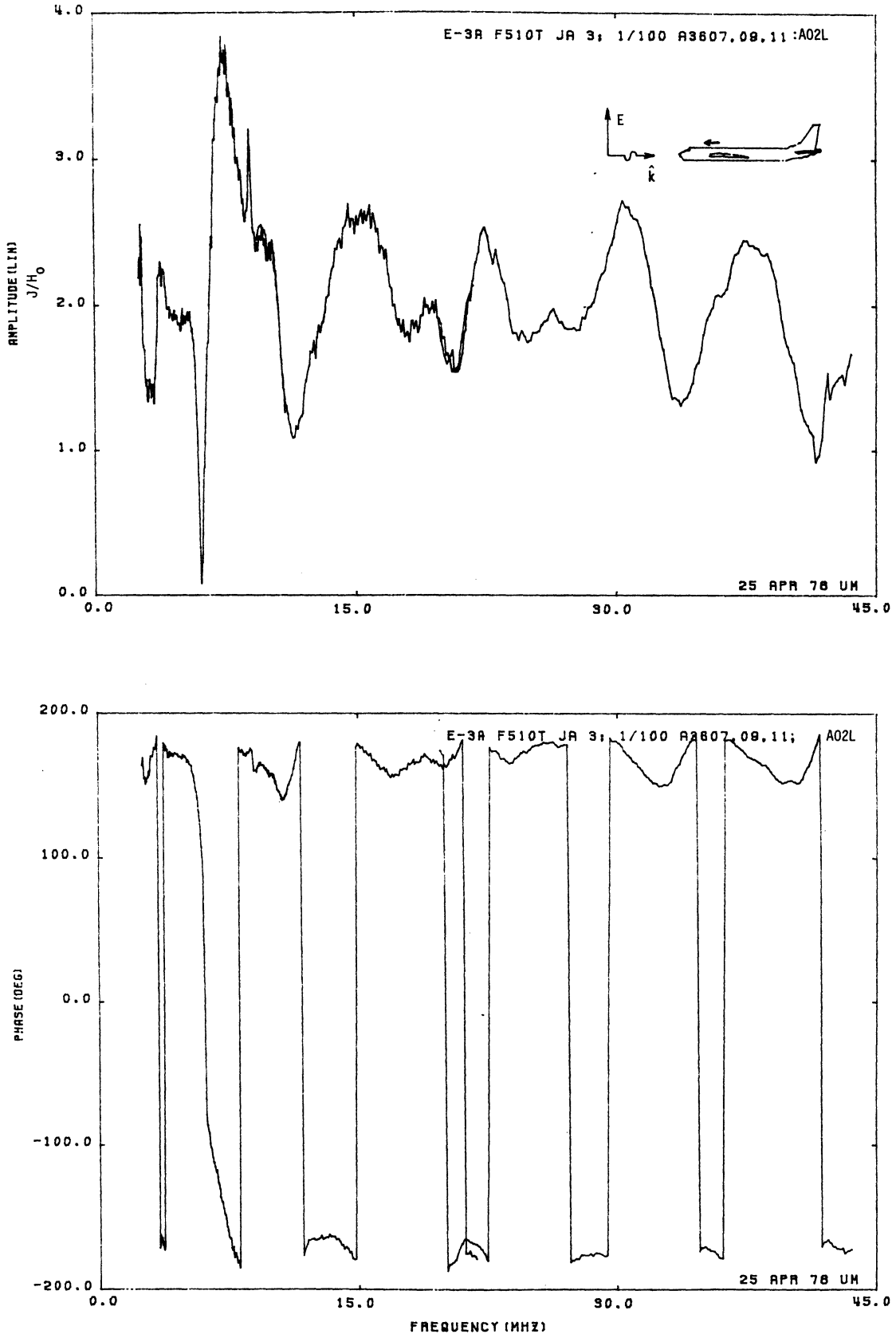

Figure 02L. Axial Current at STA:F510T, Excitation 3, 1/100 Model.

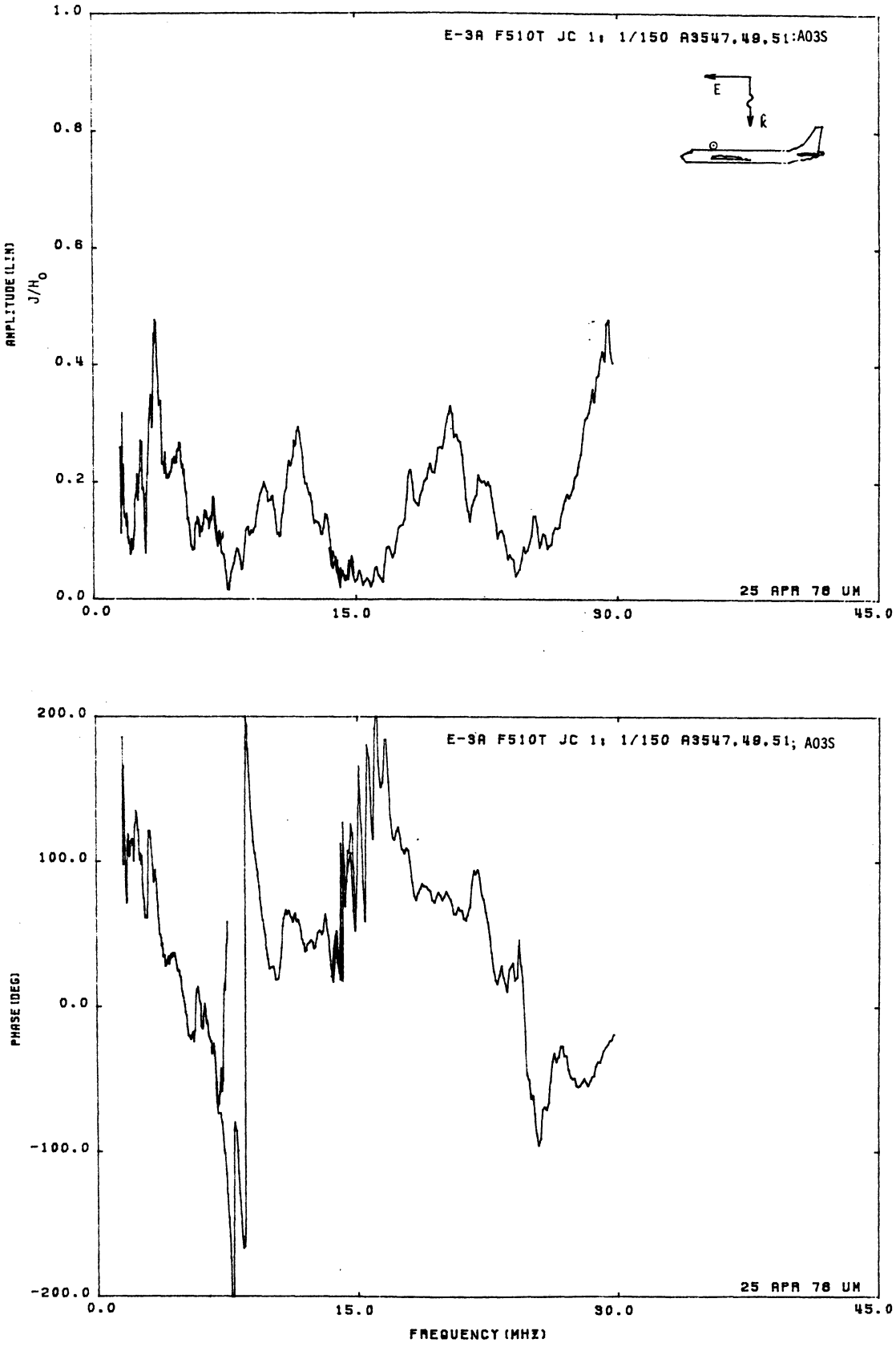

Figure 03S. Circumferential Current at STA:F510T, Excitation 1, 1/150 Model.

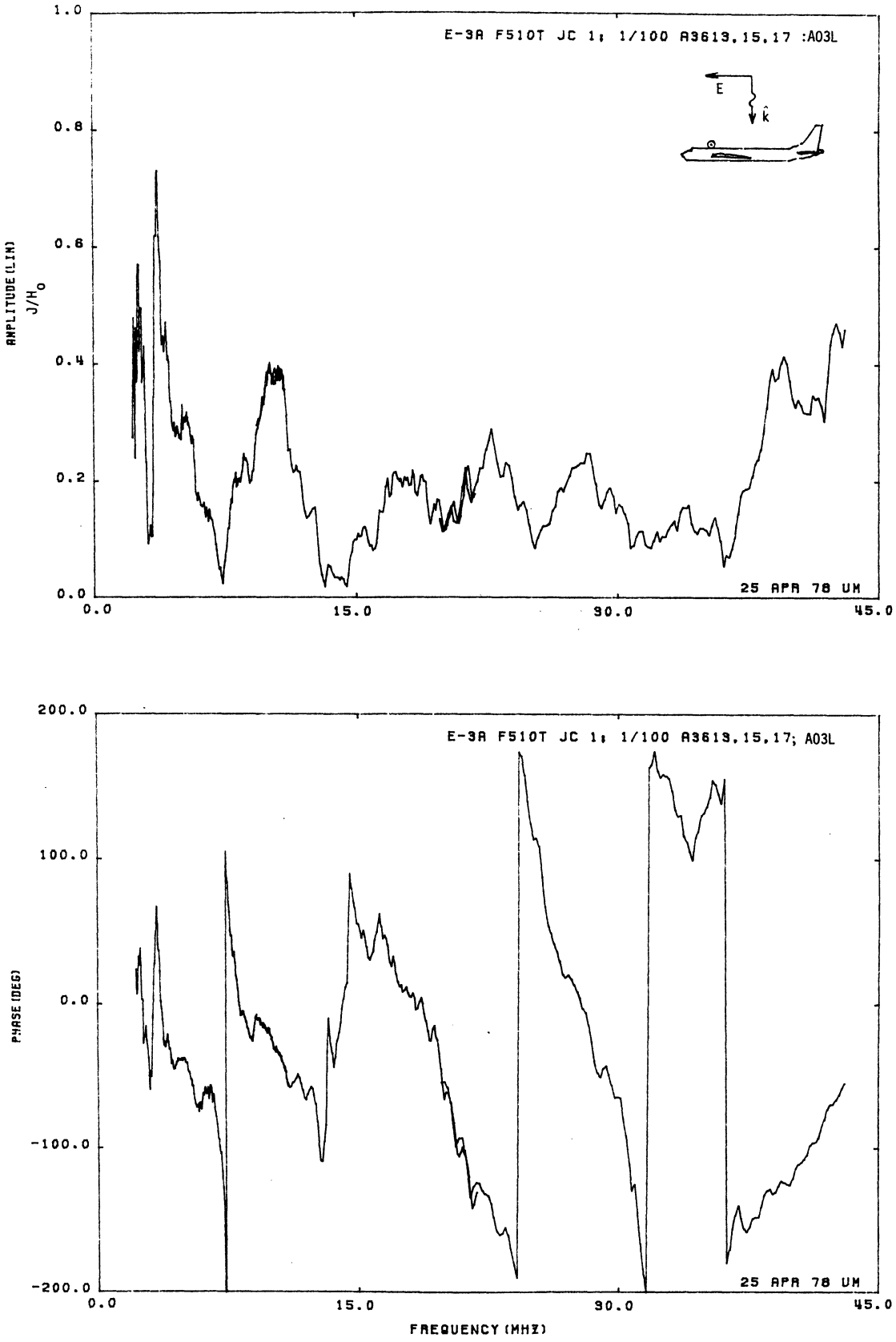

Figure 03L. Circumferential Current at STA:F510T, Excitation 1, 1/100 Model.

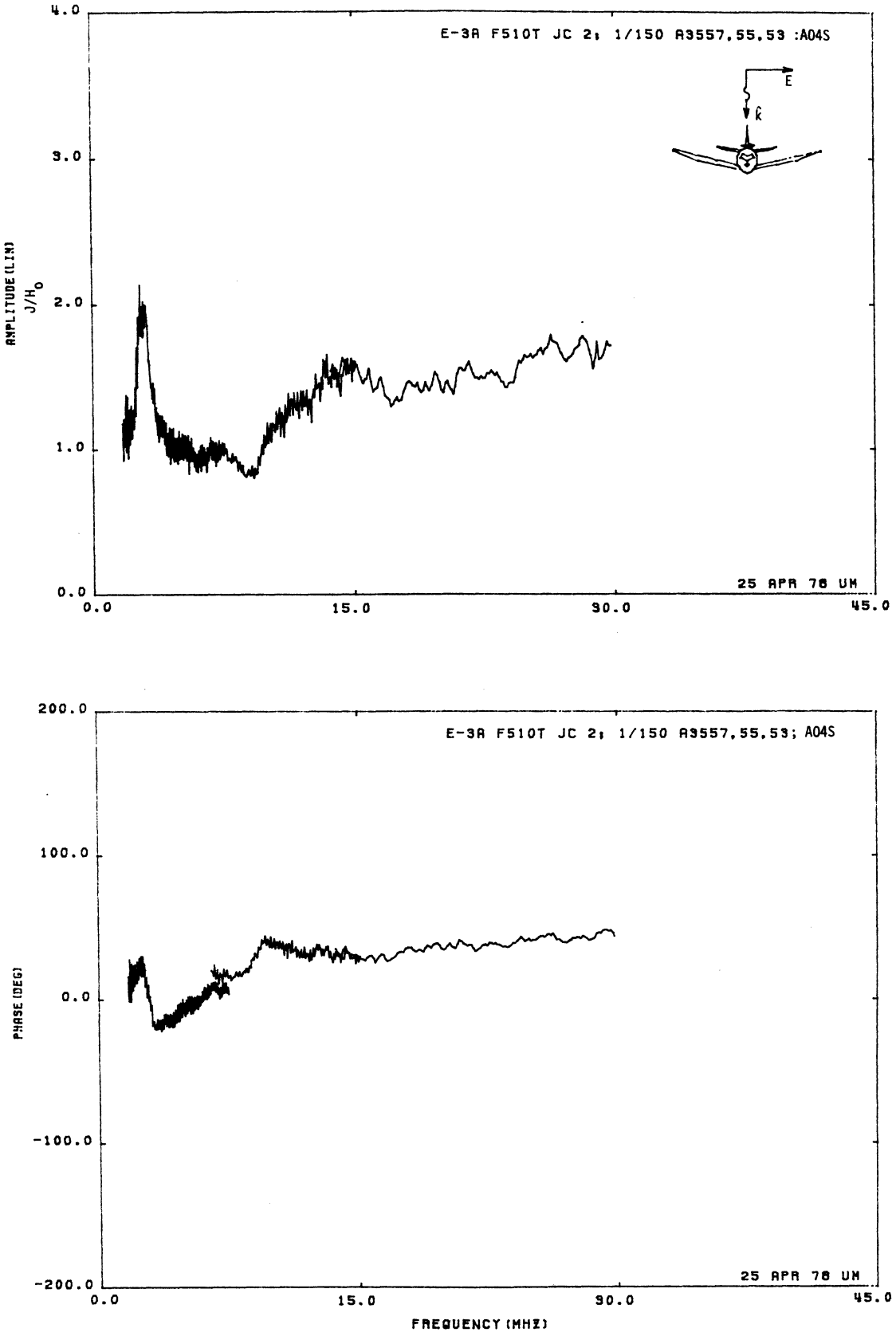

Figure 04S. Circumferential Current at STA:F510T, Excitation 2, 1/150 Model.

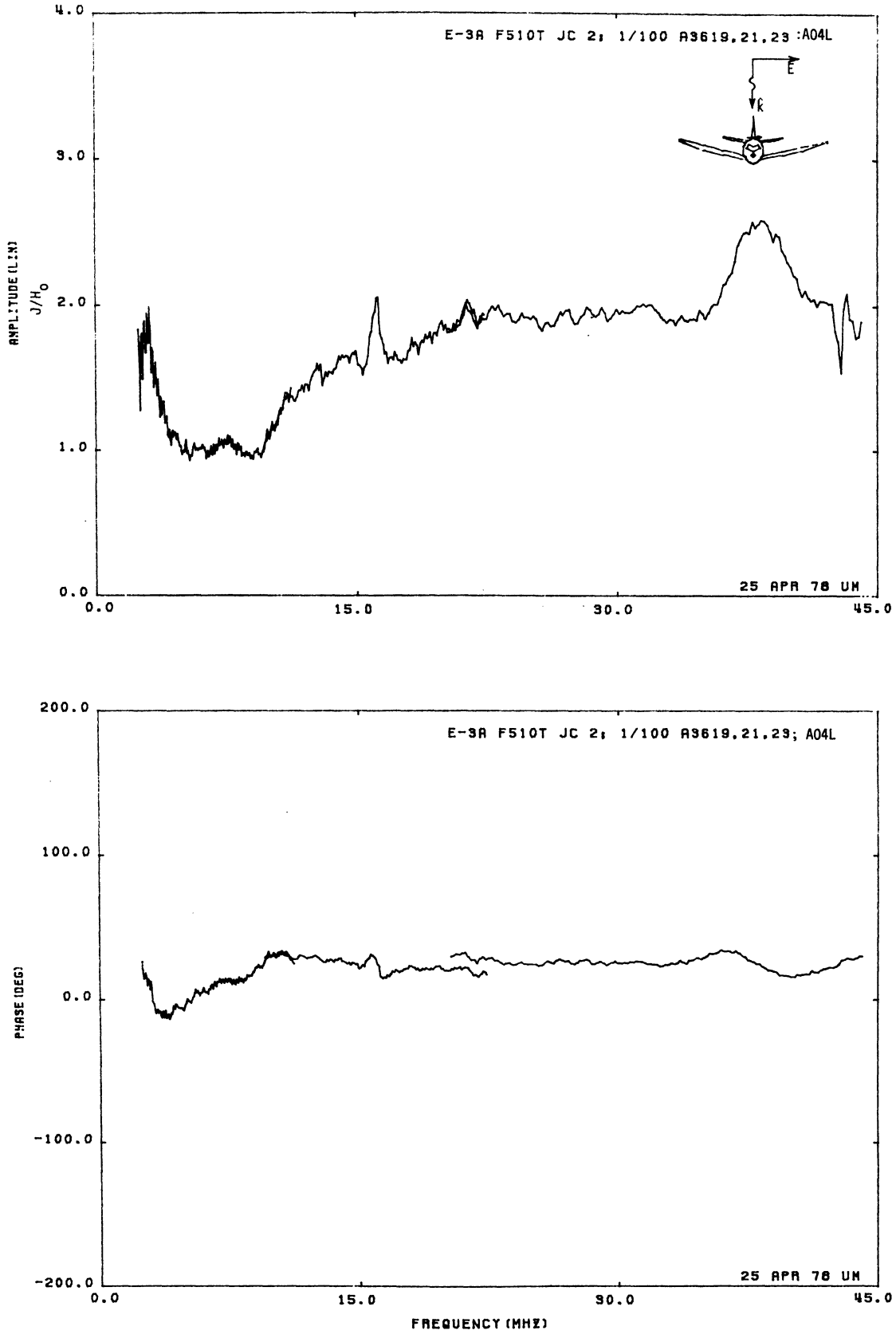

Figure 04L. Circumferential Current at STA:F510T, Excitation 2, 1/100 Model.

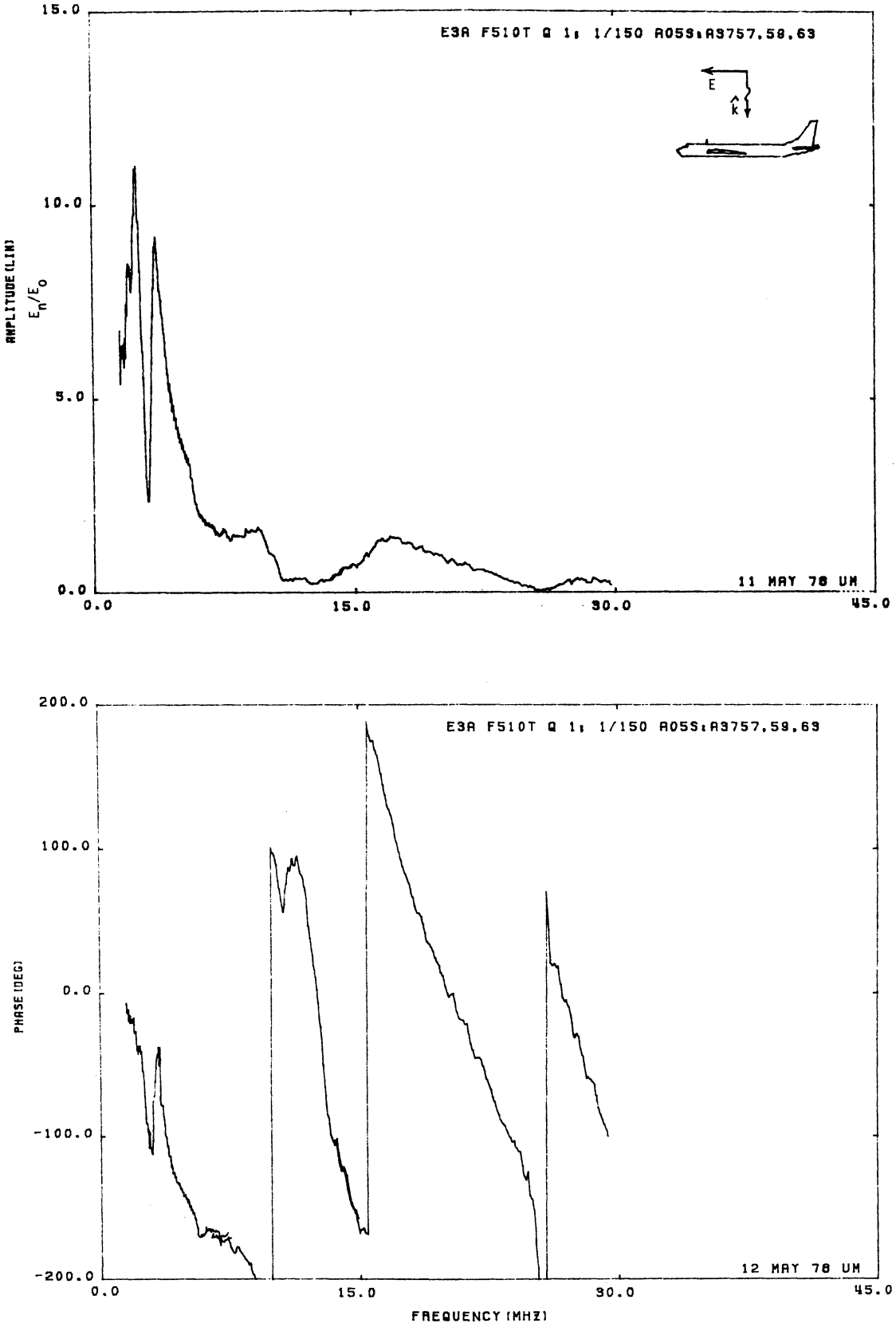

Figure 05S. Charge at STA:F510T, Excitation 1, 1/150 Model.

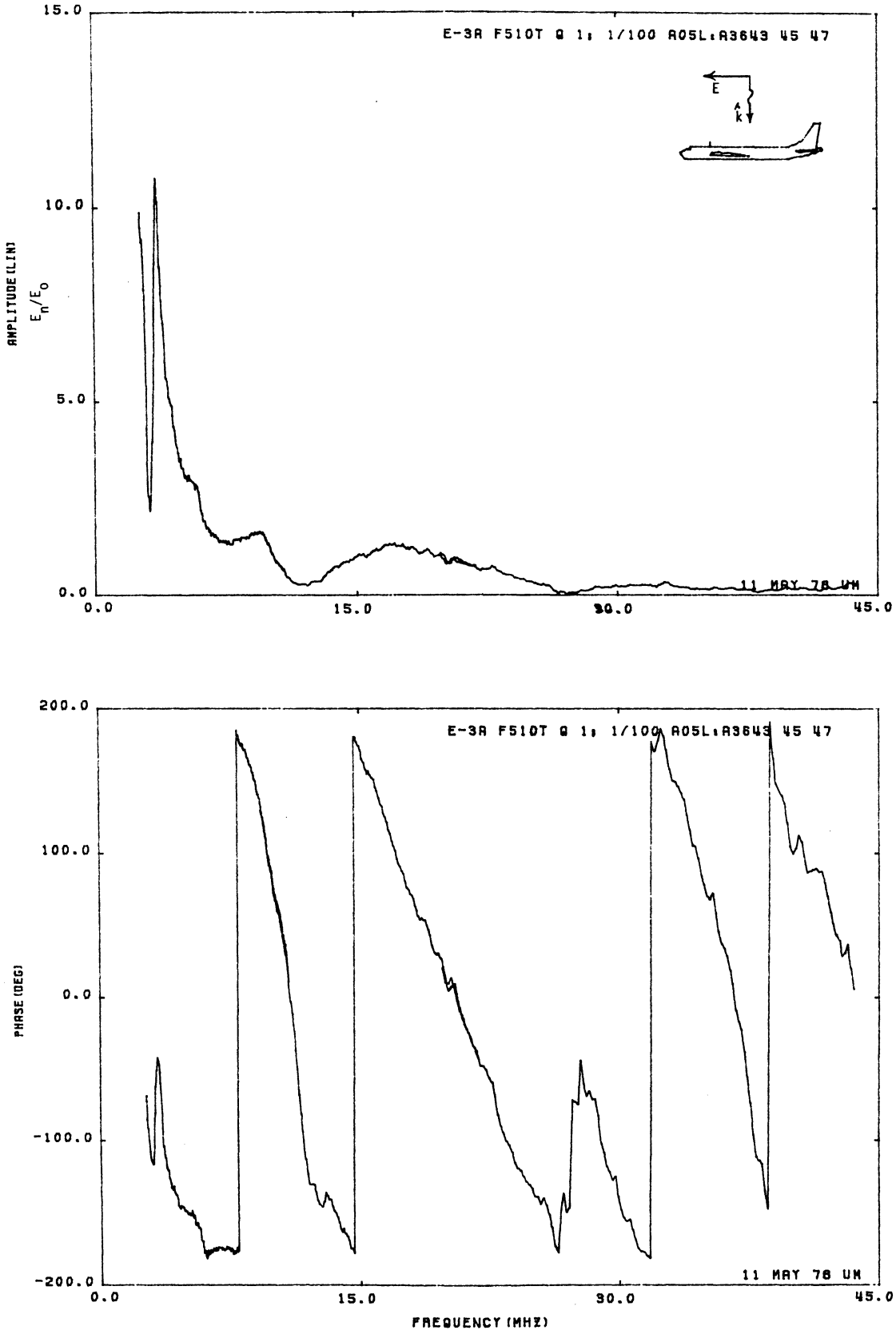

Figure 05L. Charge at STA:F510T, Excitation 1, 1/100 Model.

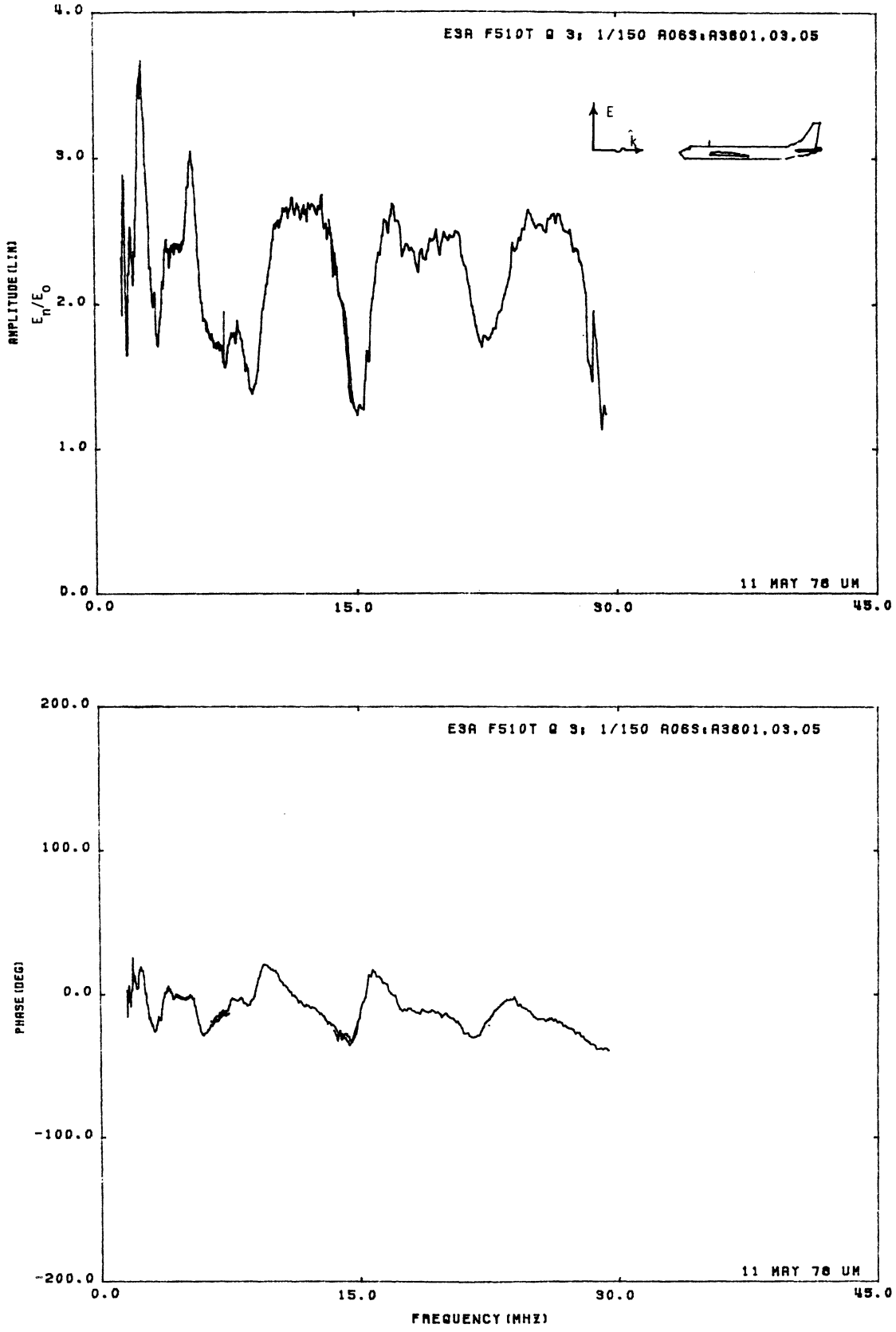

Figure 06S. Charge at STA:F510T, Excitation 3, 1/150 Model.

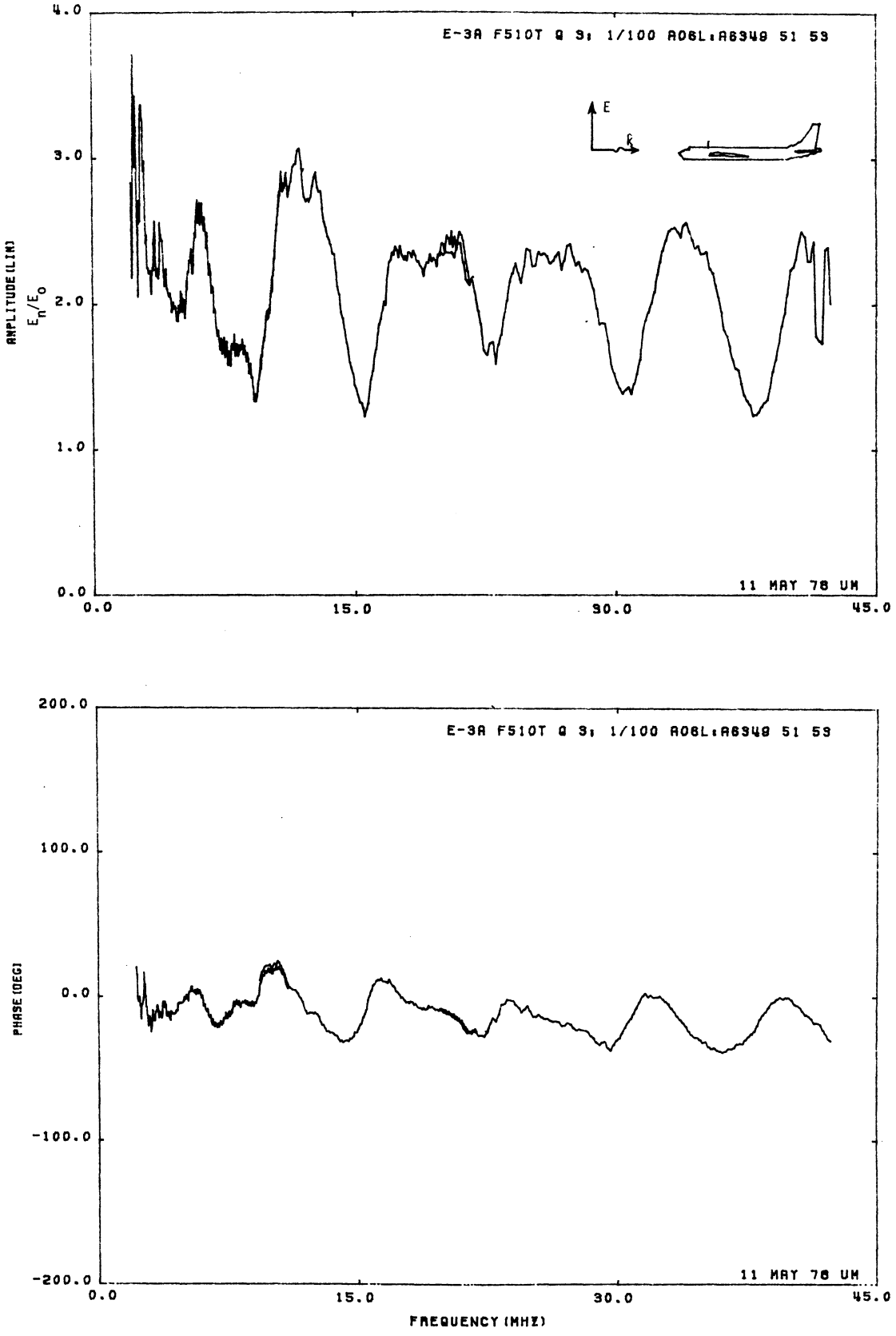

Figure 06L. Charge at STA:F510T, Excitation 3, 1/100 Model.

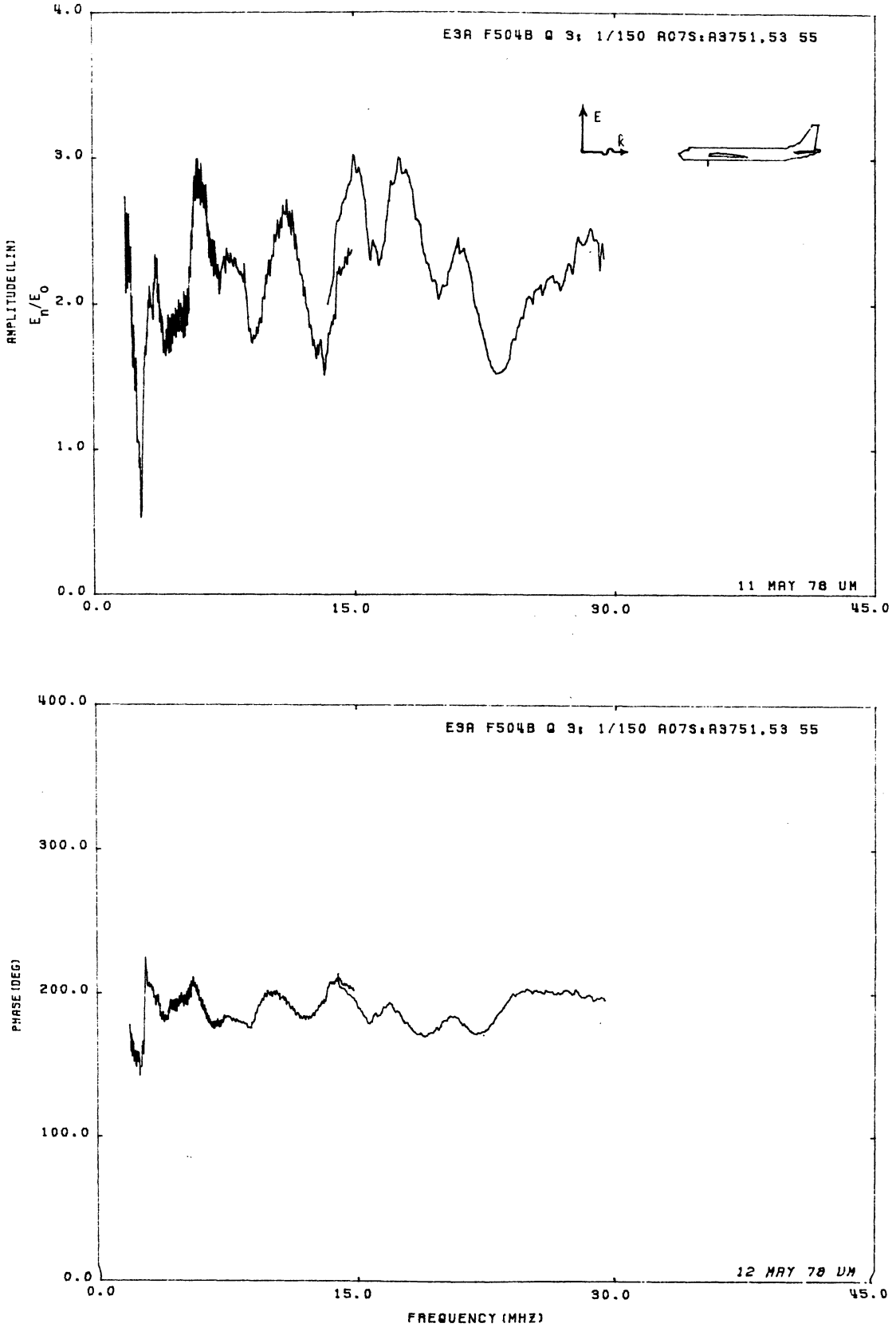

Figure 07S. Charge at STA:F504B, Excitation 3, 1/150 Model.

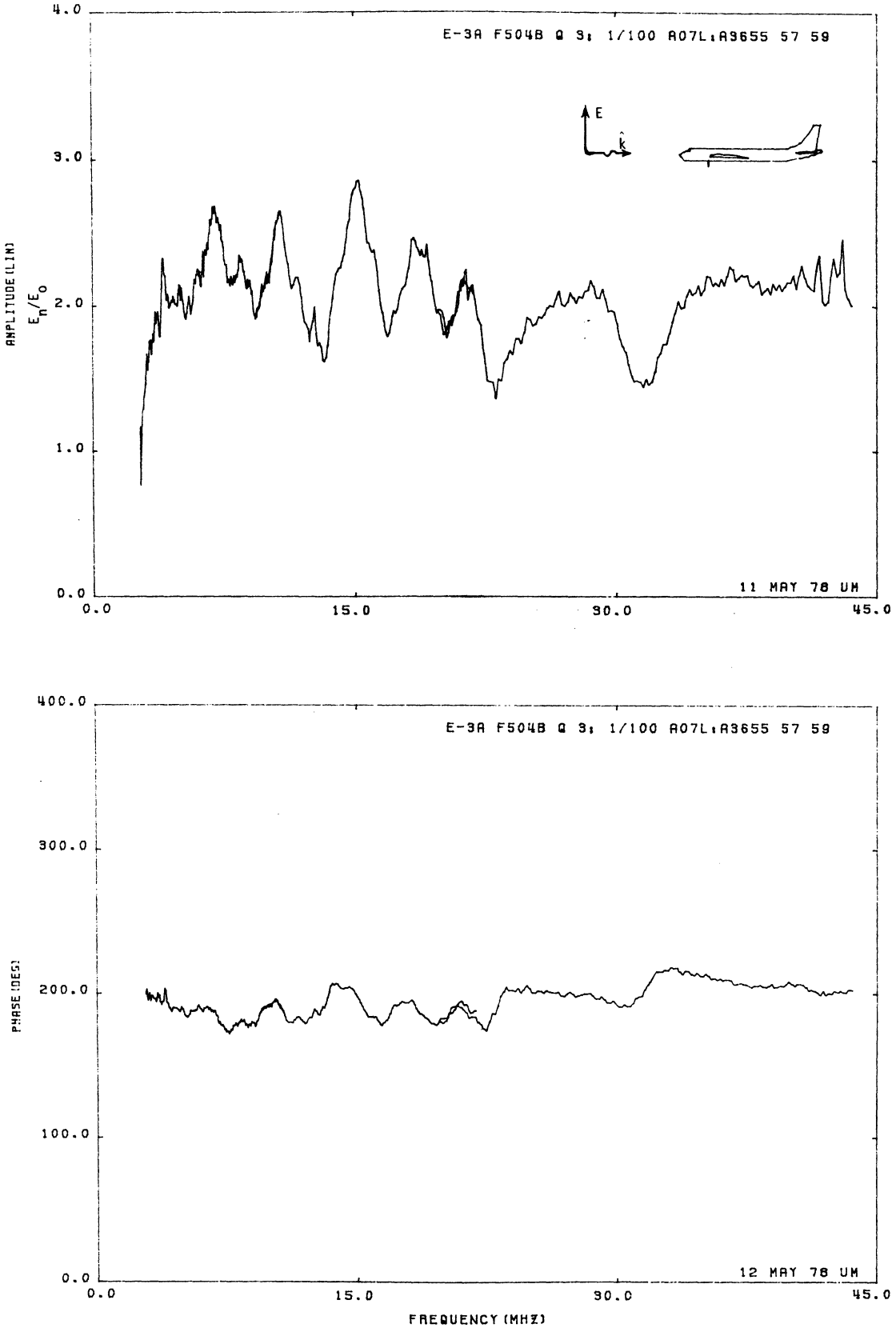

Figure 07L. Charge at STA:F504B, Excitation 3, 1/100 Model.

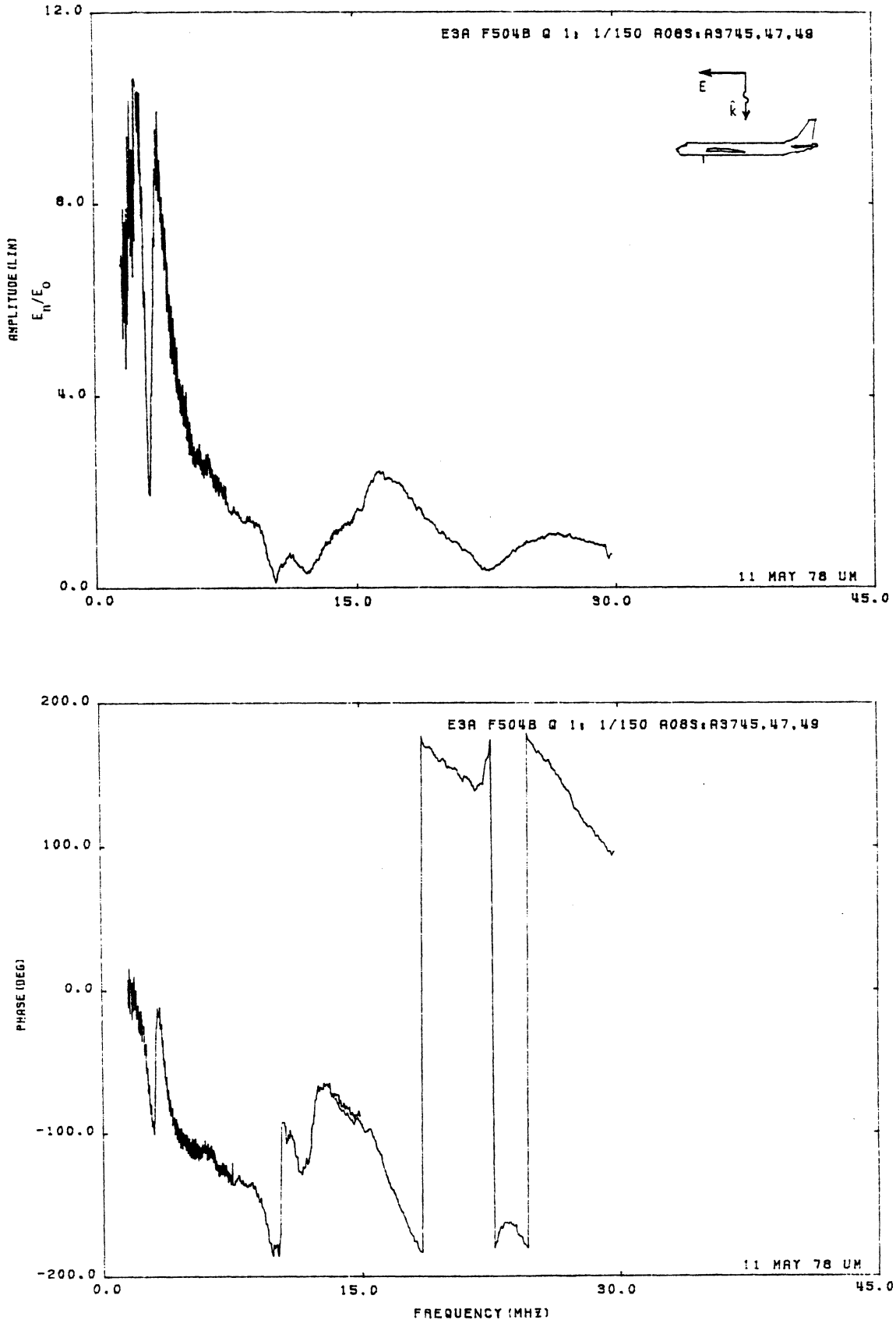

Figure 08S. Charge at STA;F504B, Excitation 1, 1/150 Model.

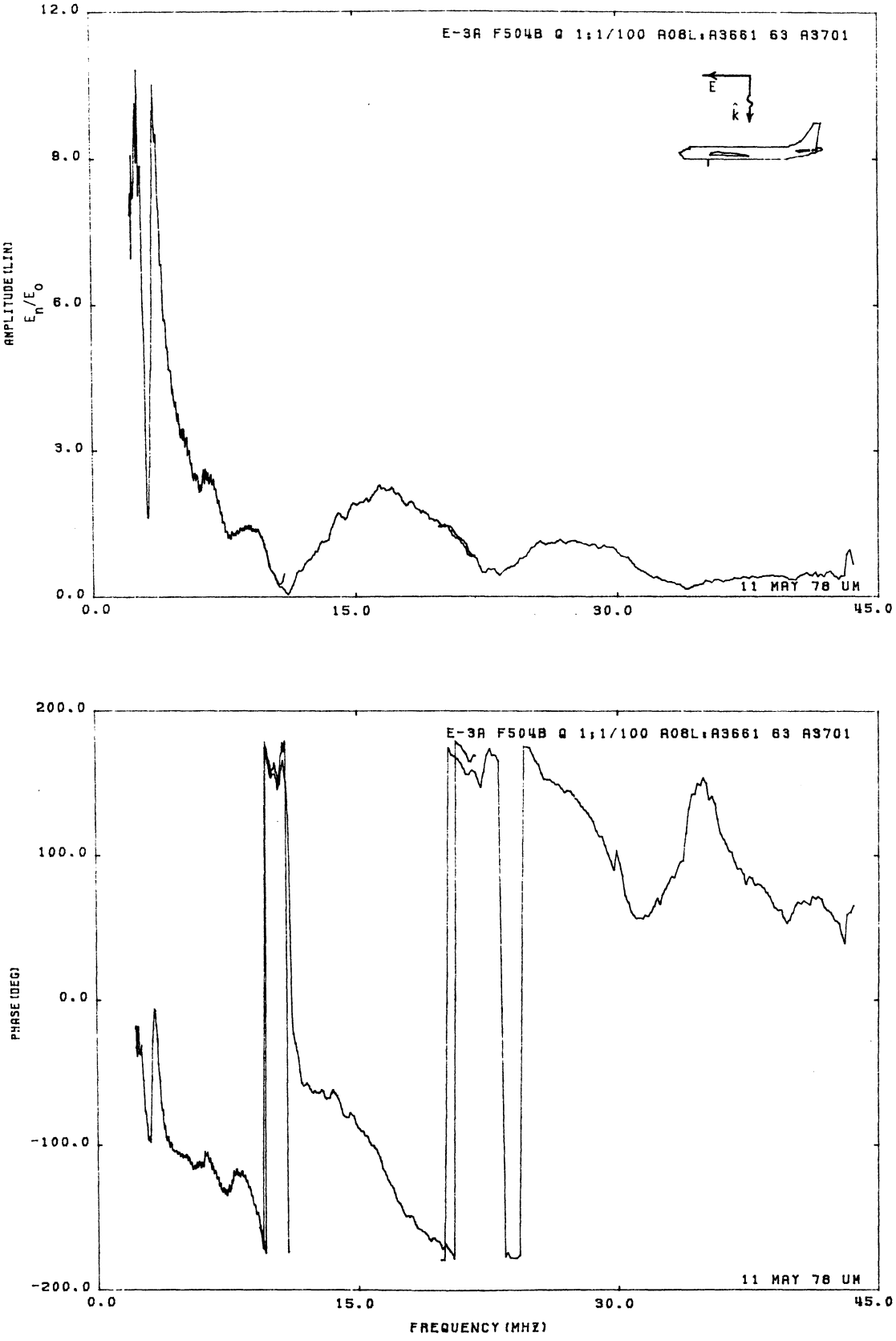

Figure 08L. Charge at STA:F504B, Excitation 1, 1/100 Model.

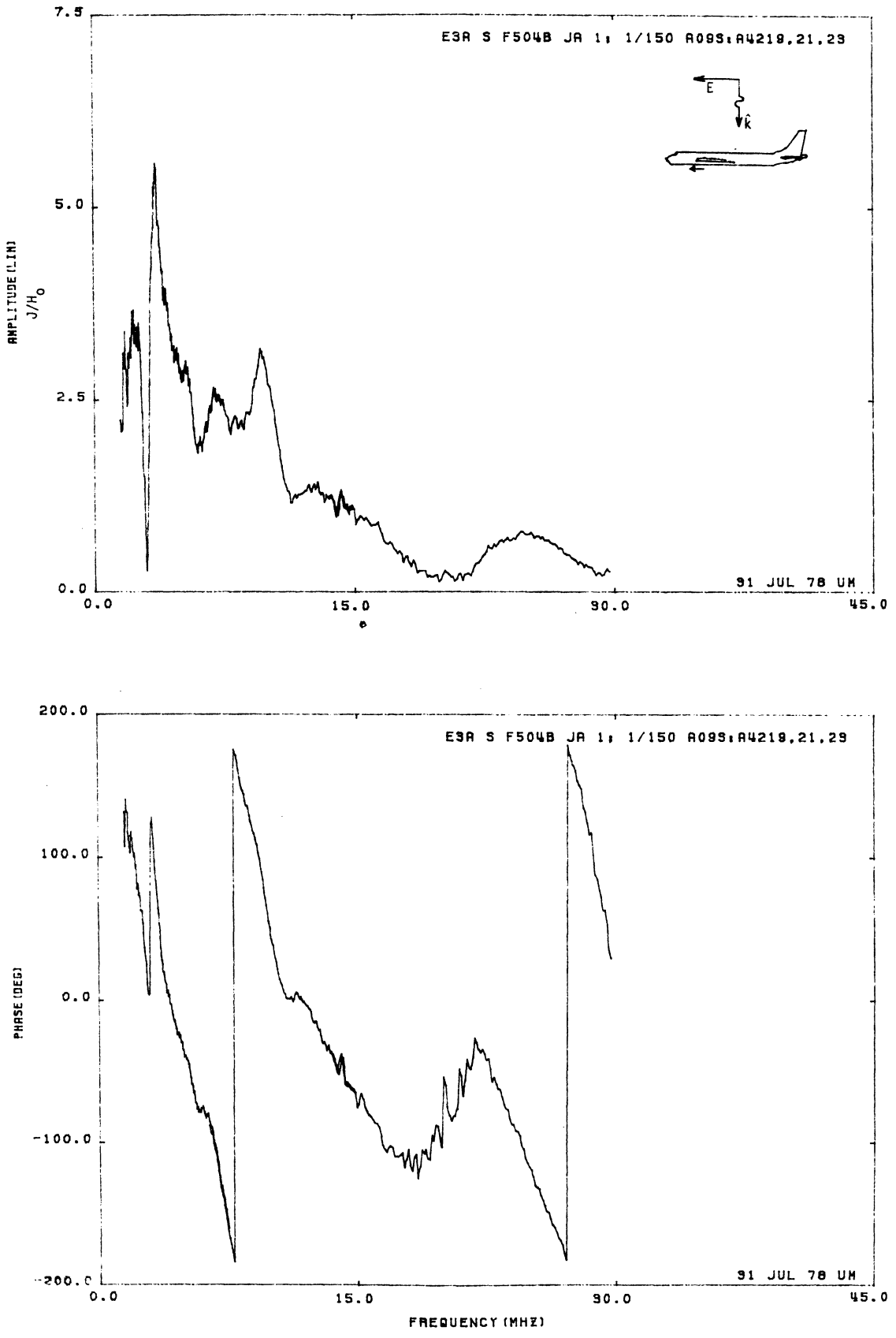

Figure 09S. Axial Current at STA:F504B, Excitation 1, 1/150 Model.

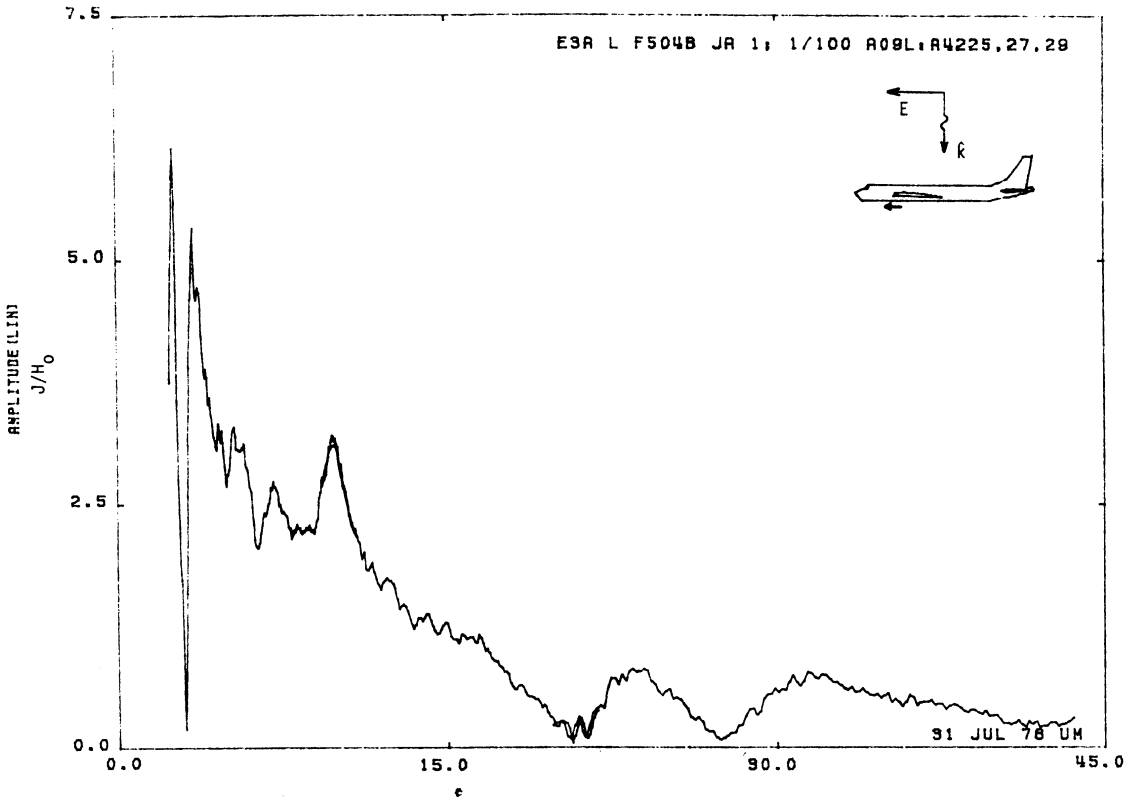

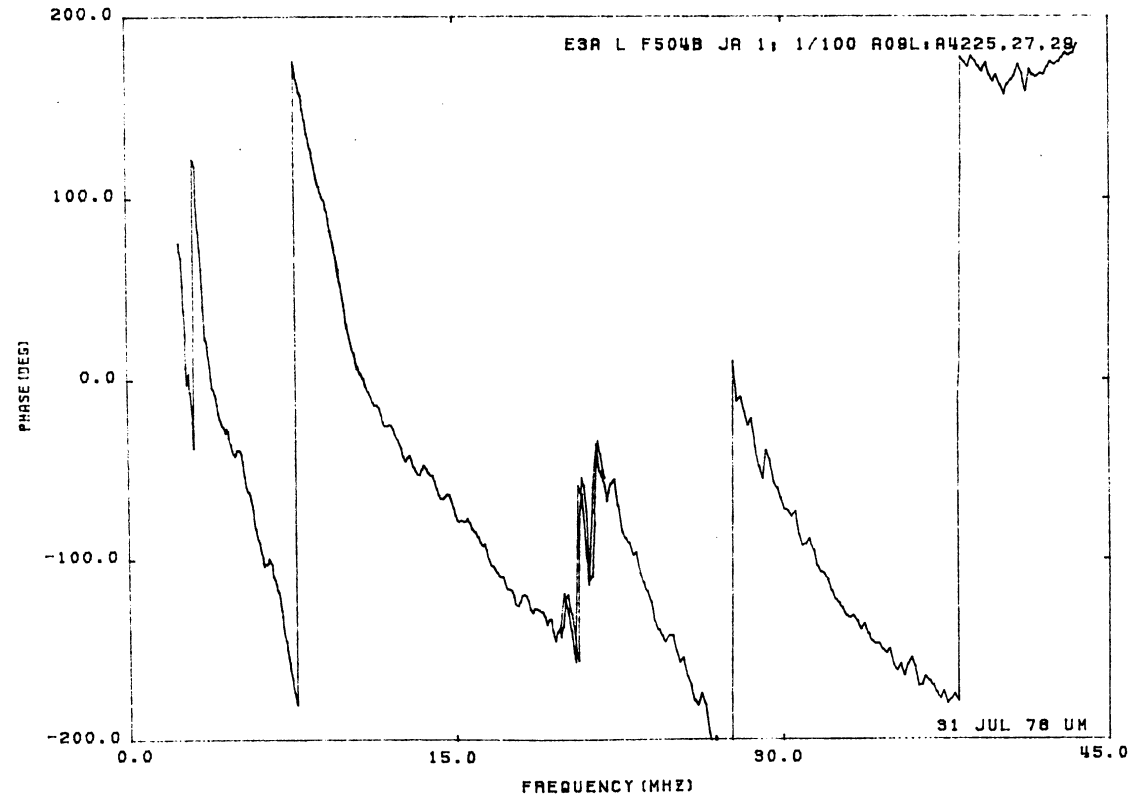

Figure 09L. Axial Current at STA:F504B, Excitation 1. 1/100 Model.

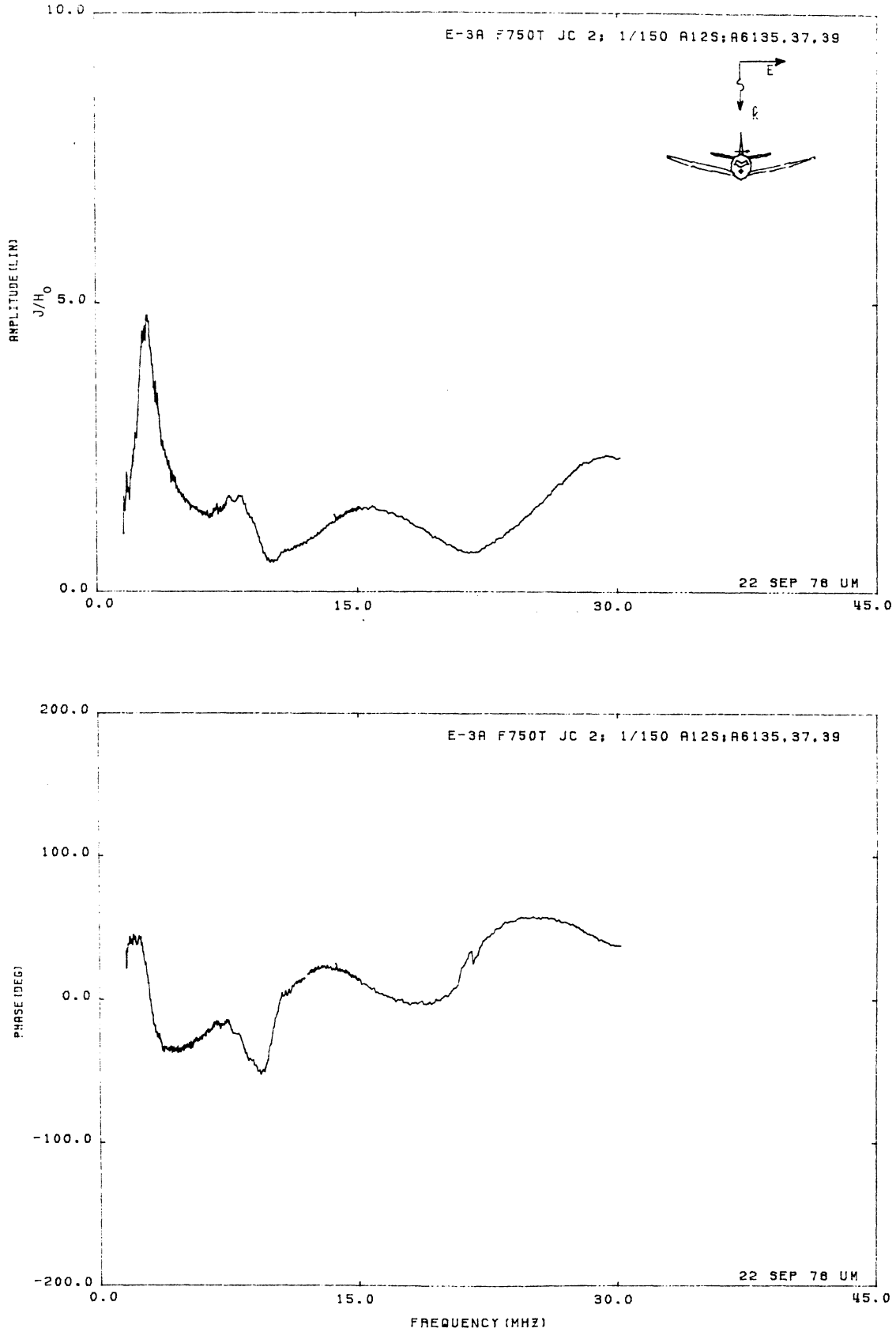

Figure 12S. Circumferential Current at STA:F750T, Excitation 2, 1/150 Model.

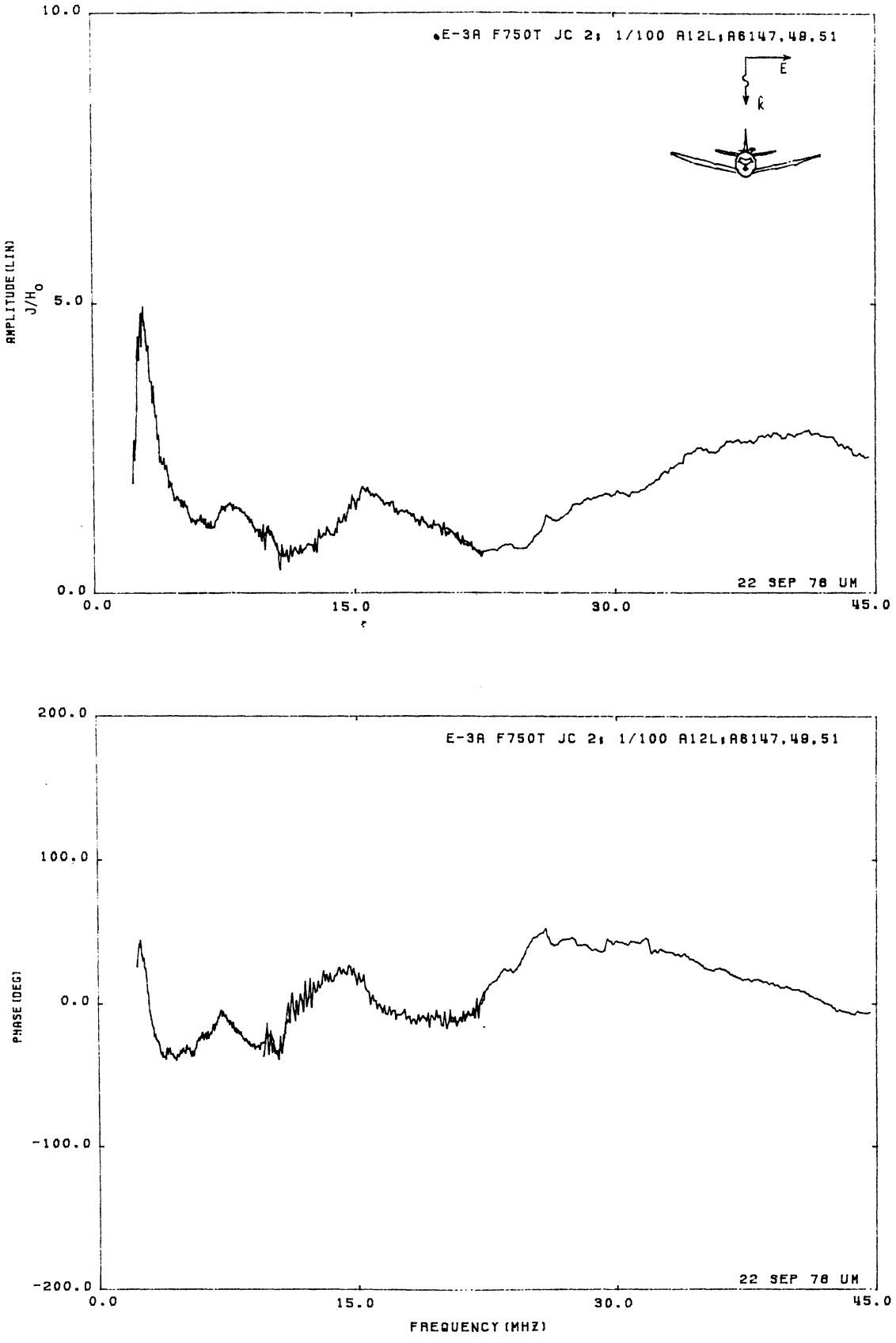

Figure 12L. Circumferential Current at STA:F750T, Excitation 2, 1/100 Model.

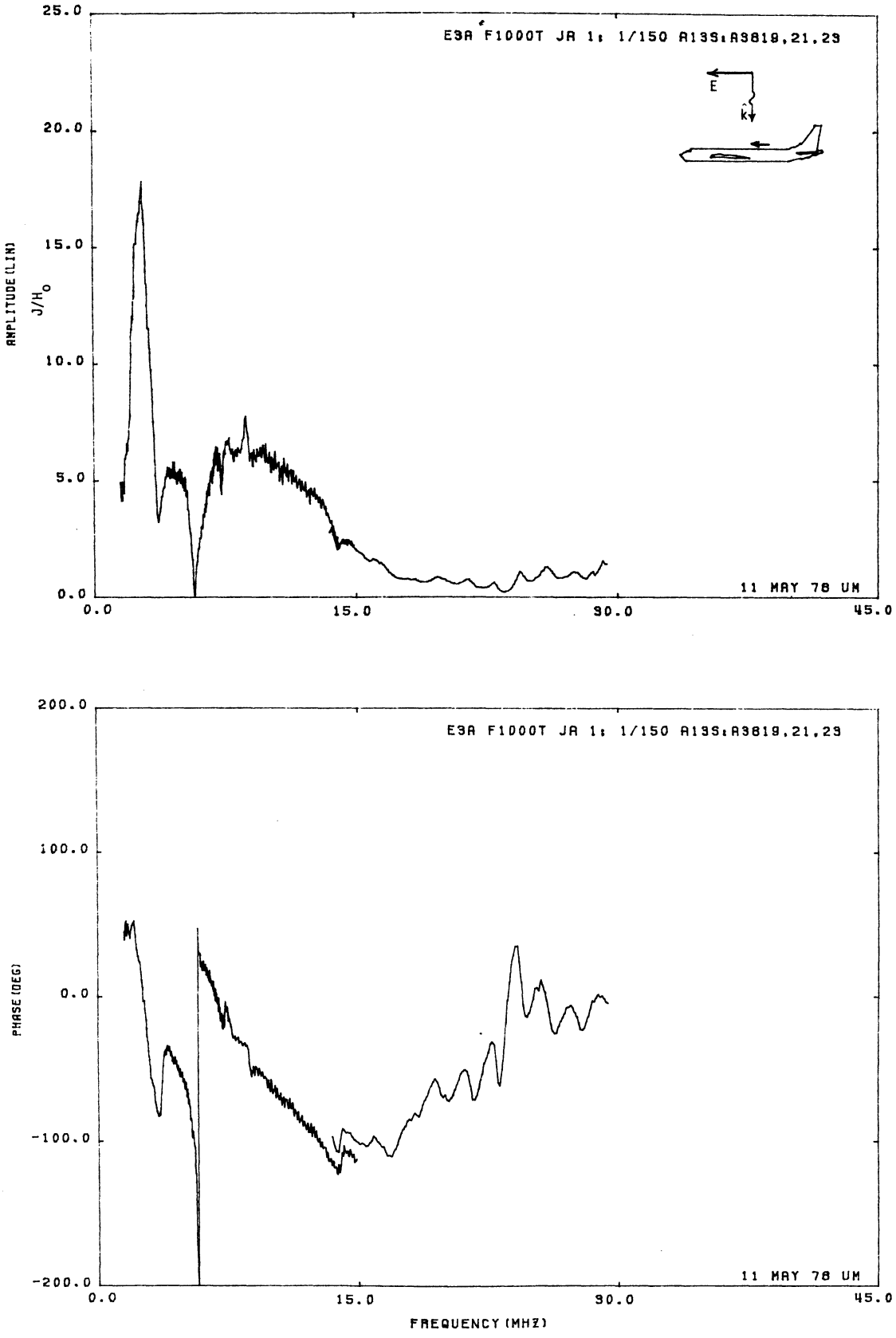

Figure 13S. Axial Current at STA:F1000T, Excitation 1, 1/150 Model.

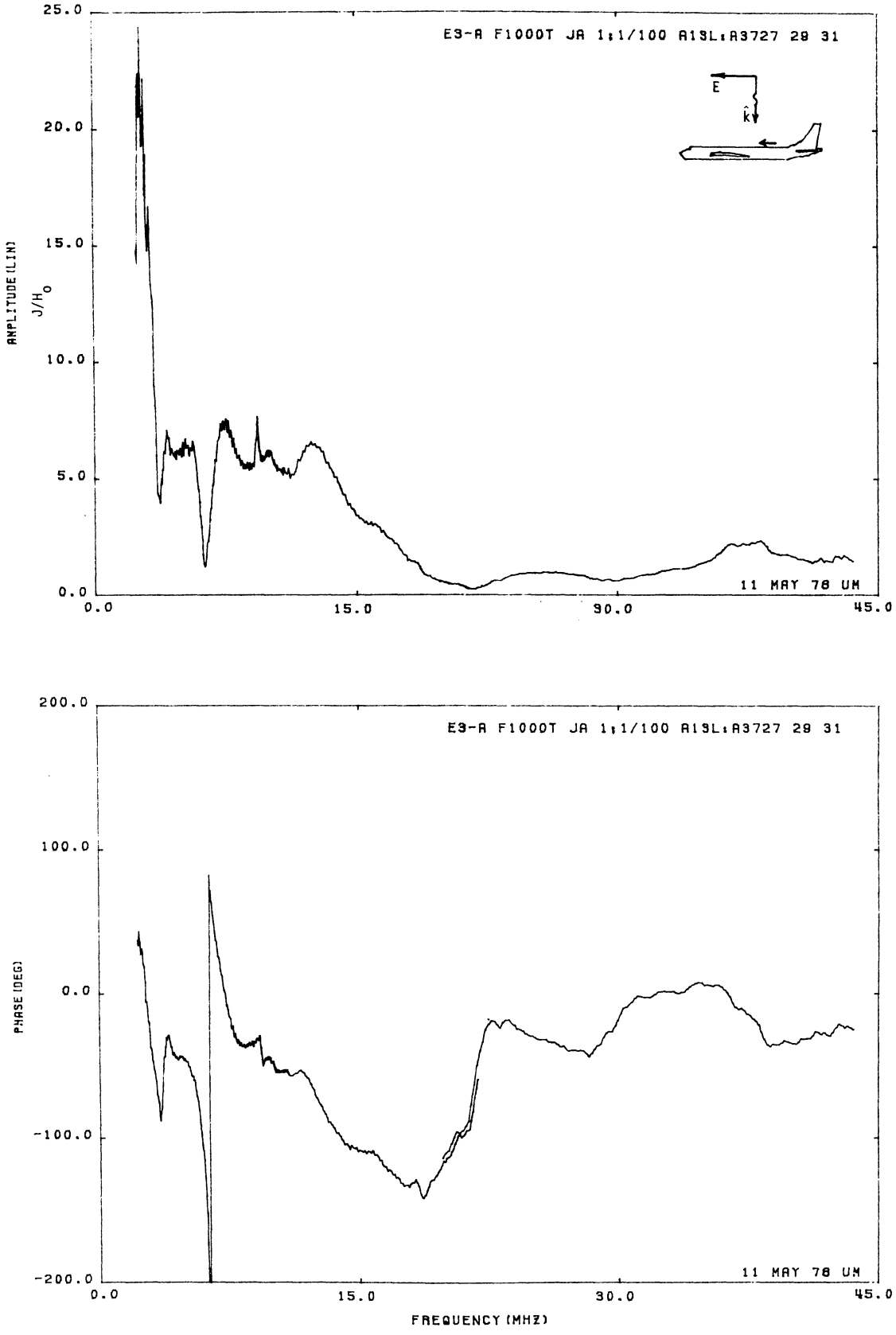

Figure 13L. Axial Current at STA:F1000T, Excitation 1, 1/100 Model.

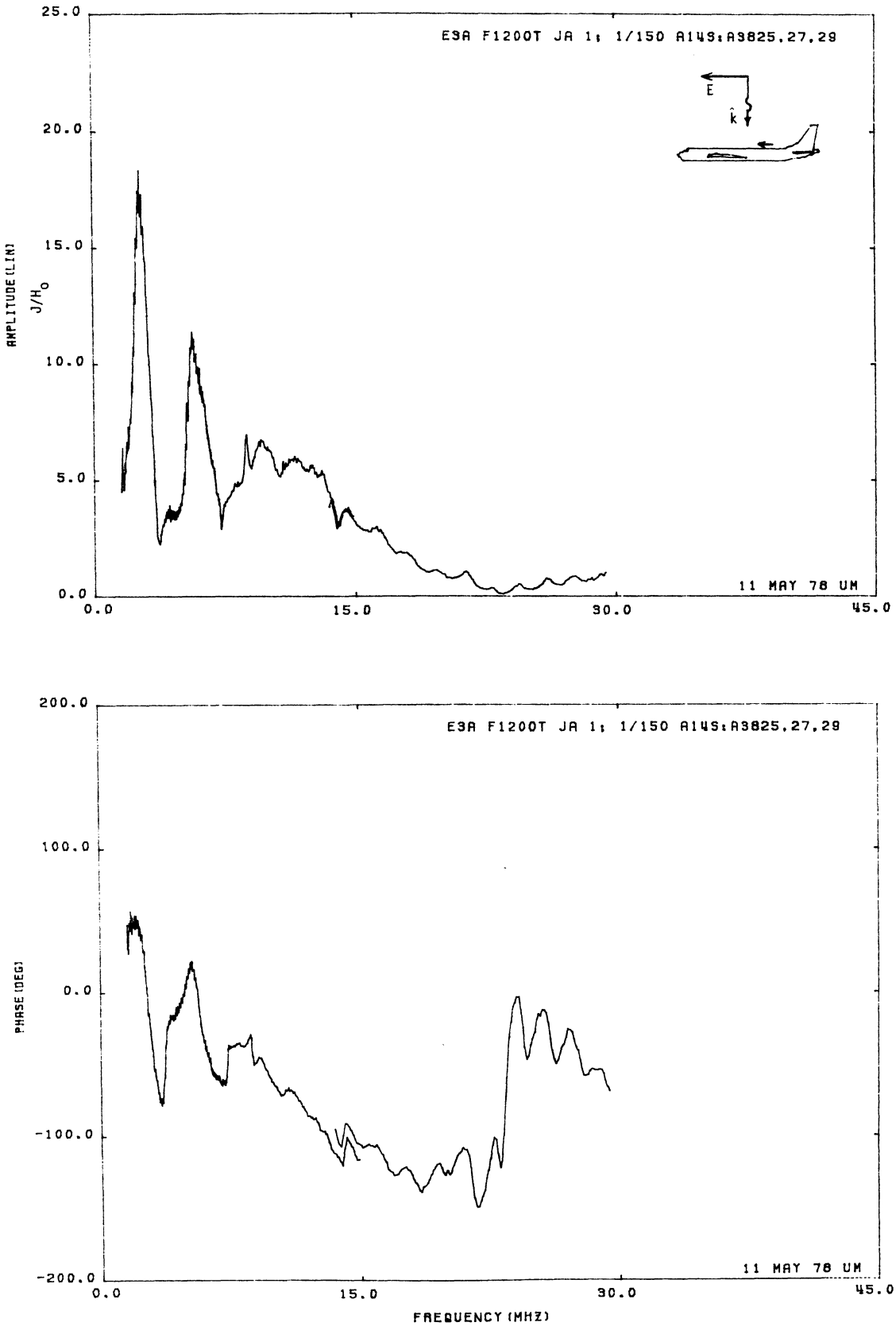

Figure 14S. Axial Current at STA:F1200T, Excitation 1, 1/150 Model.

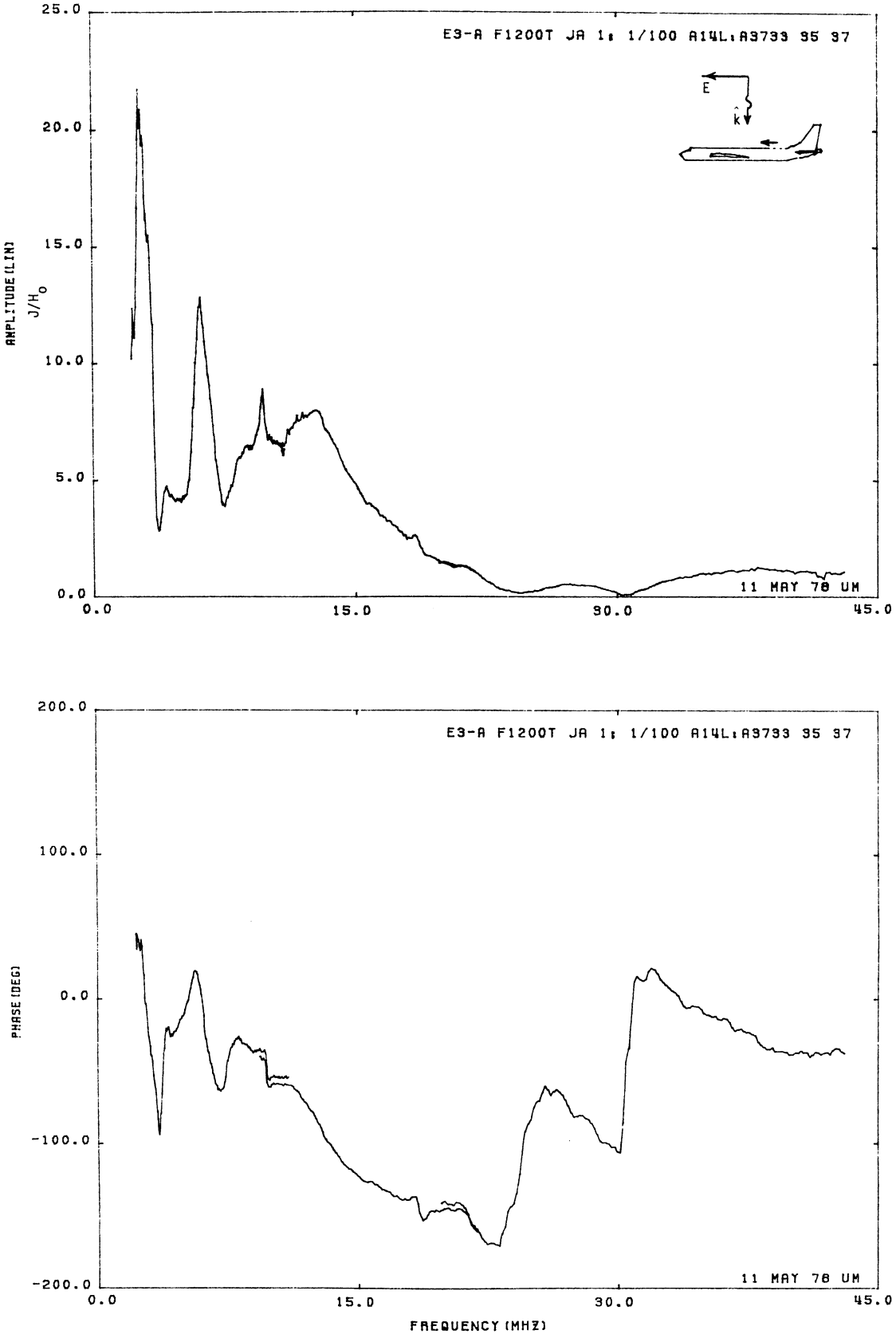

Figure 14L. Axial Current at STA:F1200T, Excitation 1, 1/100 Model.

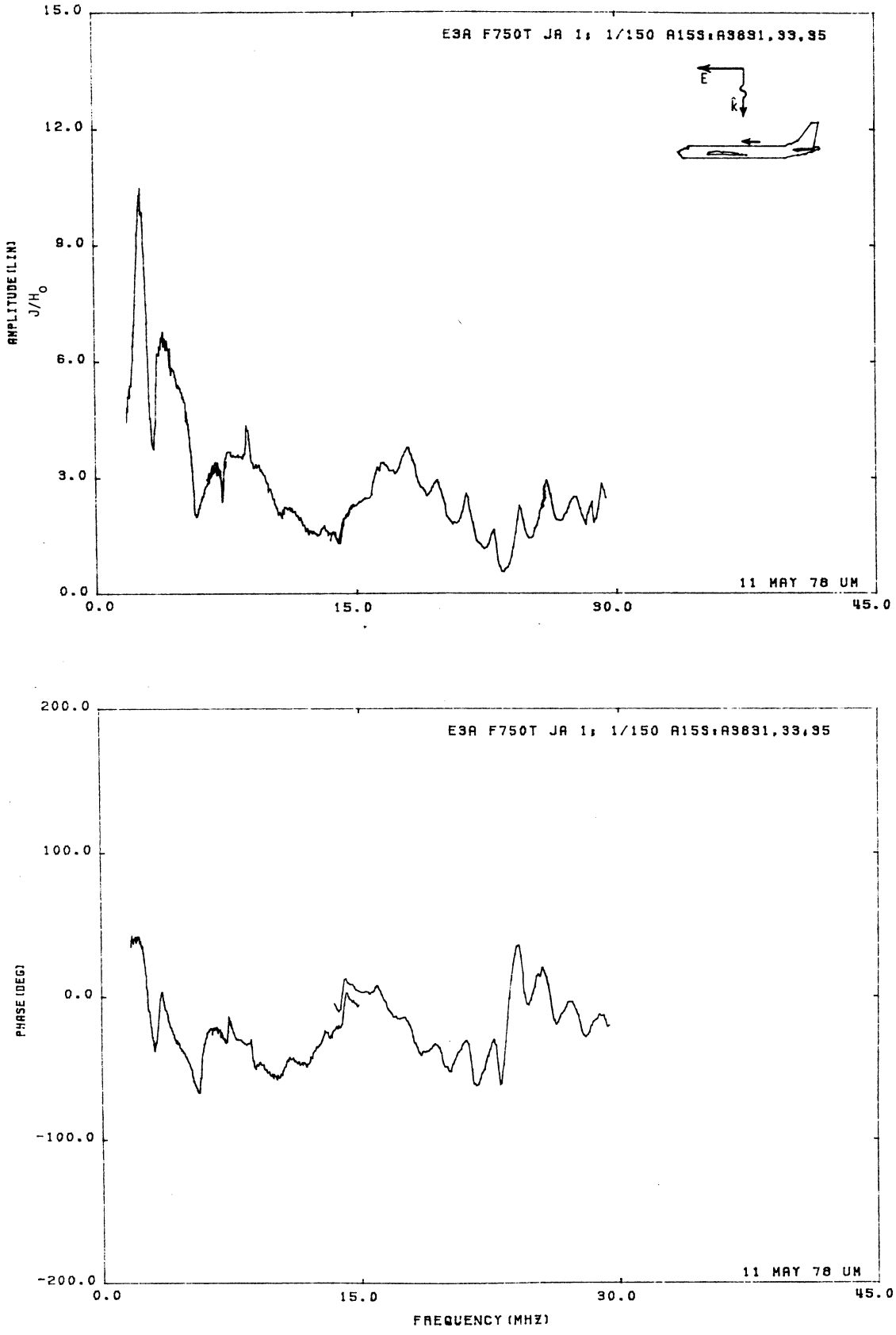

Figure 15S. Axial Current at STA:F750T, Excitation 1, 1/150 Model.

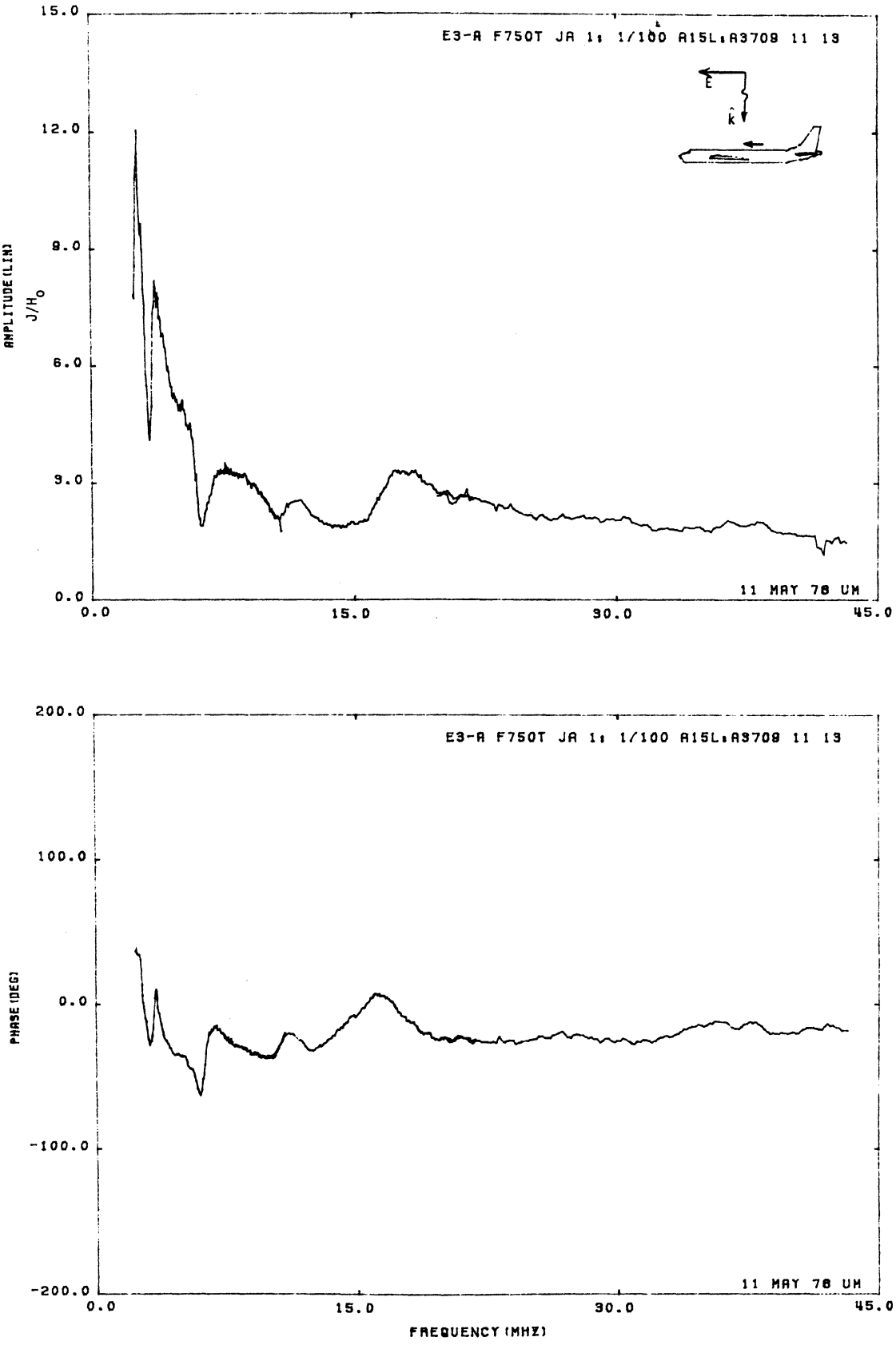

Figure 15L. Axial Current at STA:F750T, Excitation 1, 1/100 Model.

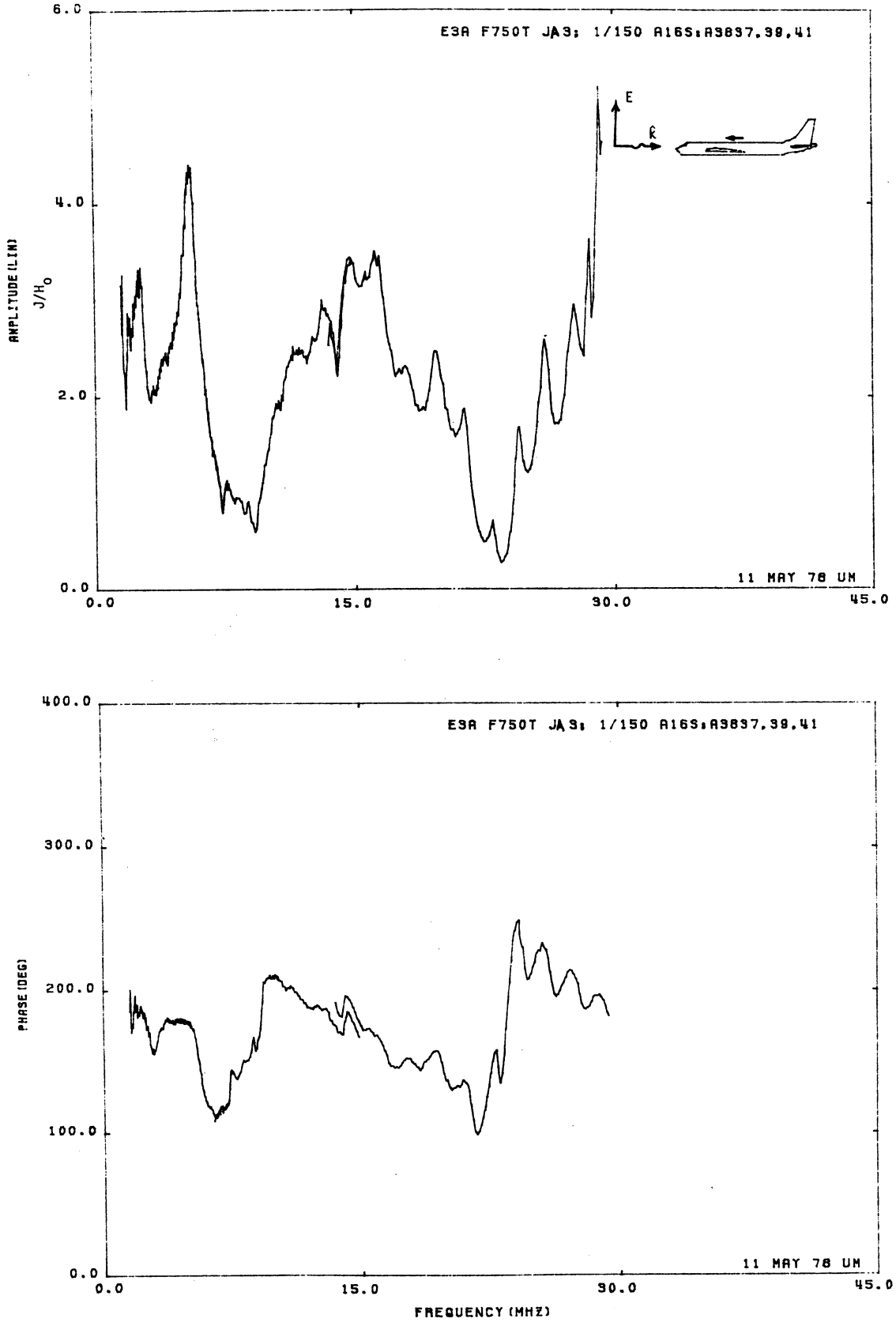

Figure 16S. Axial Current at STA:F750T, Excitation 3, 1/150 Model.

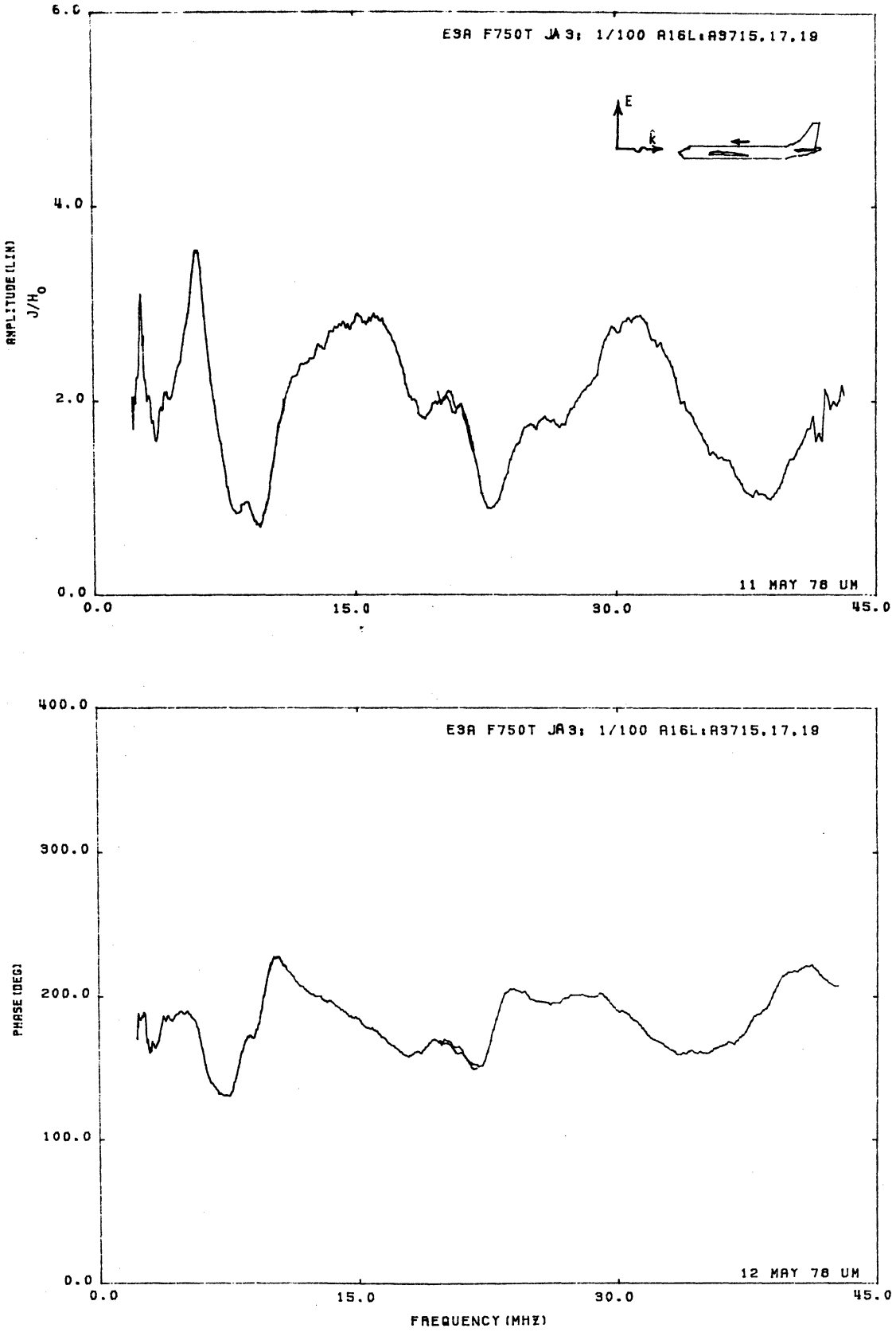

Figure 16L. Axial Current at STA:F750T, Excitation 3, 1/100 Model.

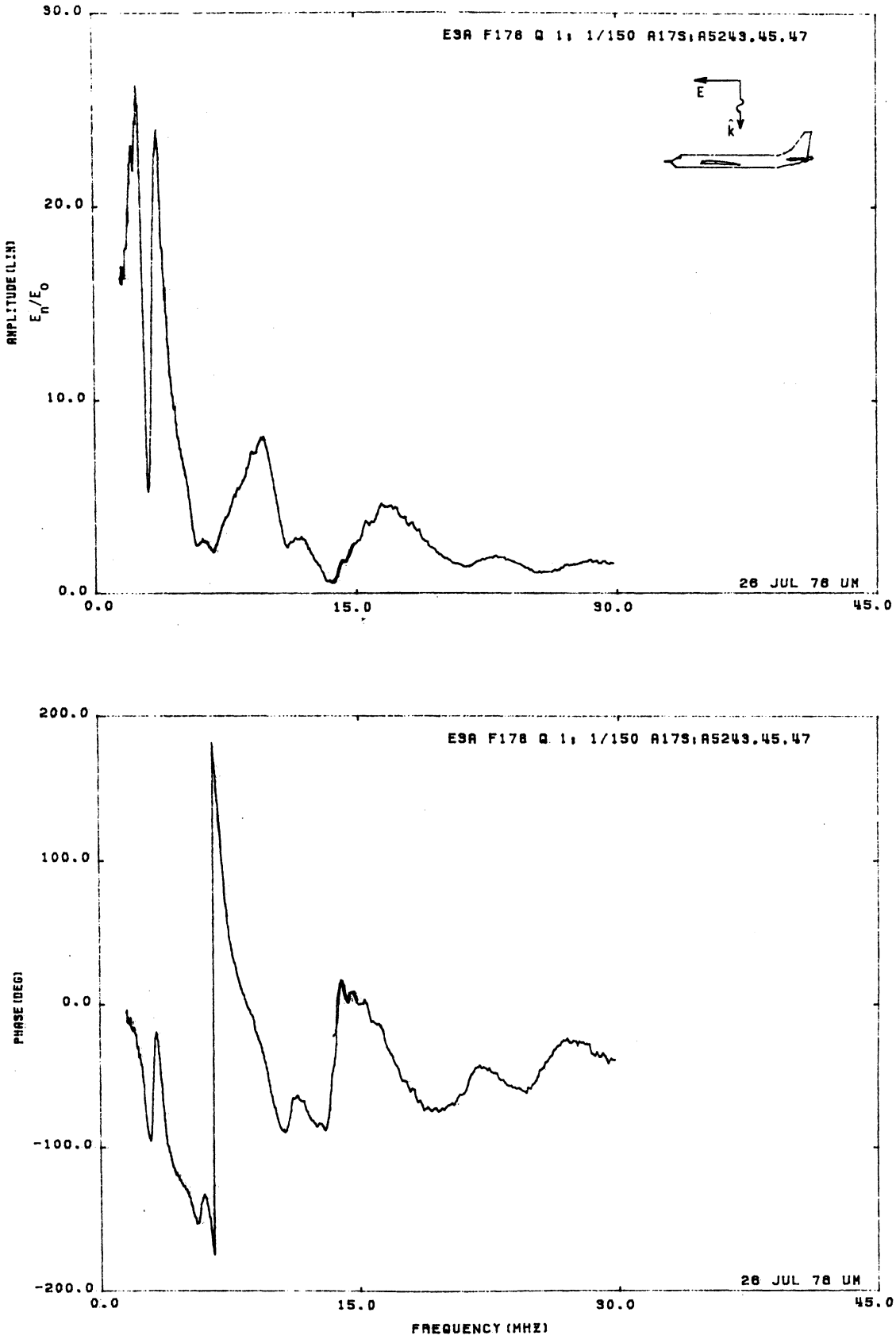

Figure 17S. Charge at STA:F178, Excitation 1, 1/150 Model.

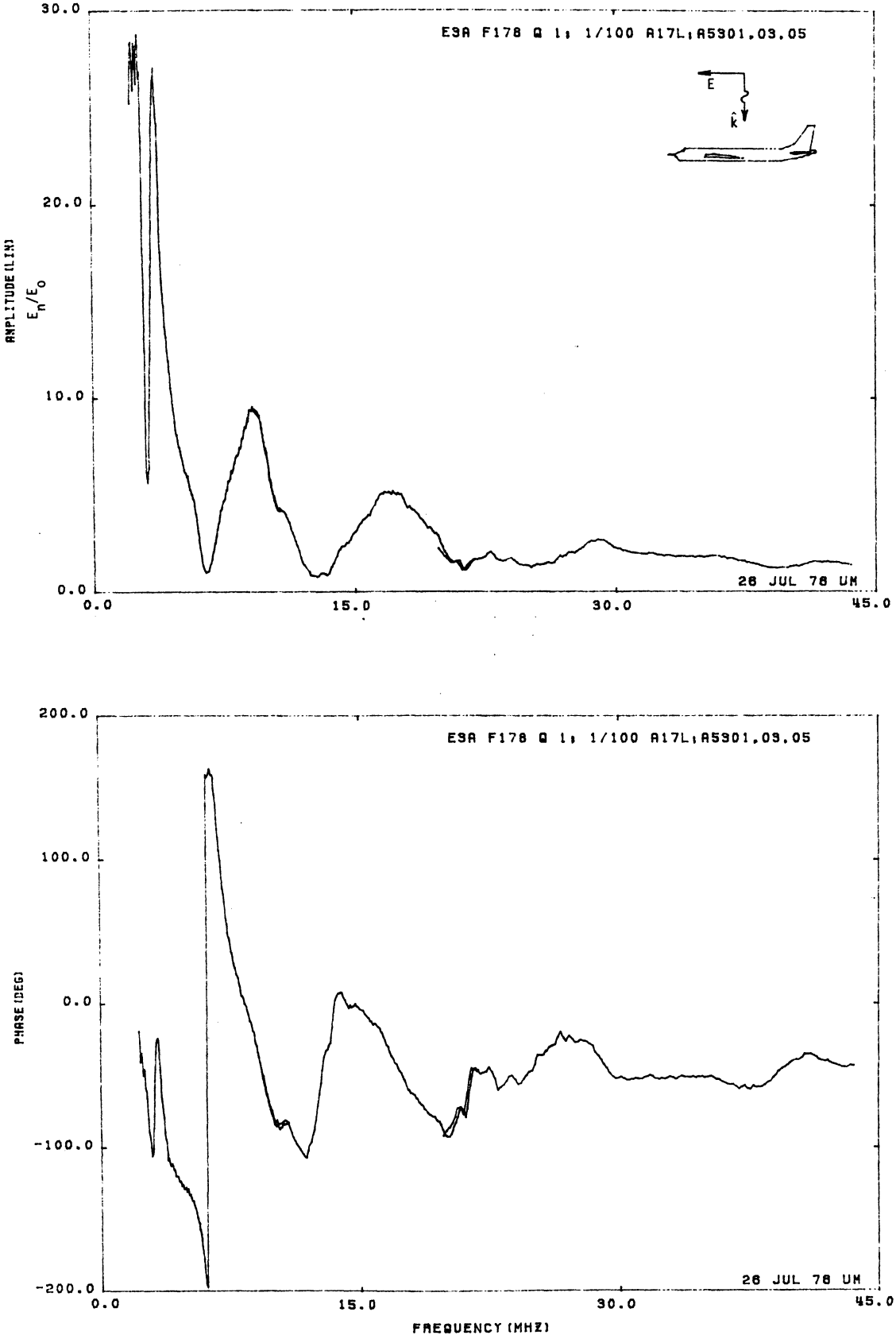

Figure 17L. Charge at STA:F178, Excitation 1, 1/100 Model.

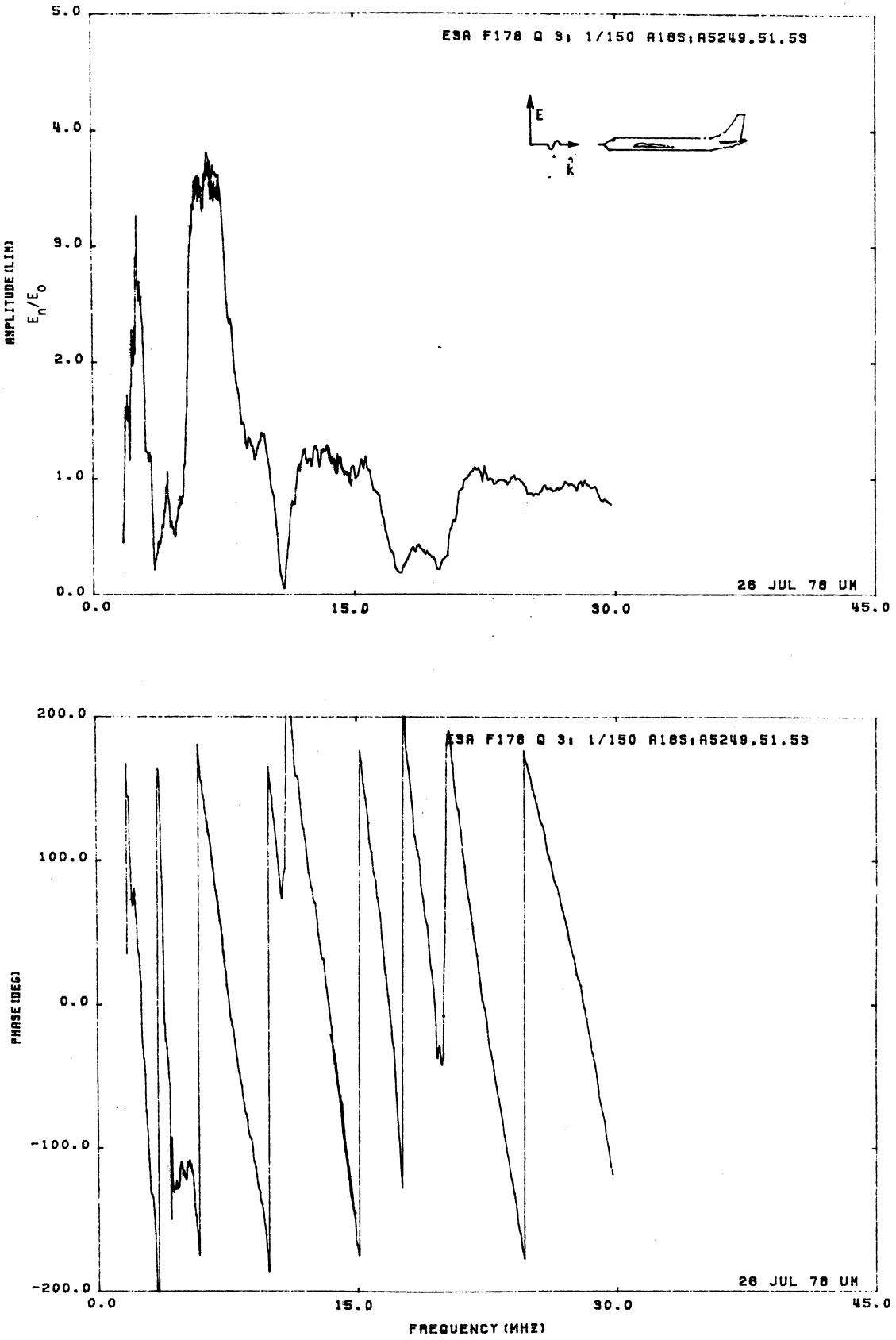

Figure 18S. Charge at STA:F178, Excitation 3, 1/150 Model.

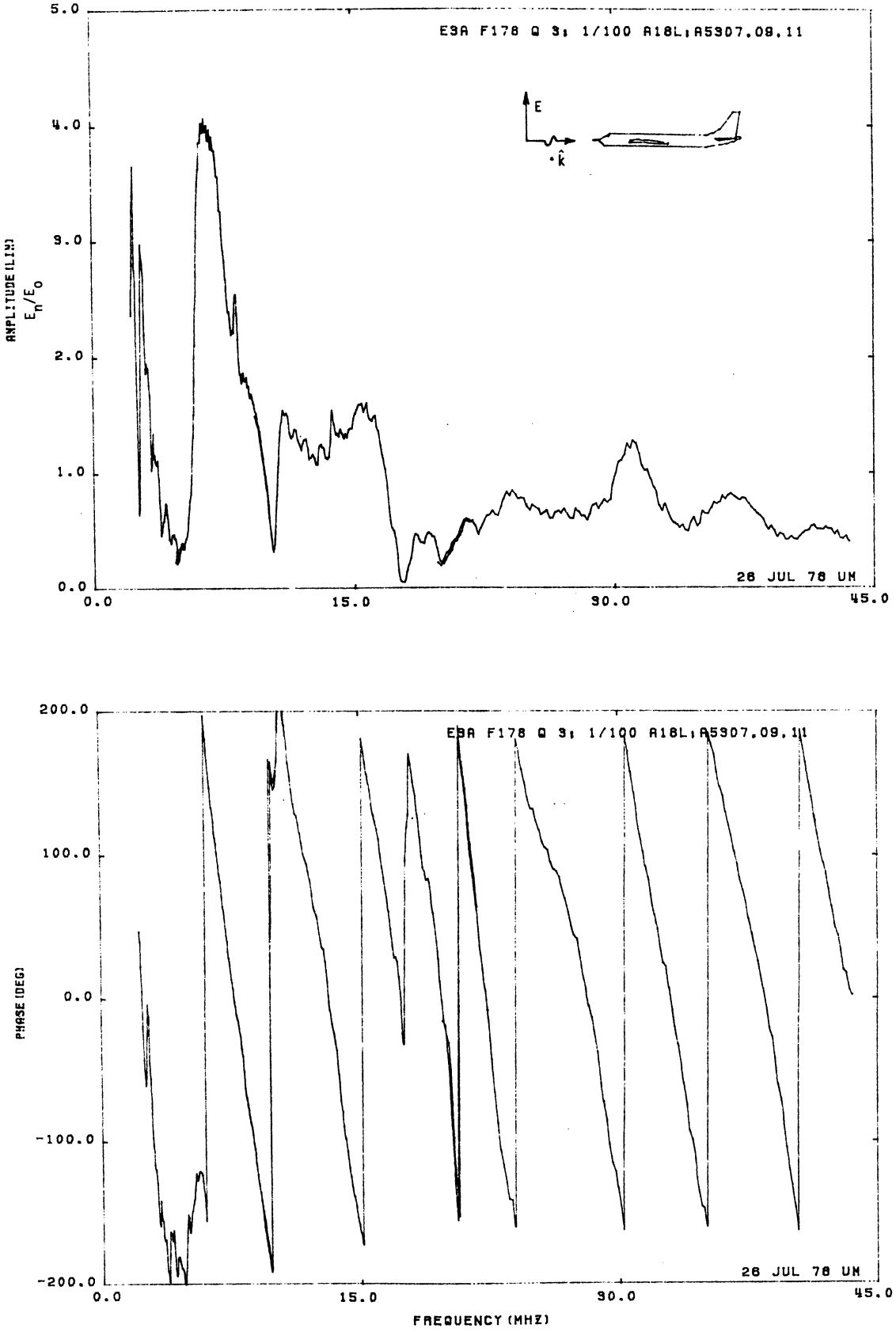

Figure 18L. Charge at STA:F178, Excitation 3, 1/100 Model.

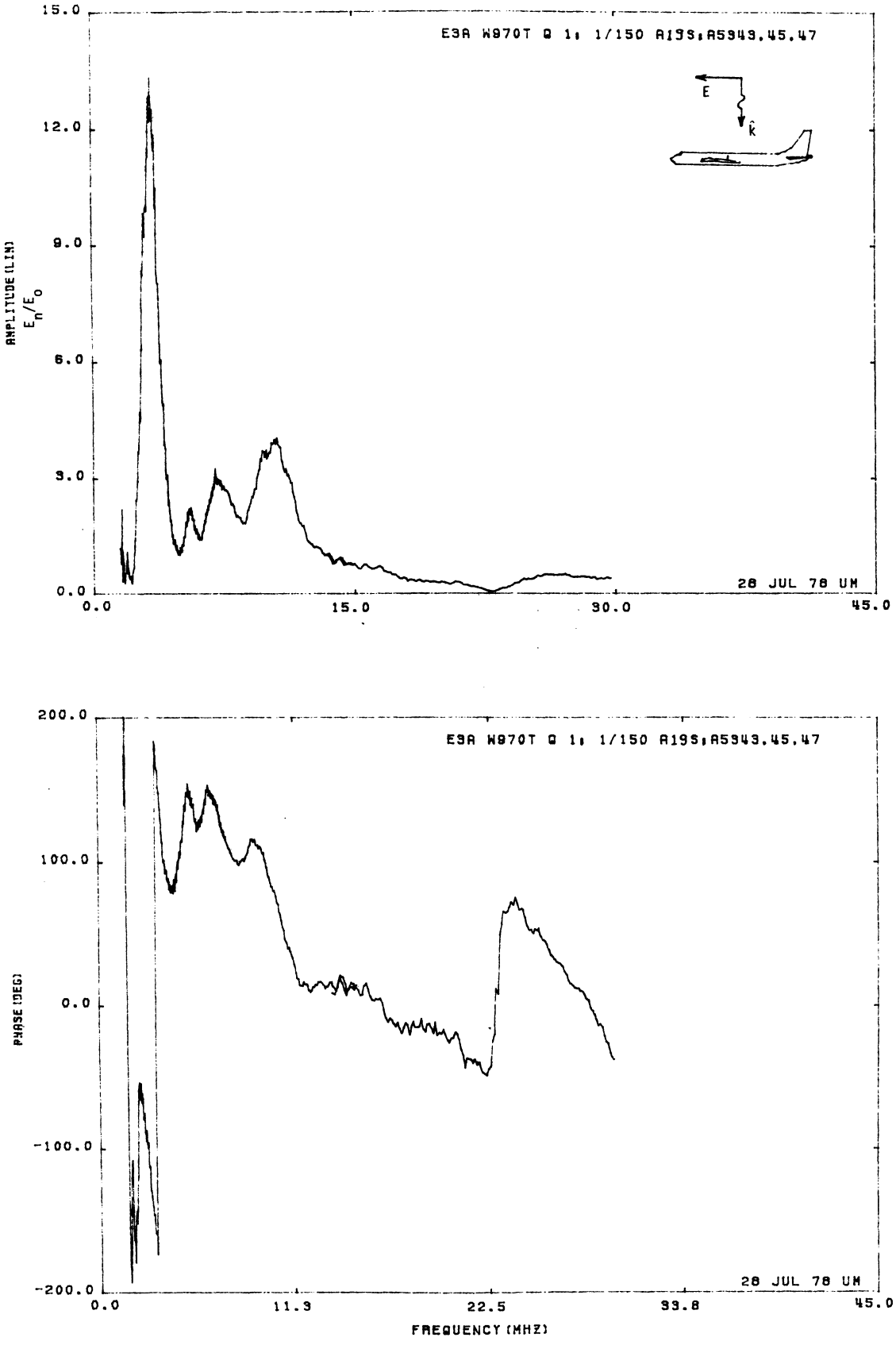

Figure 19S. Charge at STA:W970T, Excitation 1, 1/150 Model.

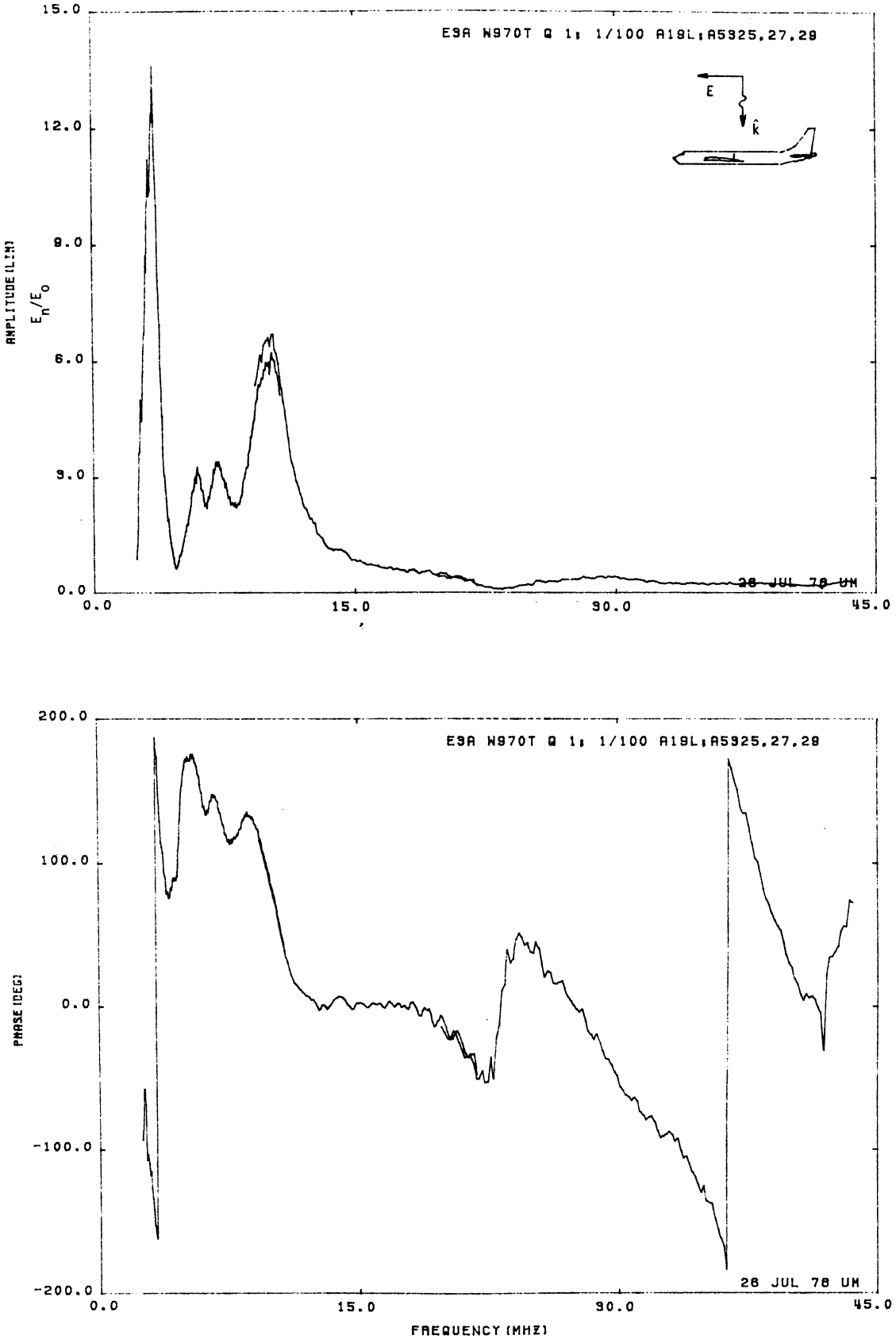

Figure 19L. Charge at STA:W970T, Excitation 1, 1/100 Model.

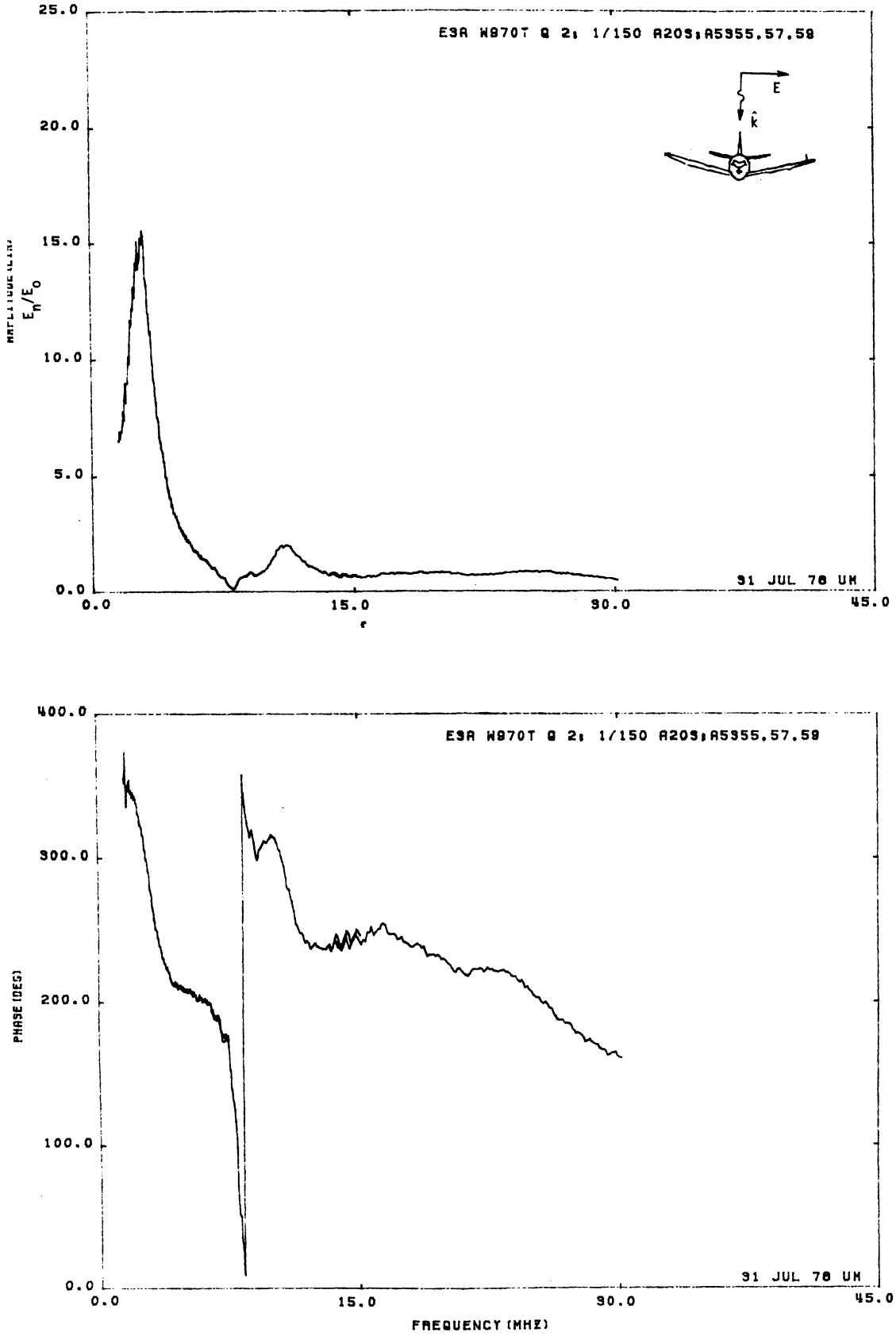

Figure 20S. Charge at STA:W970T, Excitation 2, 1/150 Model.

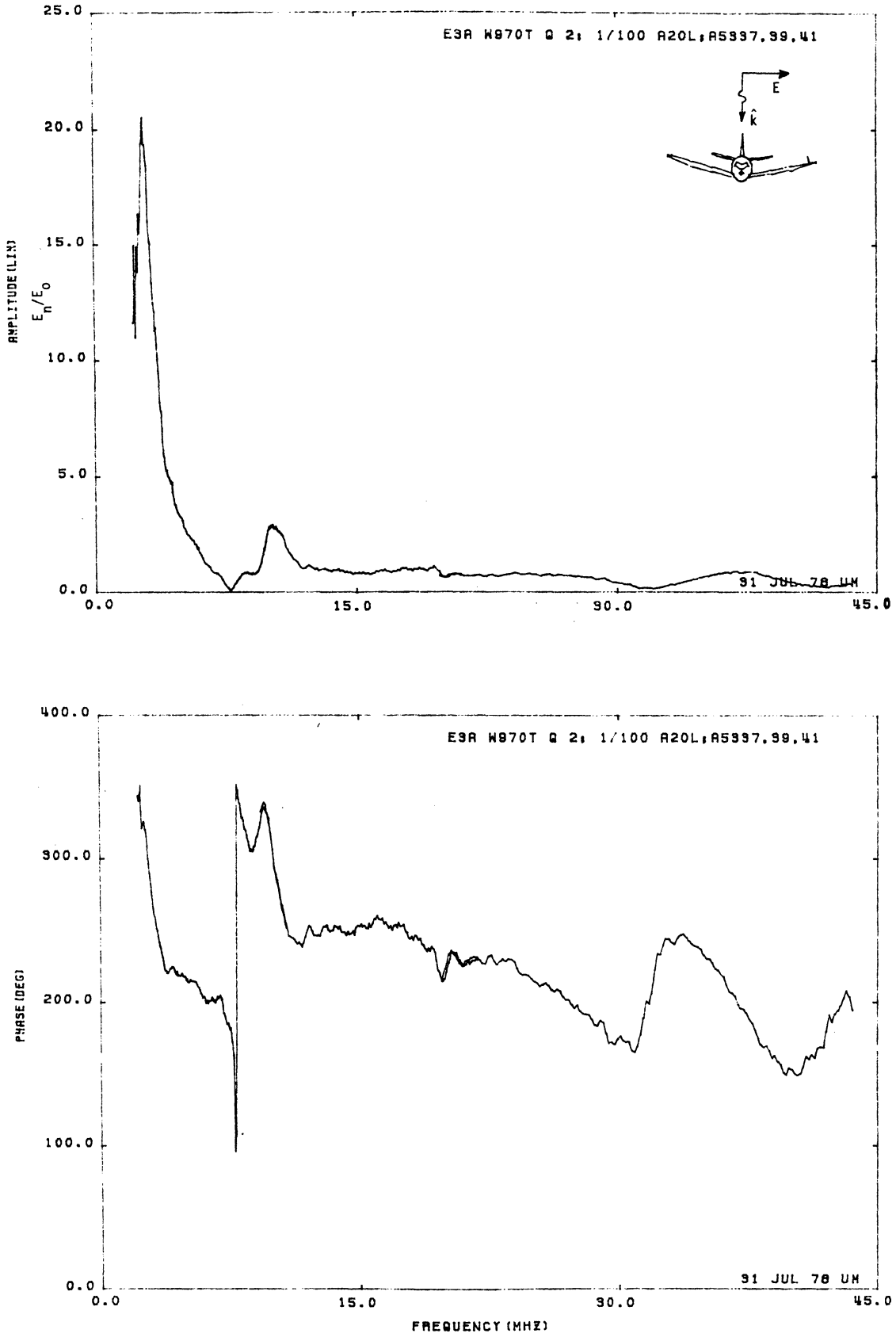

Figure 20L. Charge at STA:W970T, Excitation 2, 1/100 Model.

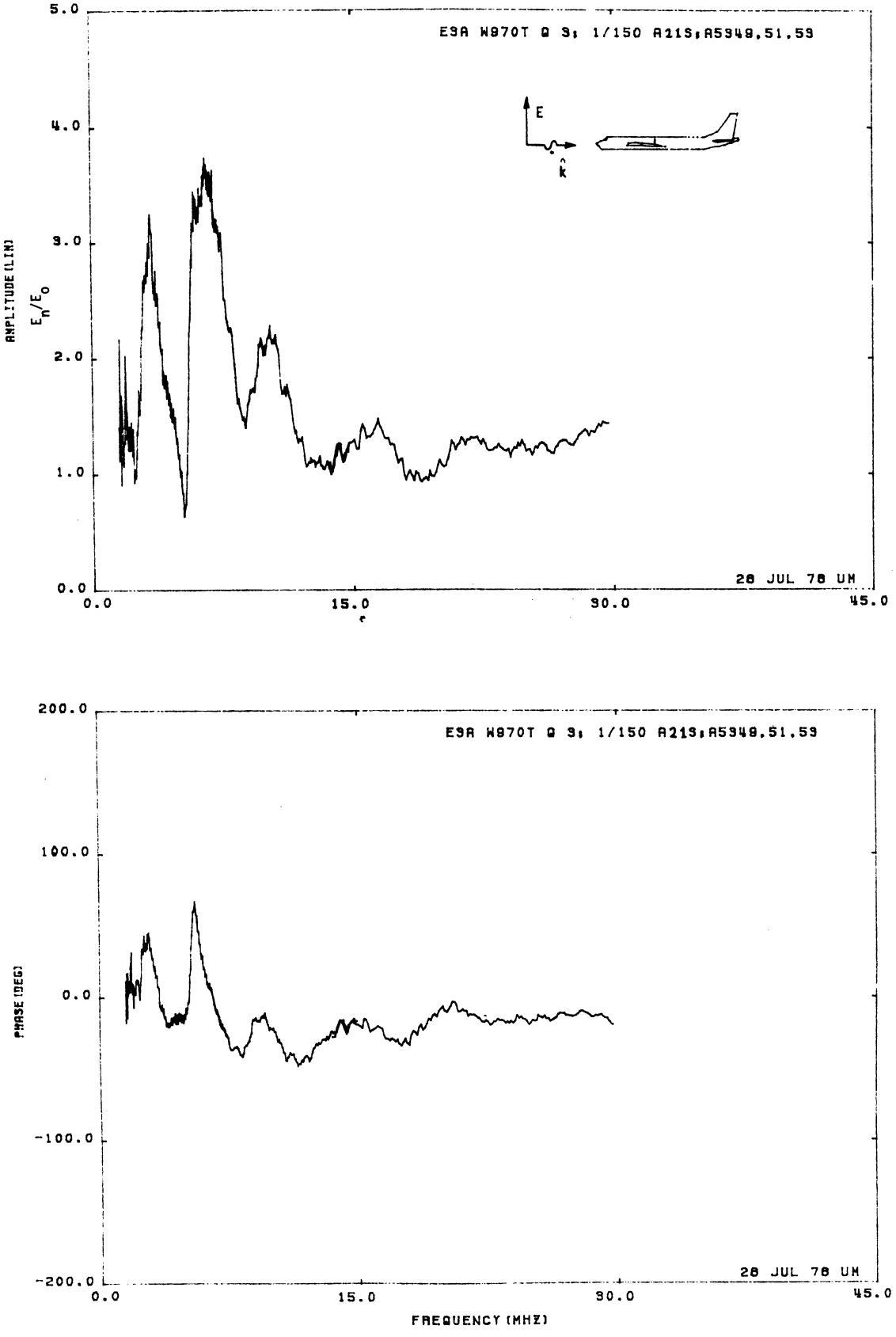

Figure 21S. Charge at STA:W970T, Excitation 3, 1/150 Model.

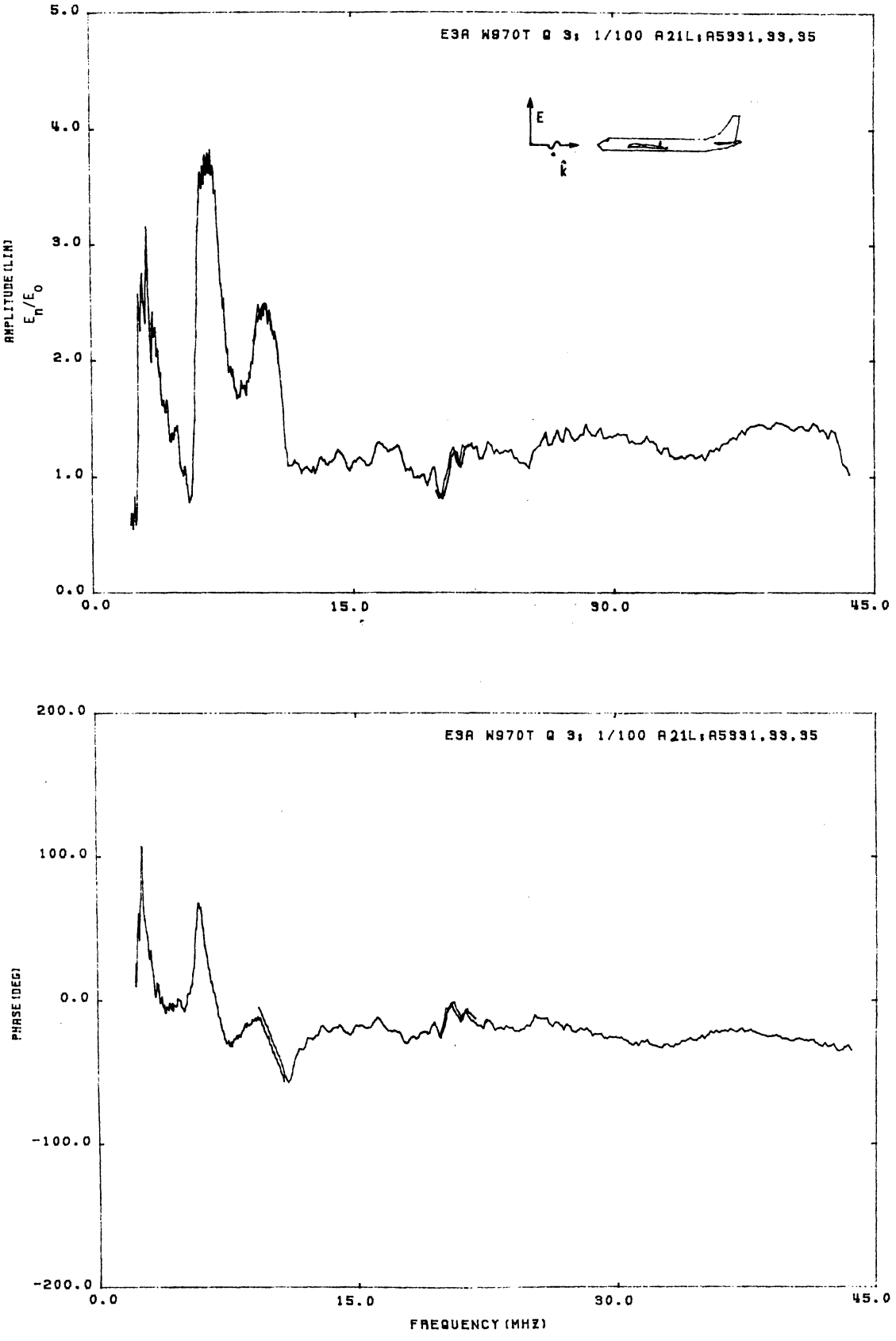

Figure 21L. Charge at STA:W970T, Excitation 3, 1/100 Model.

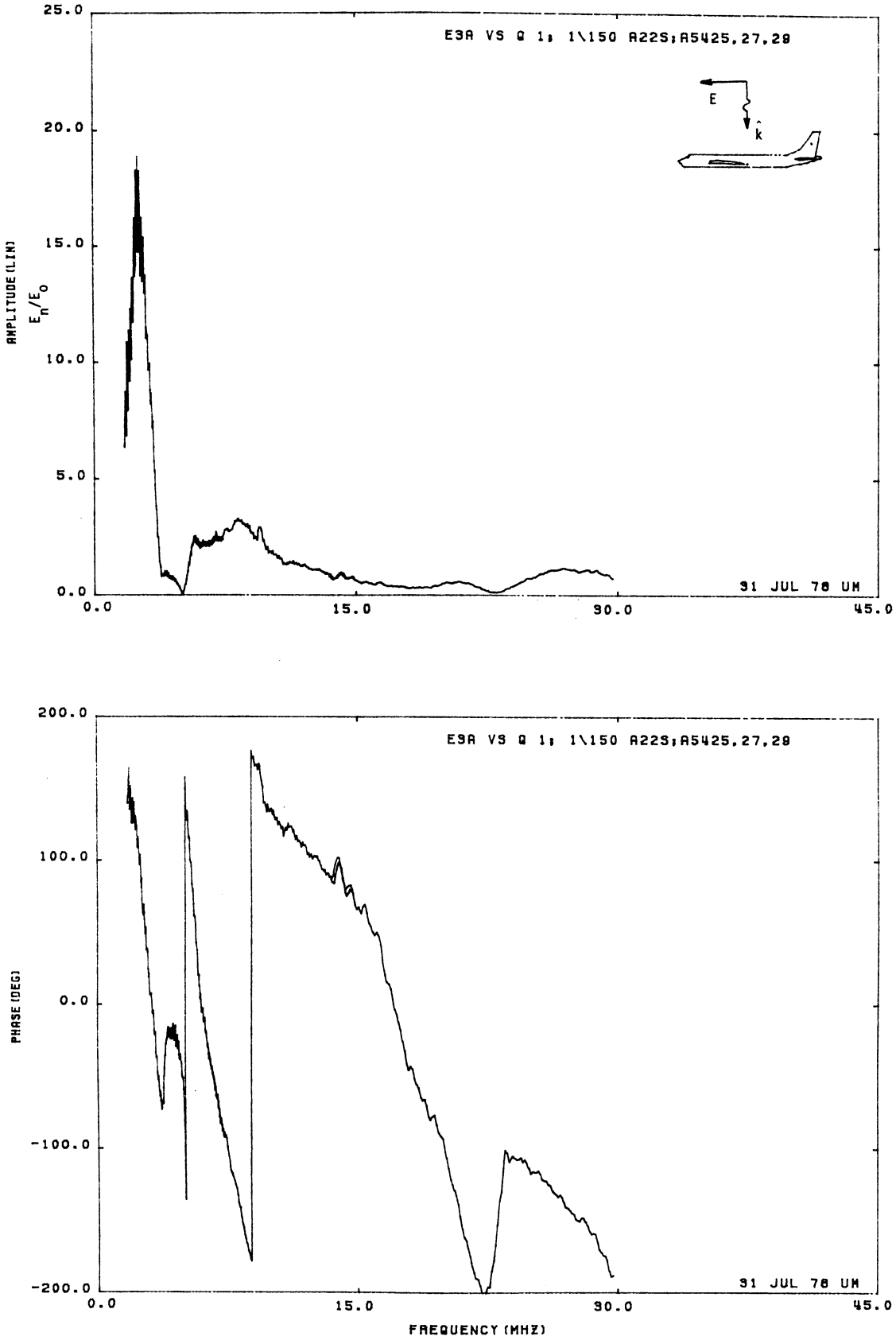

Figure 22S. Charge at STA:VS, Excitation 1, 1/150 Model.

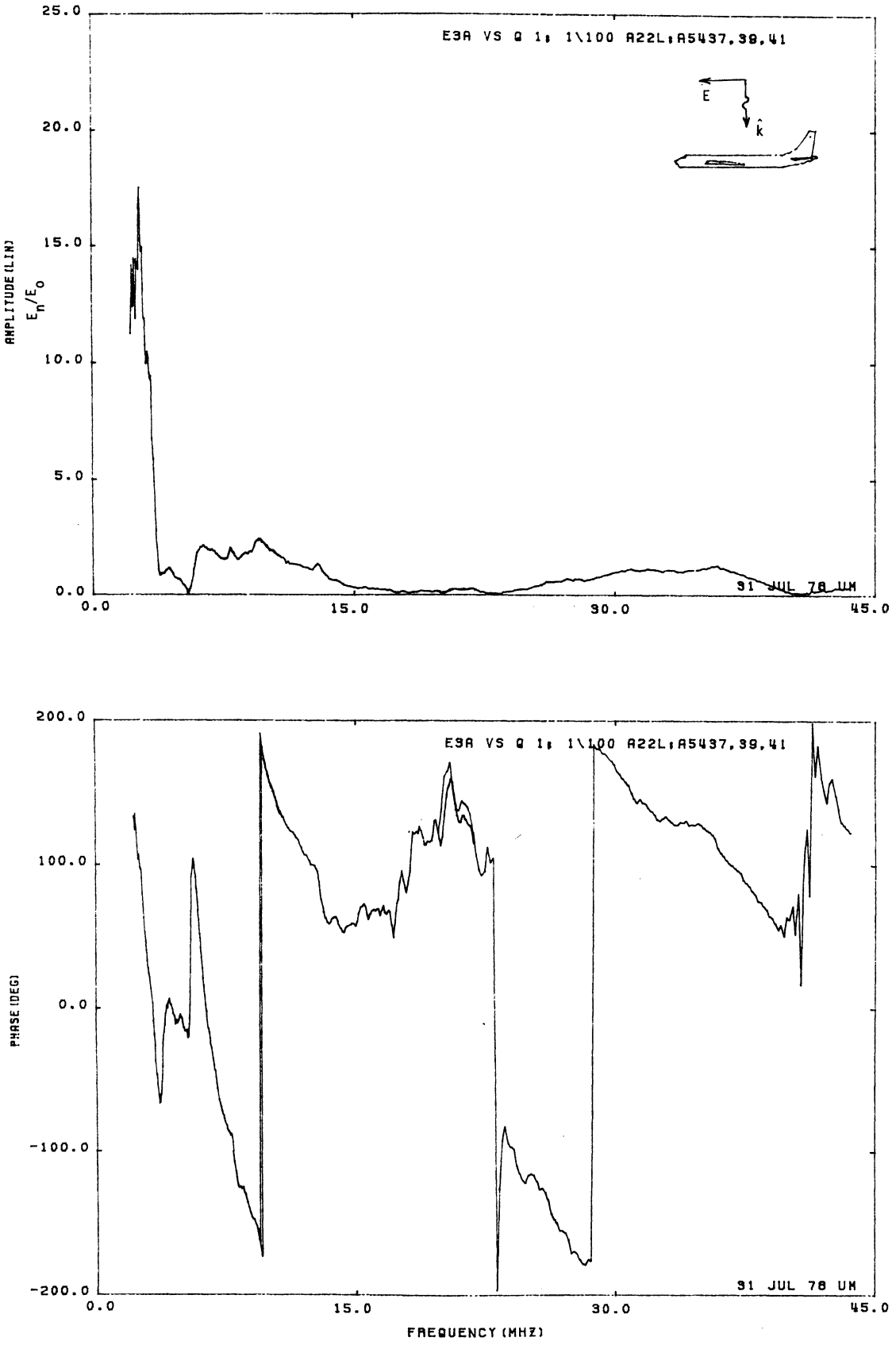

Figure 22L. Charge at STA:VS, Excitation 1, 1/100 Model.

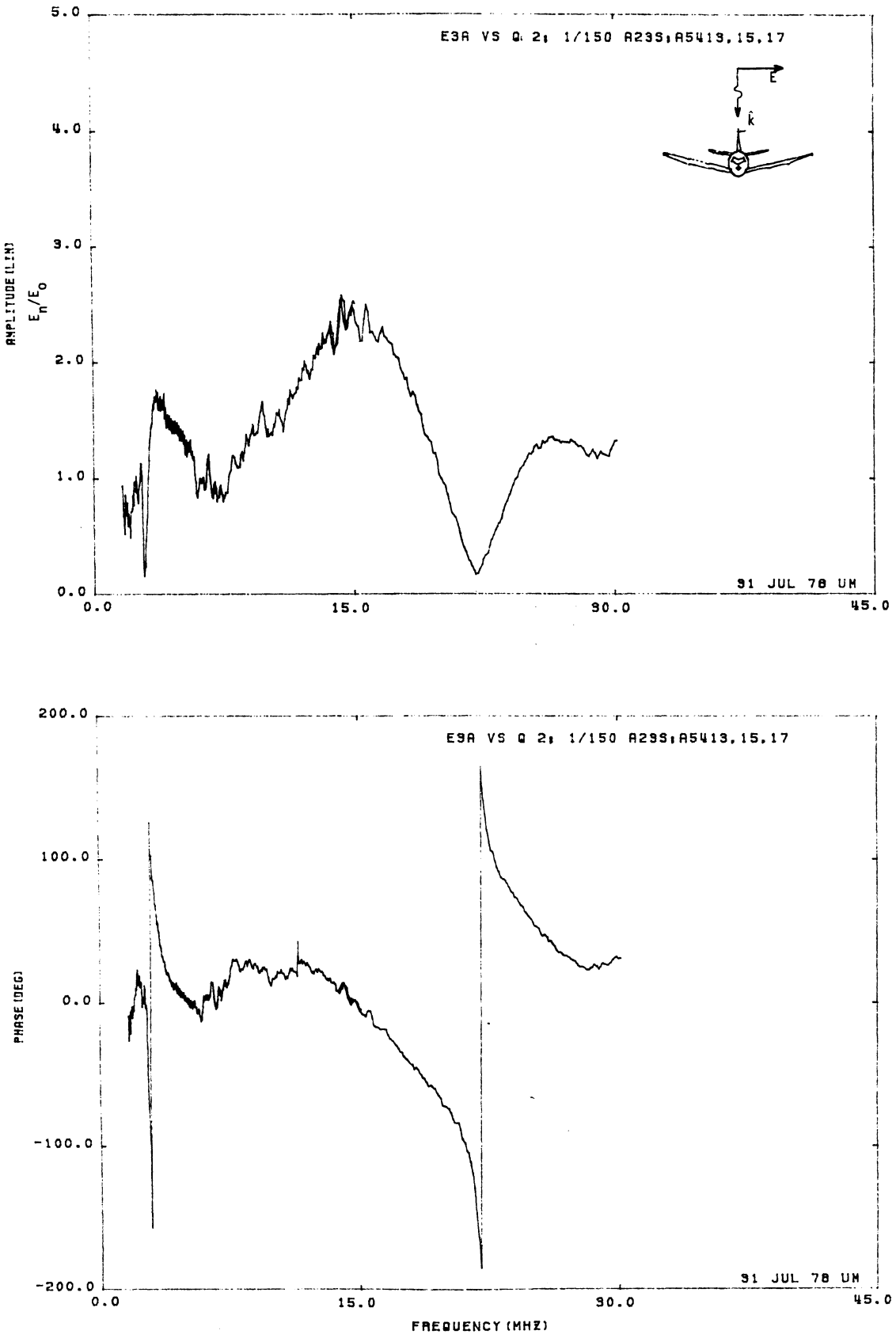

Figure 23S. Charge at STA:VS, Excitation 2, 1/150 Model.

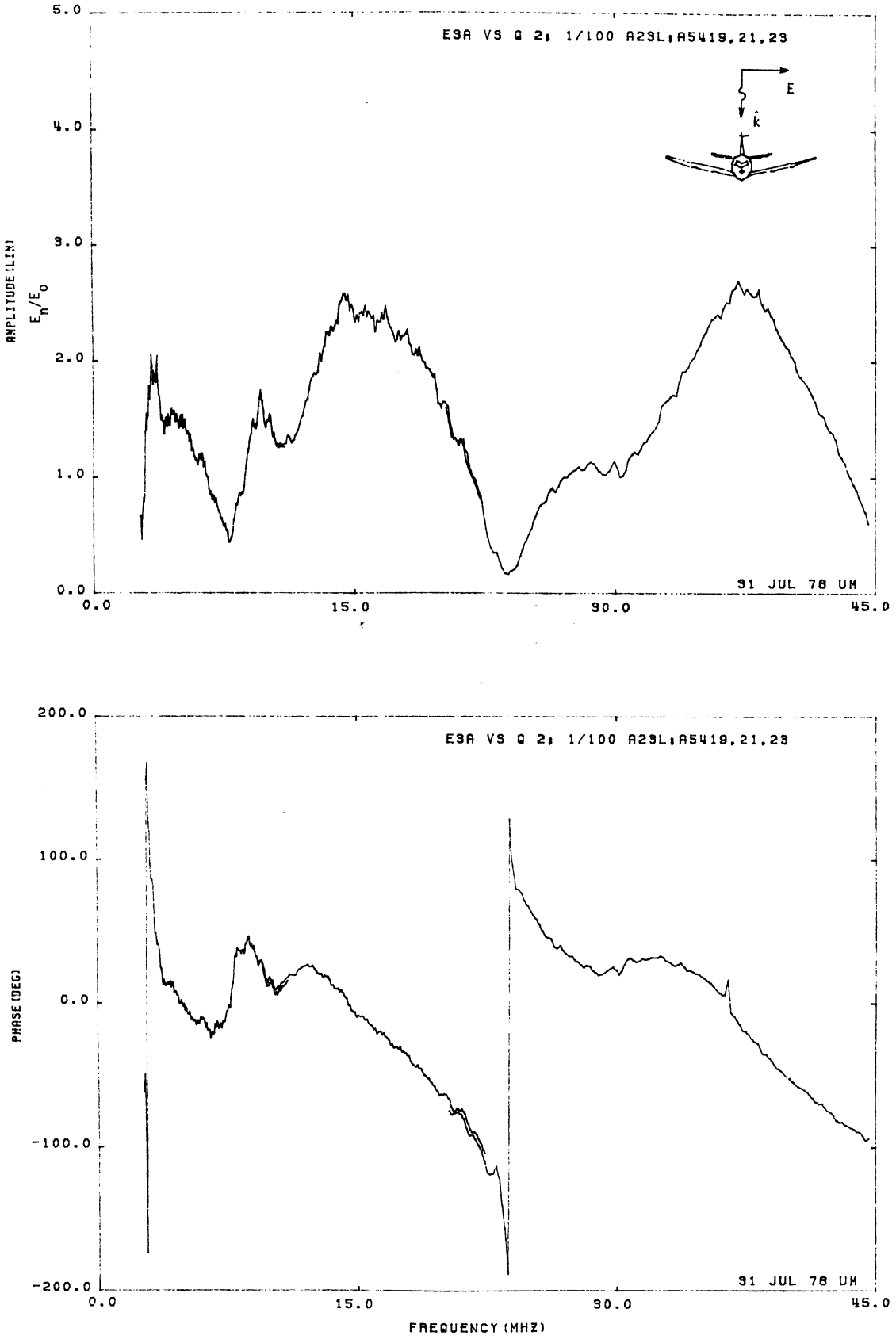

Figure 23L. Charge at STA:VS, Excitation 2, 1/100 Model.

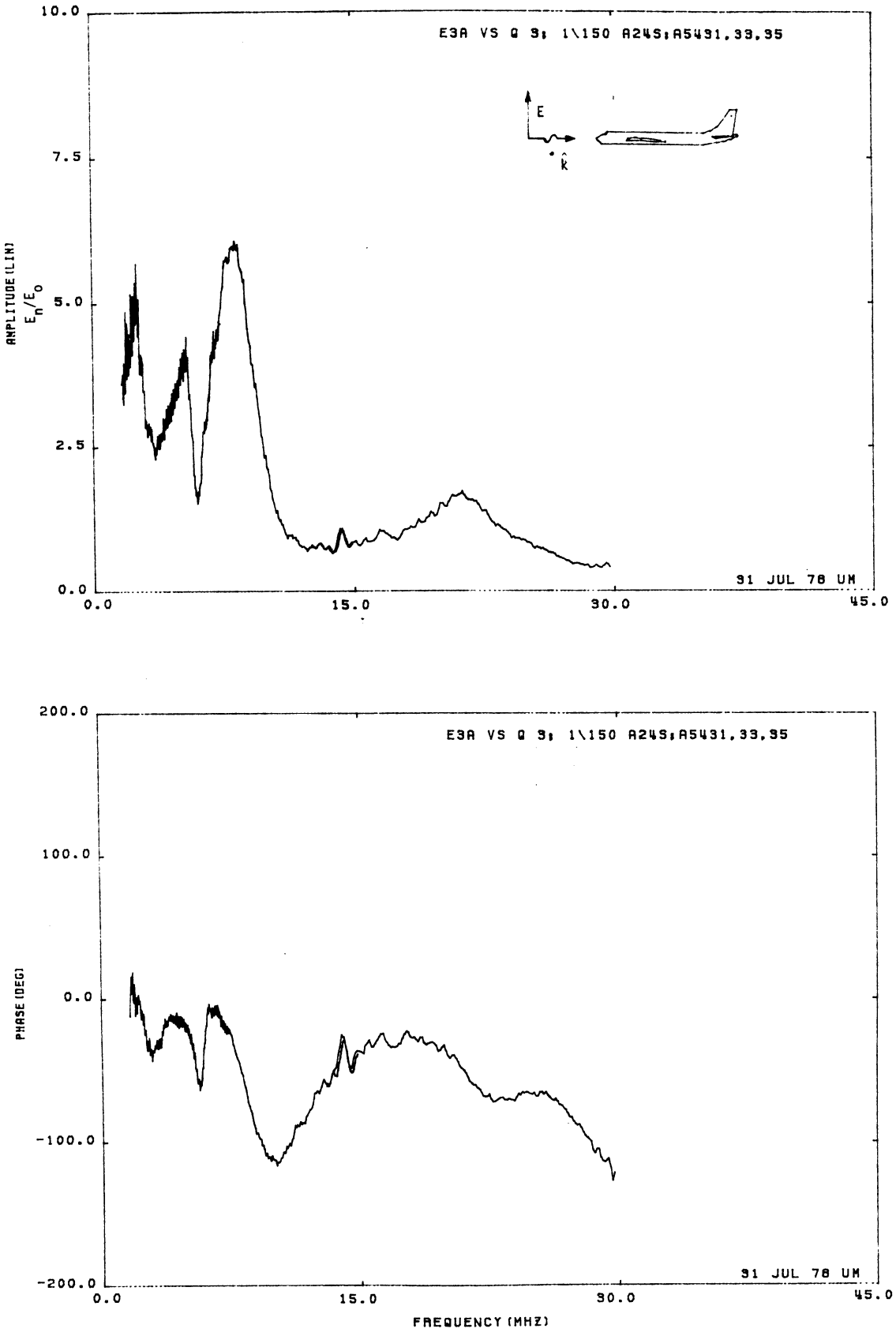

Figure 24S. Charge at STA:VS, Excitation 3, 1/150 Model.

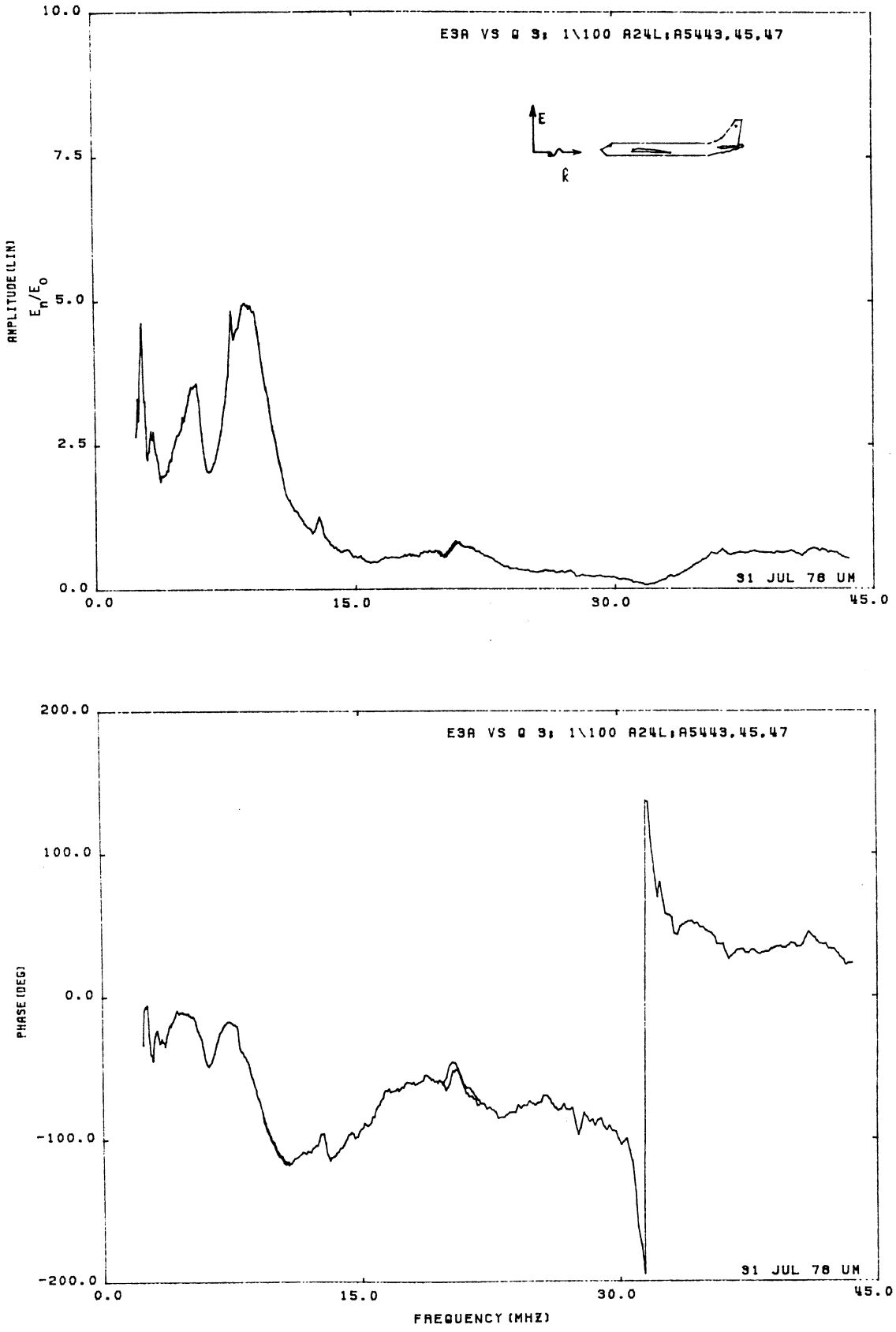

Figure 24L. Charge at STA:VS, Excitation 3, 1/100 Model.

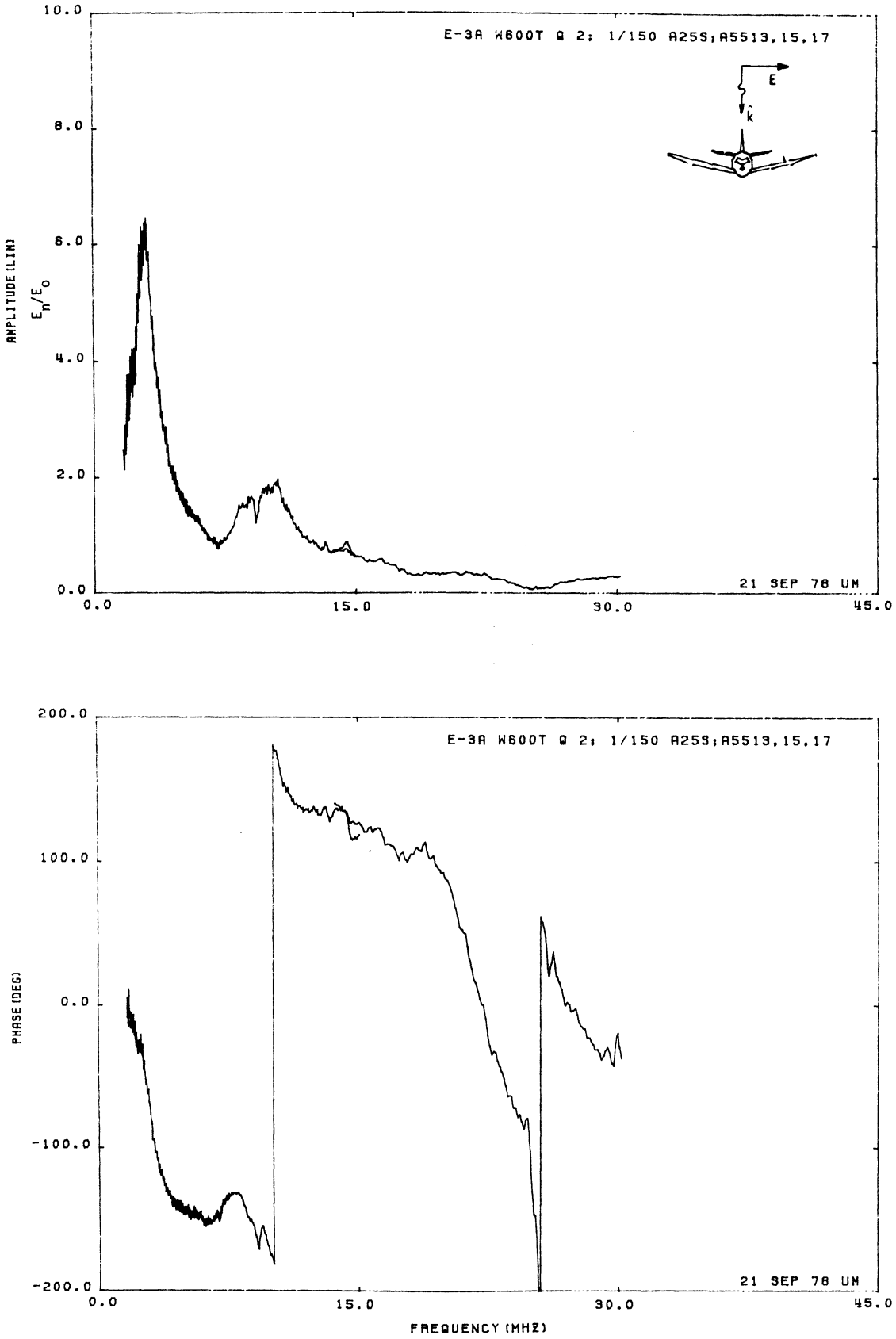

Figure 25S. Charge at STA:W600T, Excitation 2, 1/150 Model.

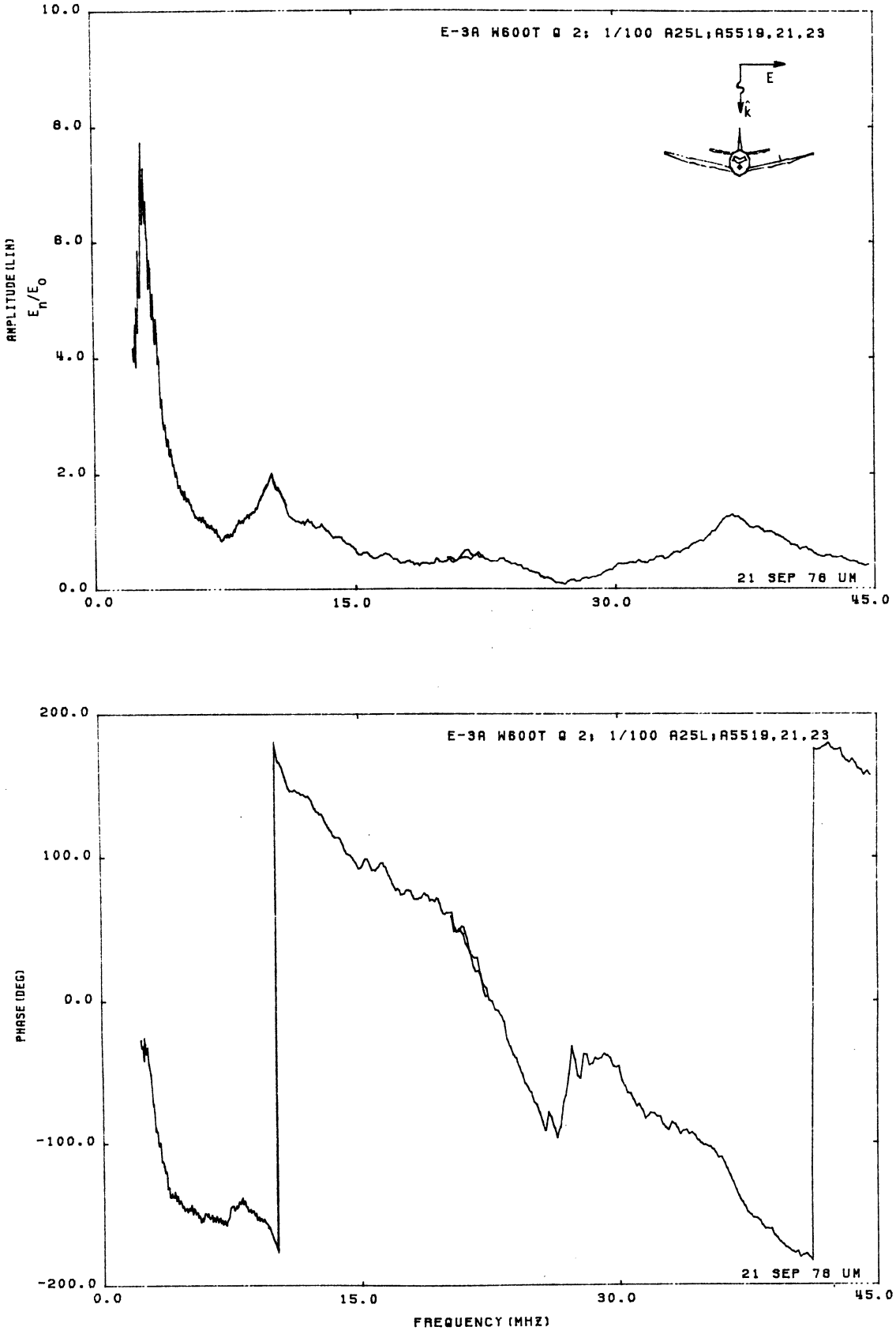

Figure 25L. Charge at STA:W600T, Excitation 2, 1/100 Model.

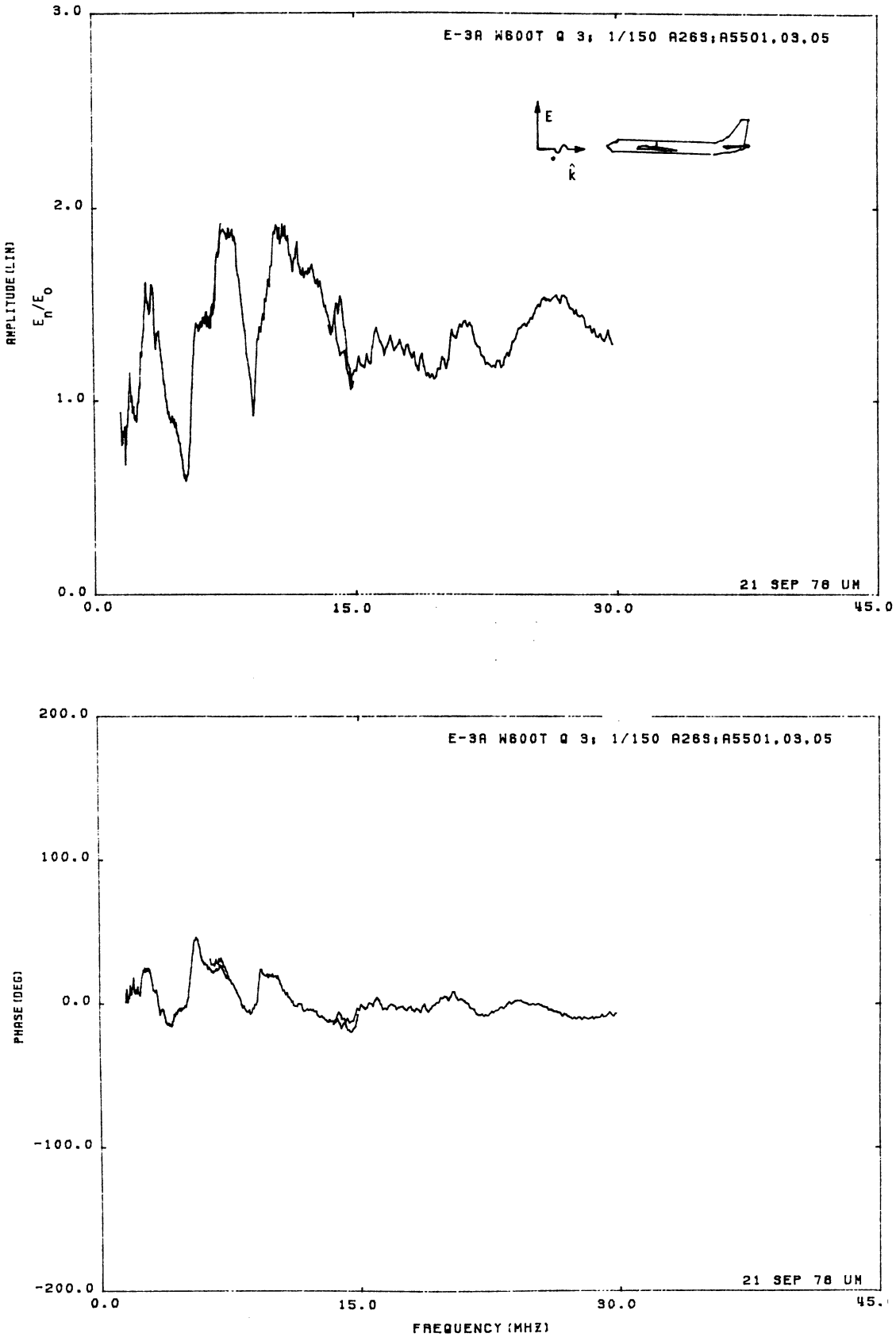

Figure 26S. Charge at STA:W600T, Excitation 3, 1/150 Model.

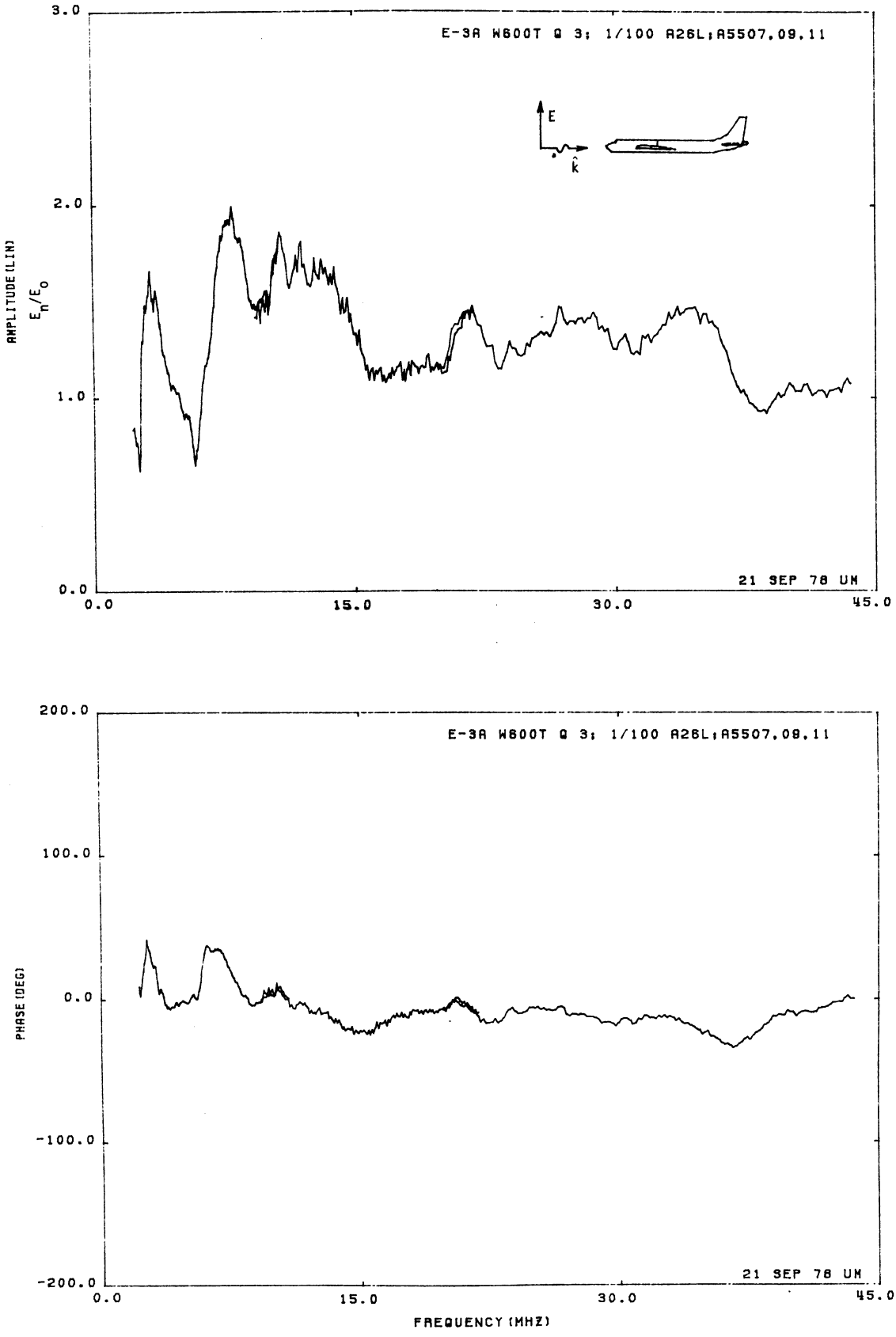

Figure 26L. Charge at STA:W600T, Excitation 3, 1/100 Model.

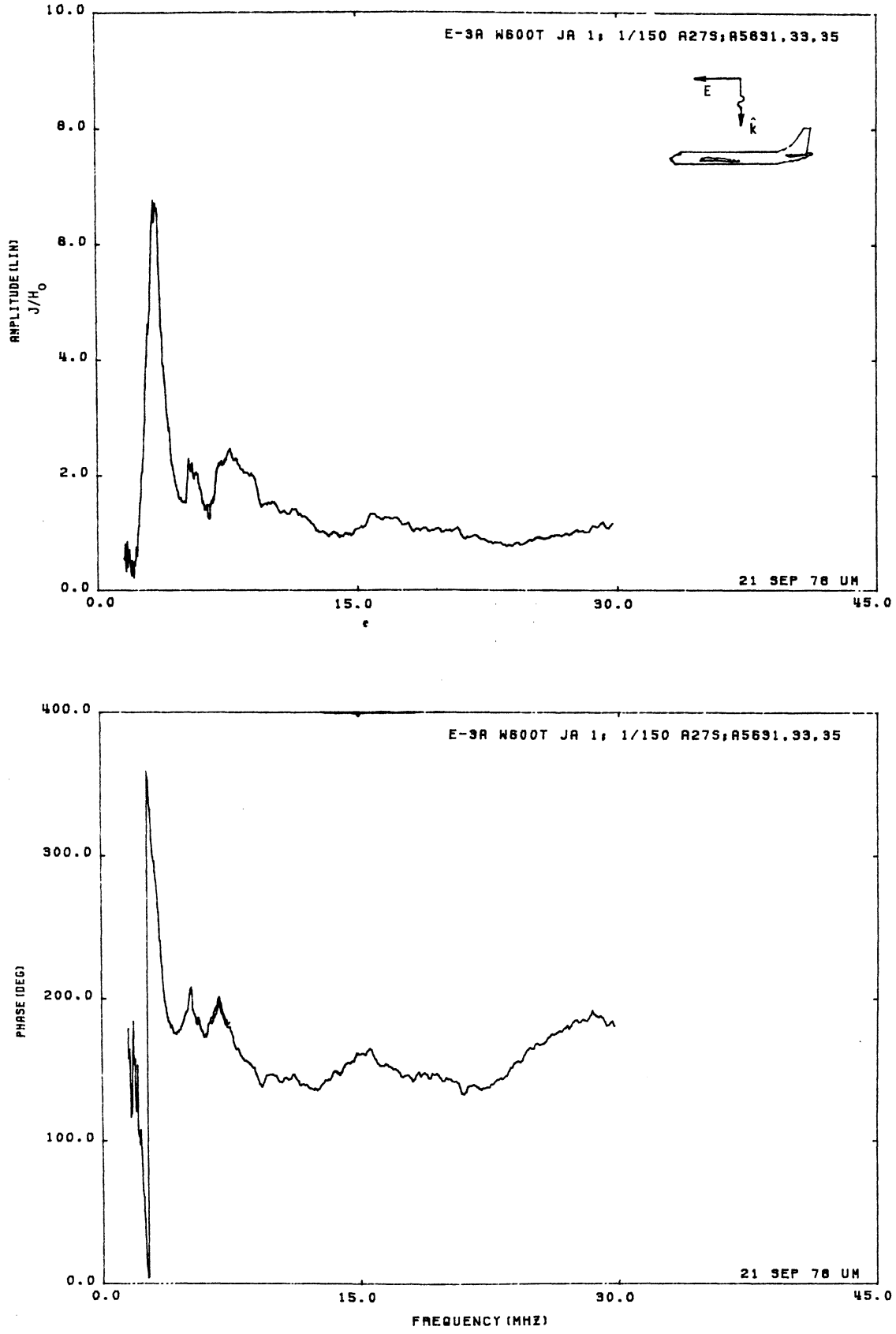

Figure 27S. Axial Current at STA:W600T, Excitation 1, 1/150 Model.

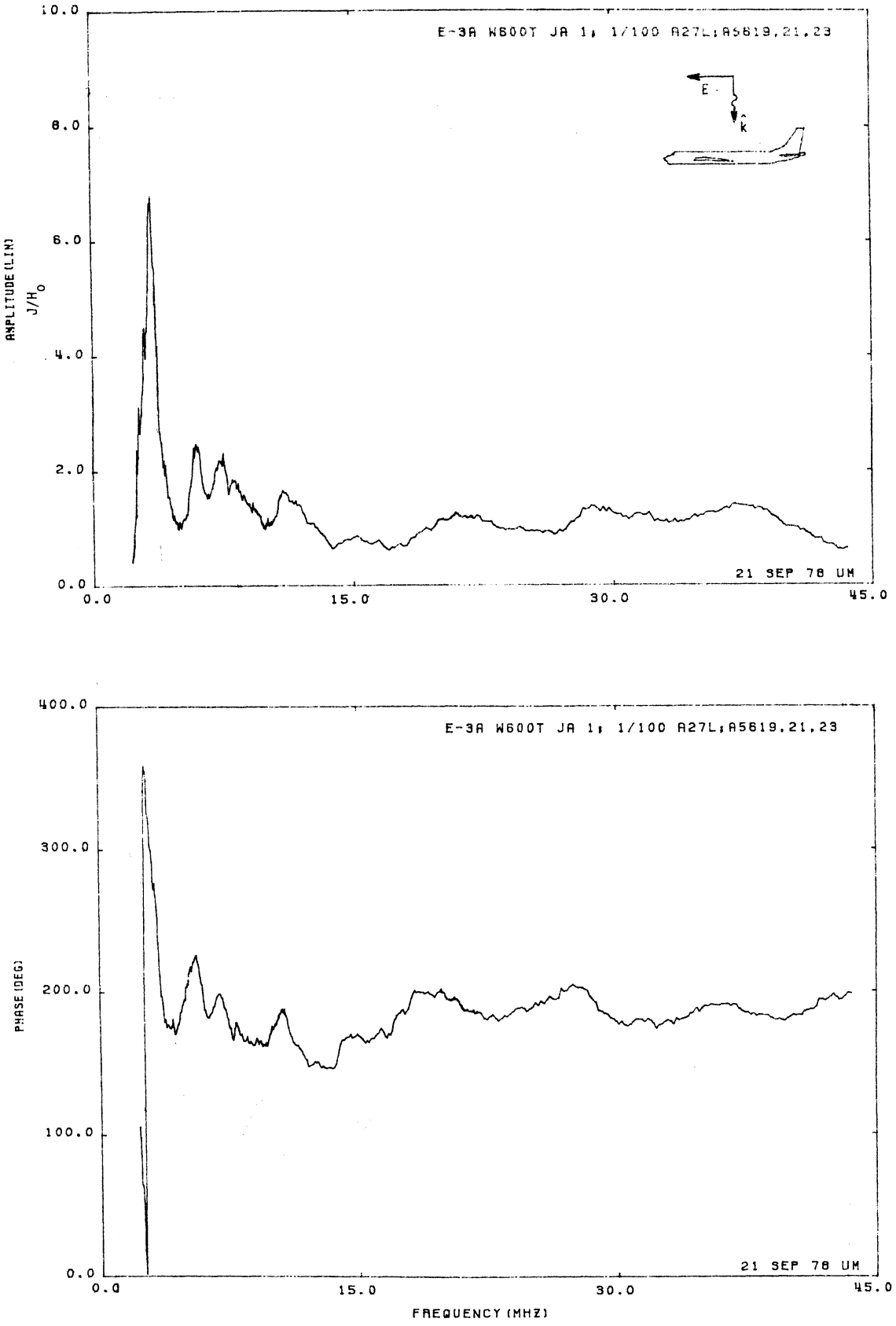

Figure 27L. Axial Current at STA:W600T, Excitation 1, 1/100 Model.

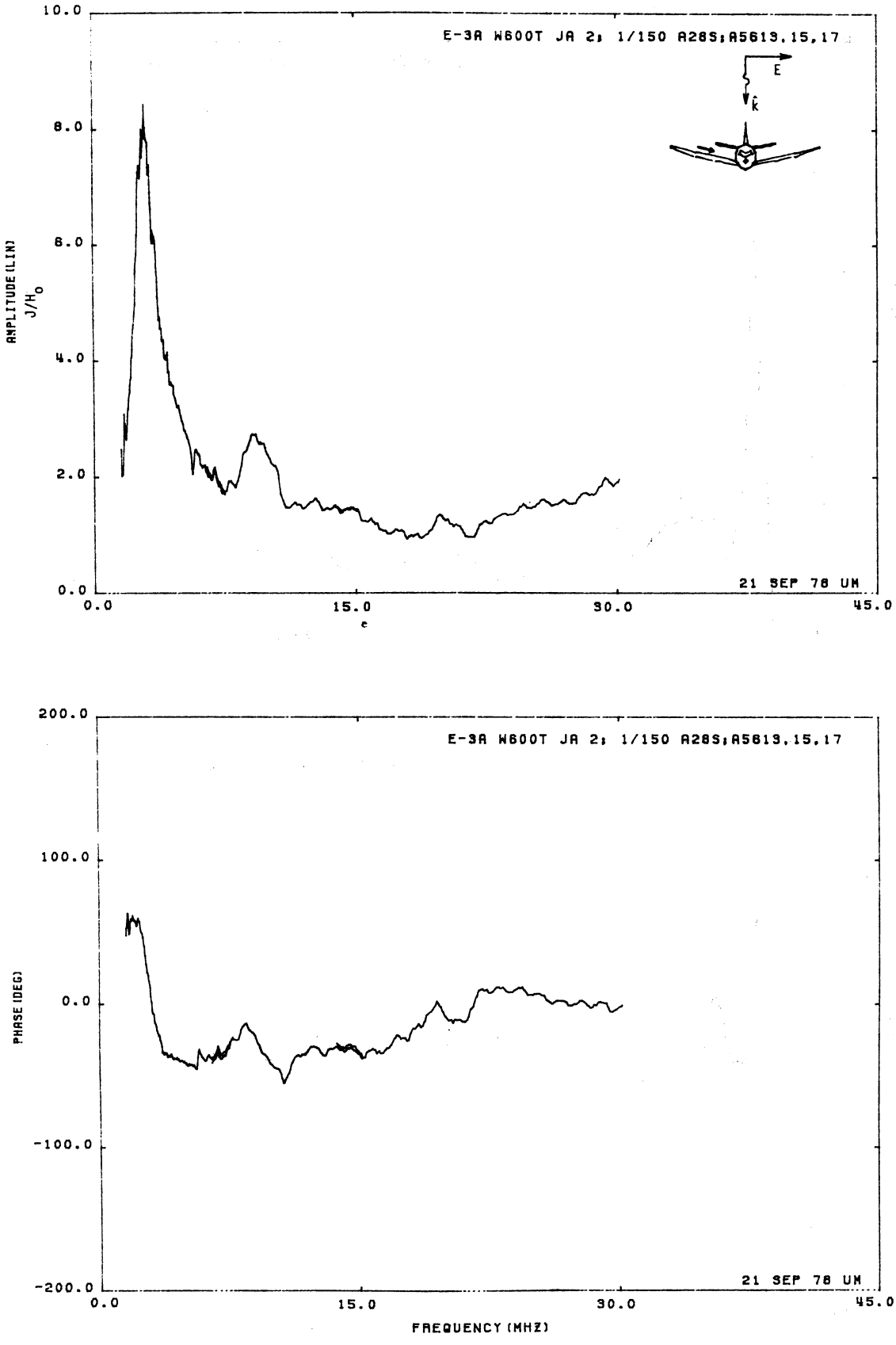

Figure 28S. Axial Current at STA:W600T, Excitation 2, 1/150 Model.

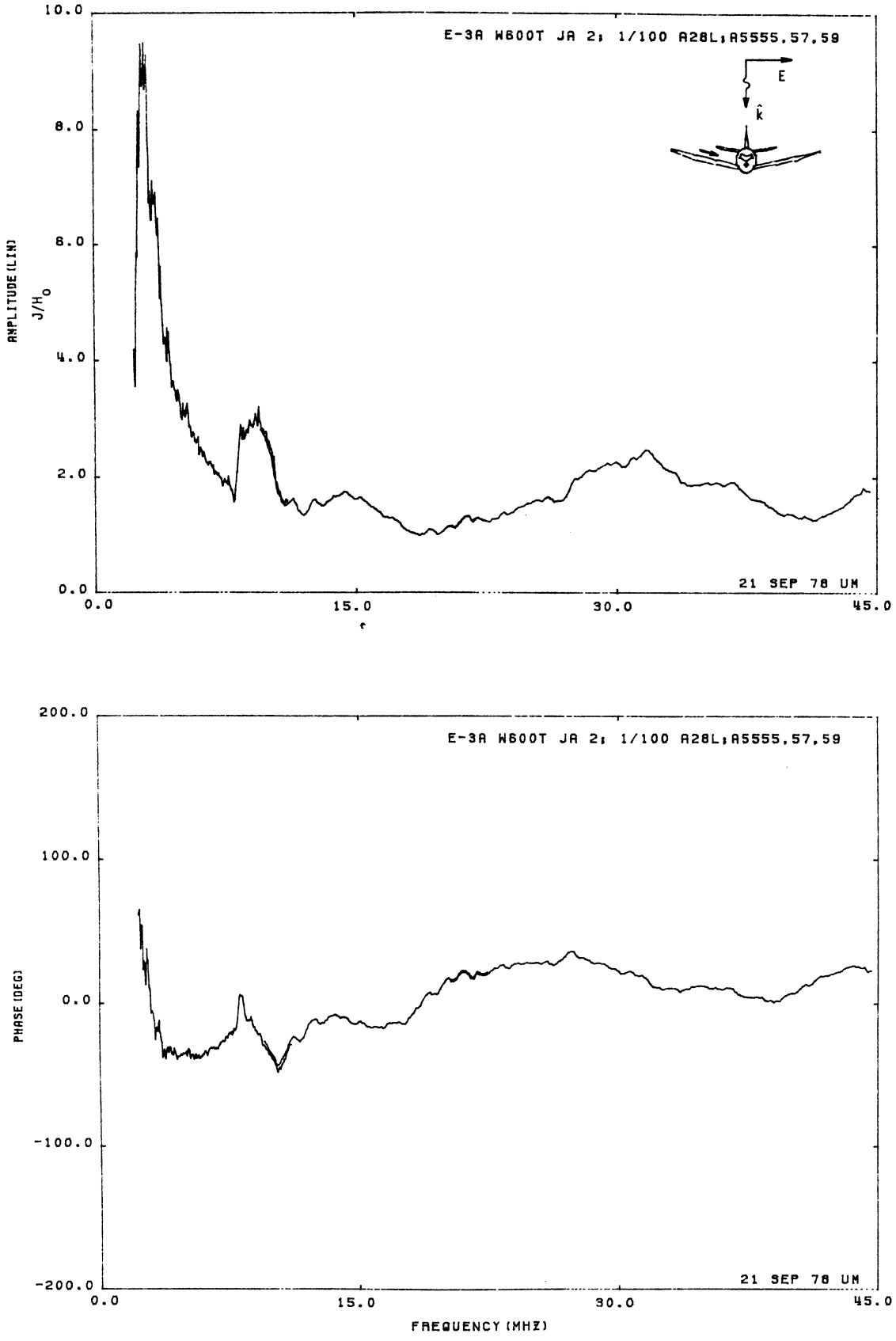

Figure 28L. Axial Current at STA:W600T, Excitation 2, 1/100 Model.

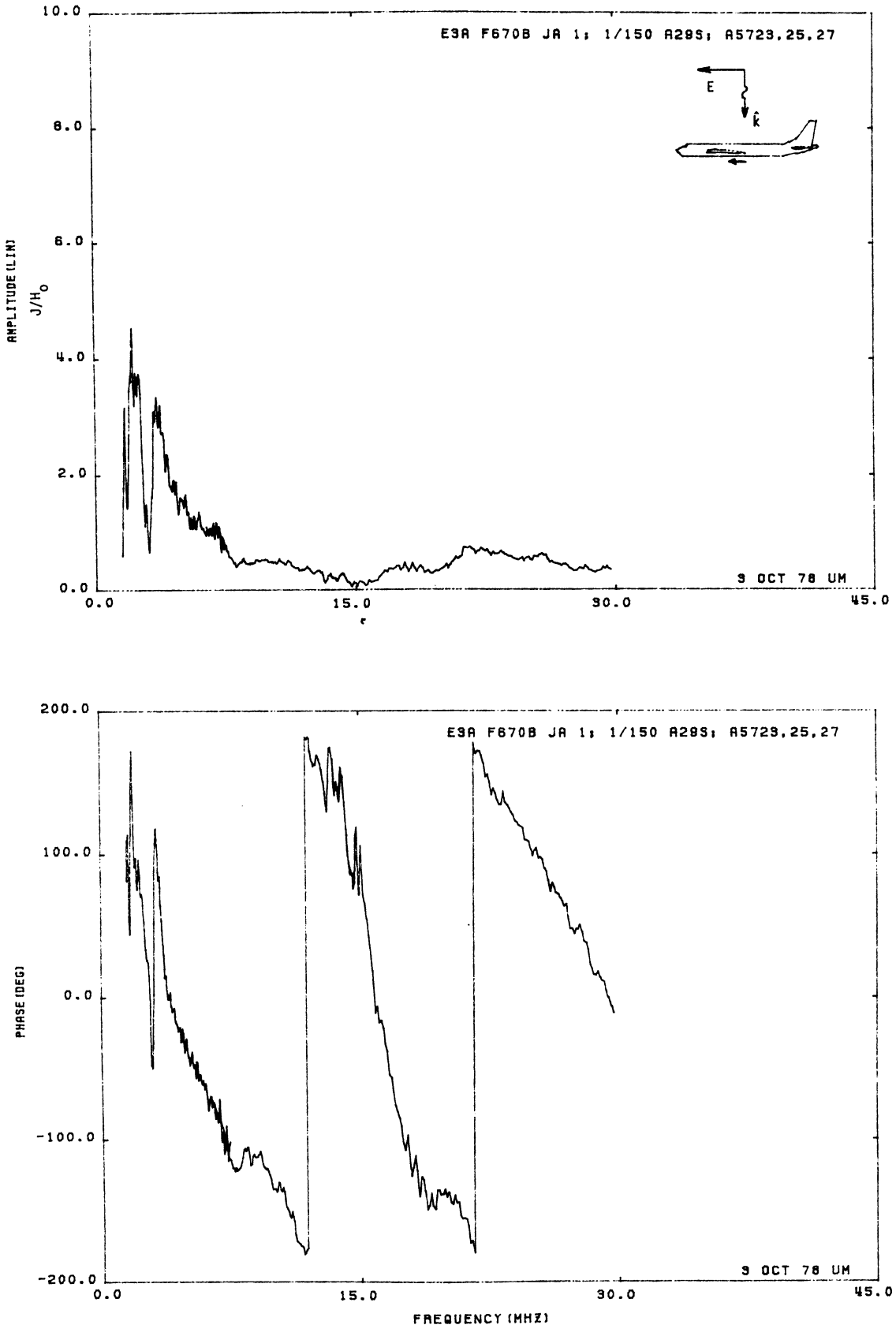

Figure 29S. Axial Current at STA:F670B, Excitation 1, 1/150 Model.

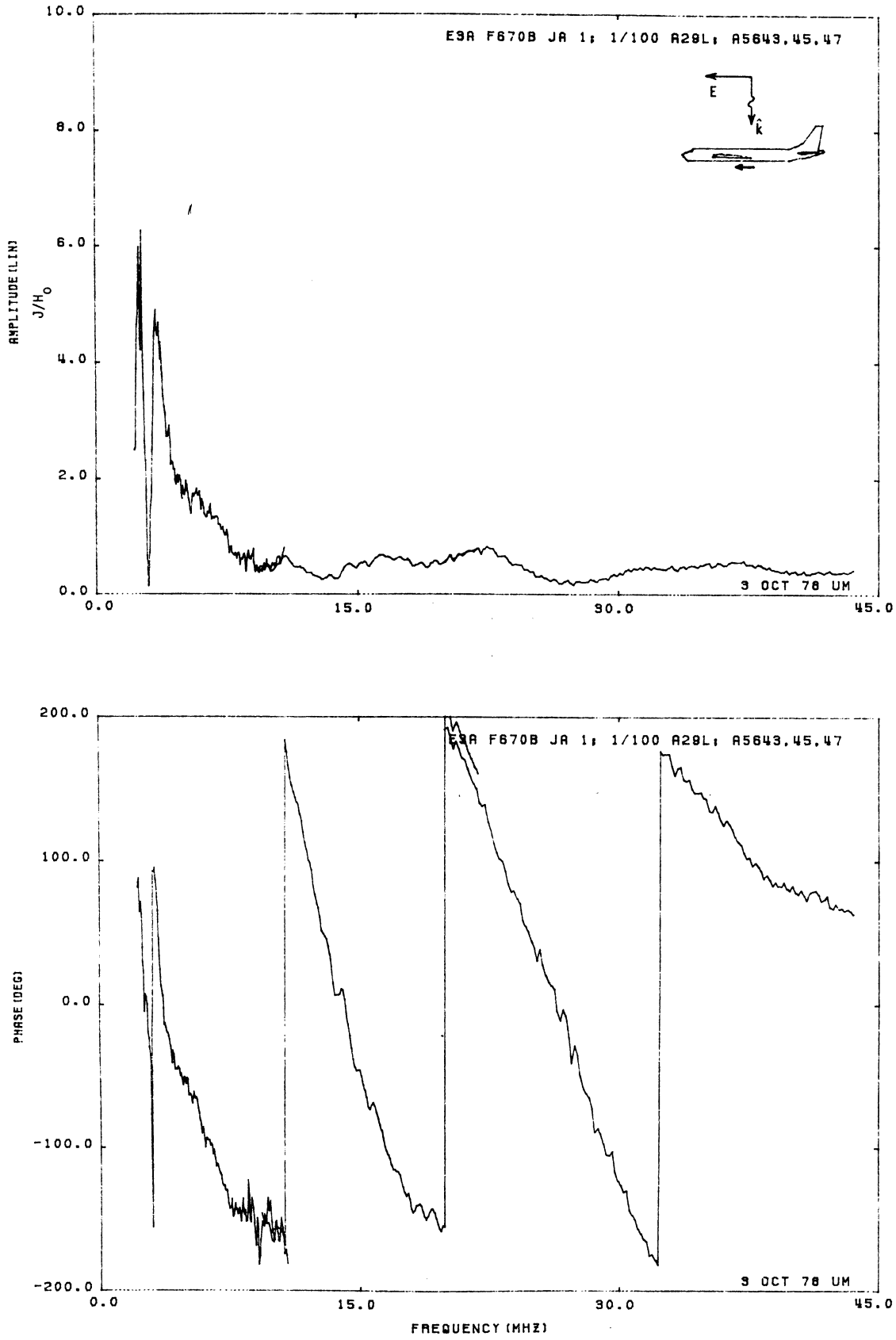

Figure 29L. Axial Current at STA:F670B, Excitation 1, 1/100 Model.

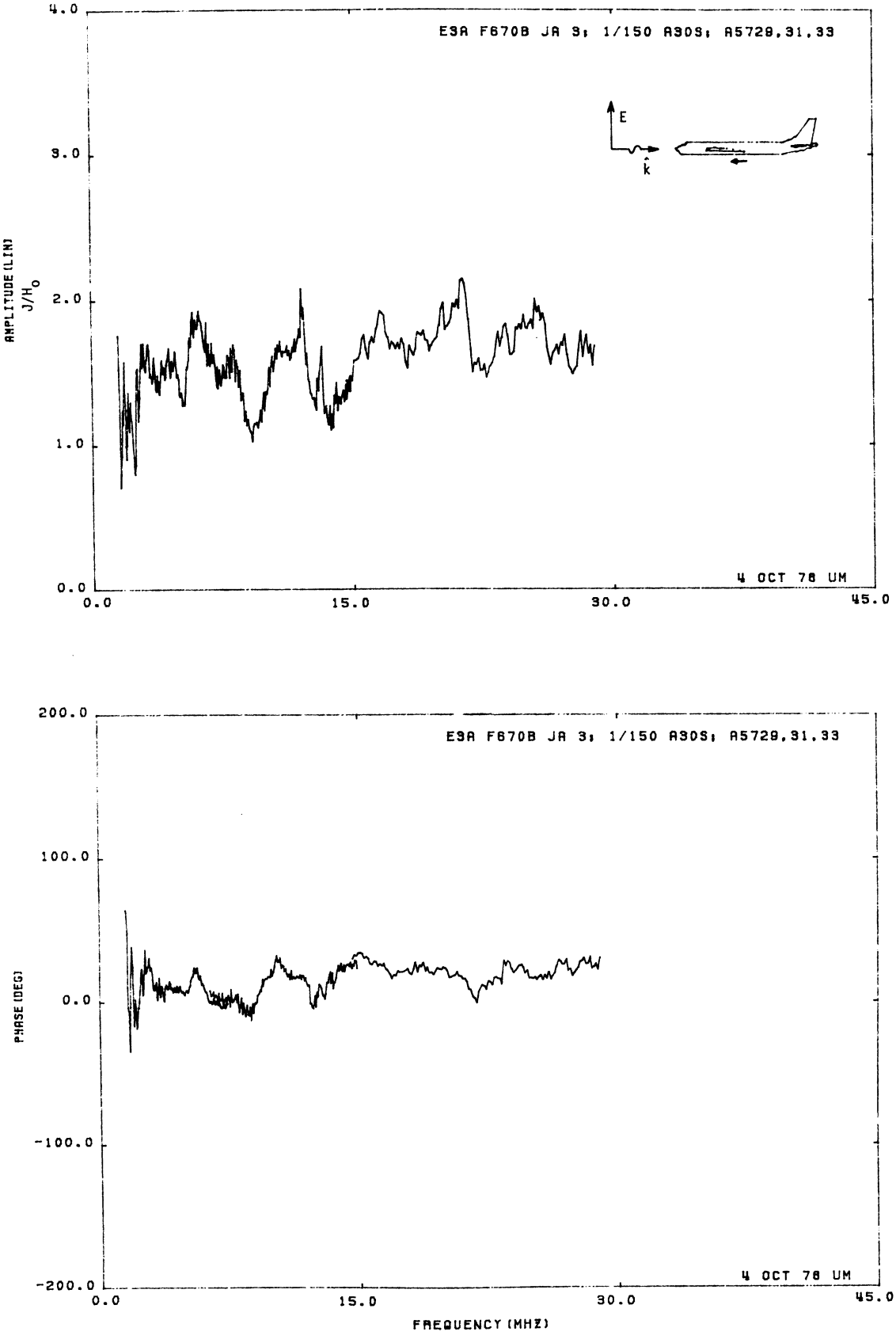

Figure 30S. Axial Current at STA:F670B, Excitation 3, 1/150 Model.

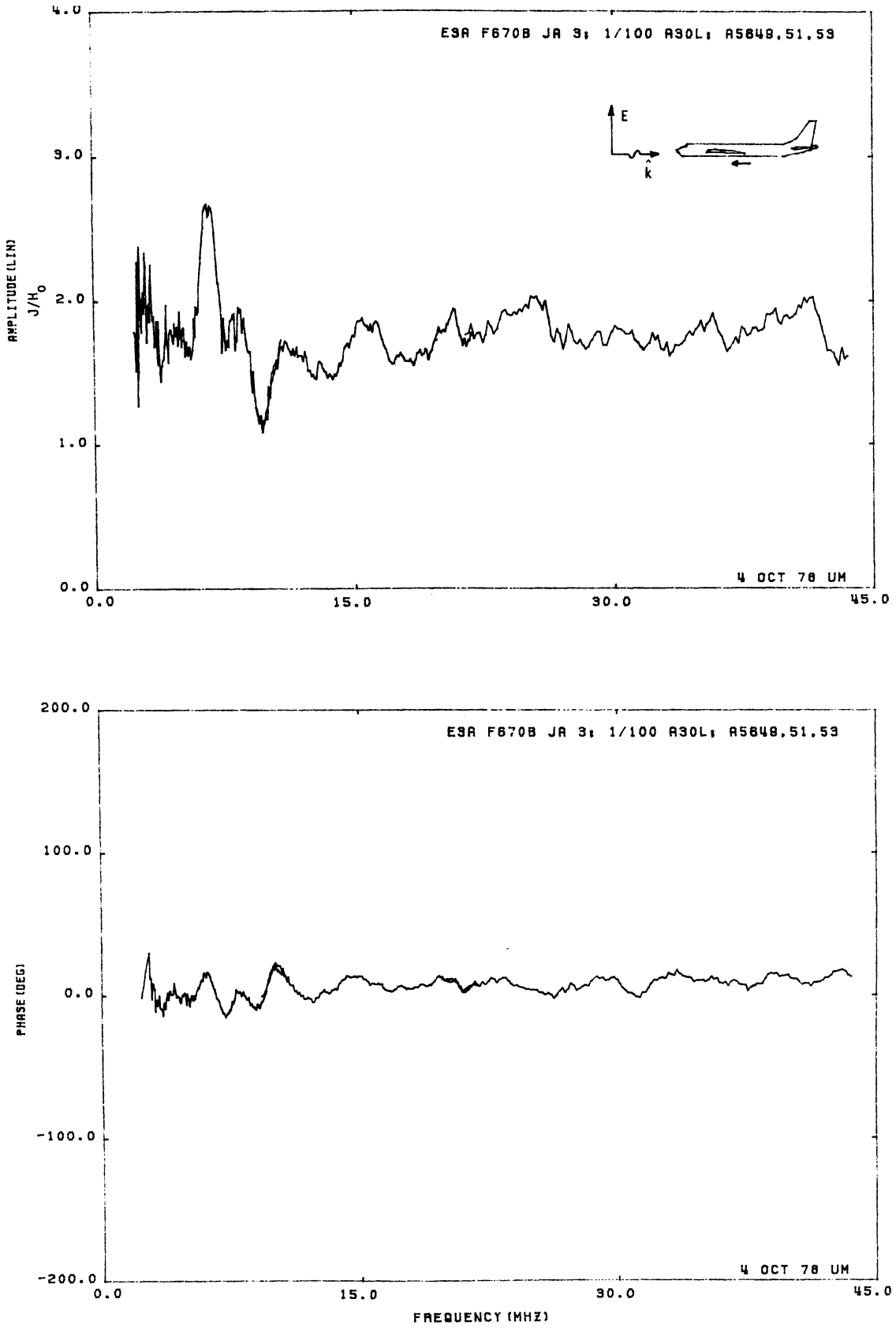

Figure 30L. Axial Current at STA:F670B, Excitation 3, 1/100 Model.

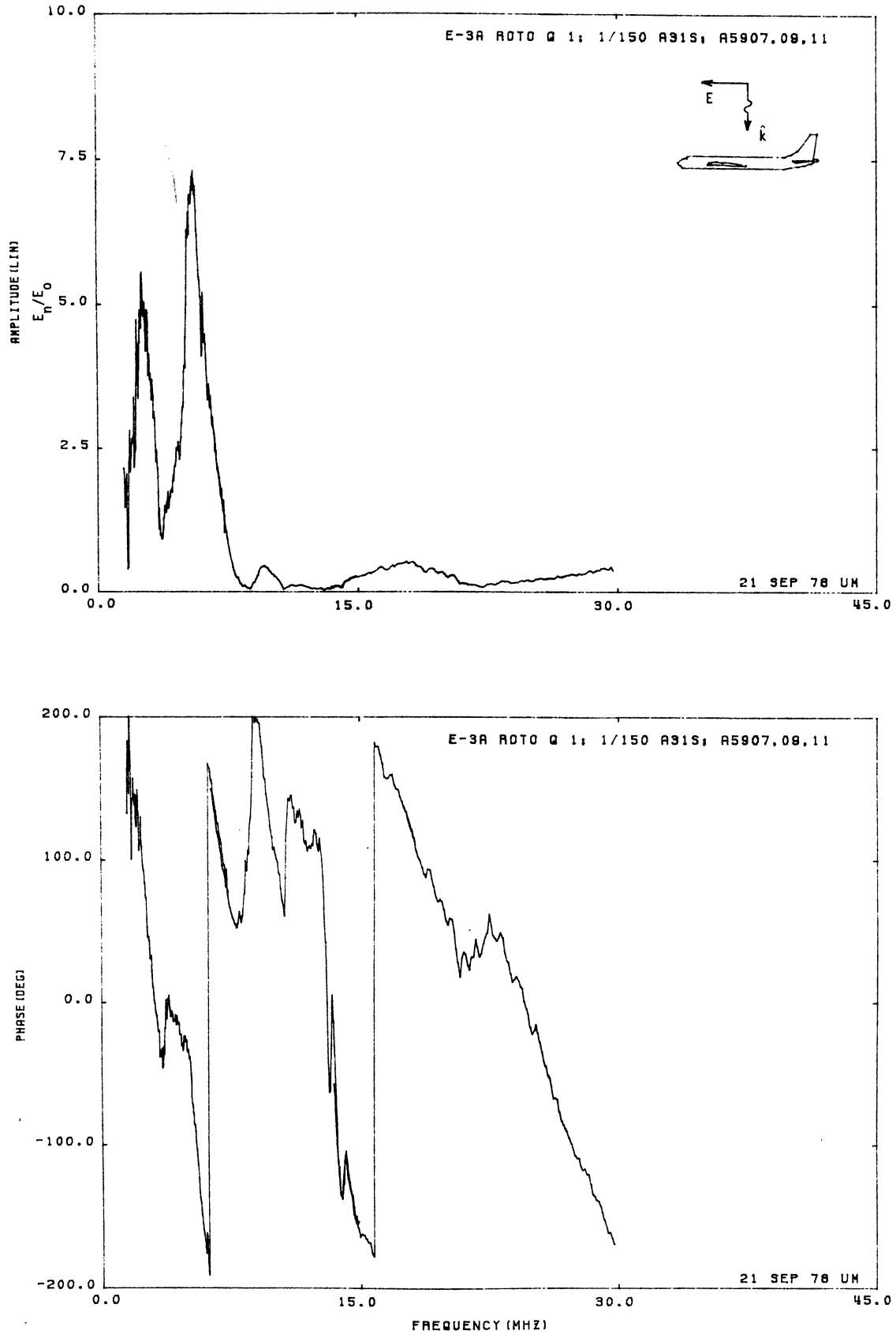

Figure 31S. Charge at STA:ROTO, Excitation 1, 1/150 Model.

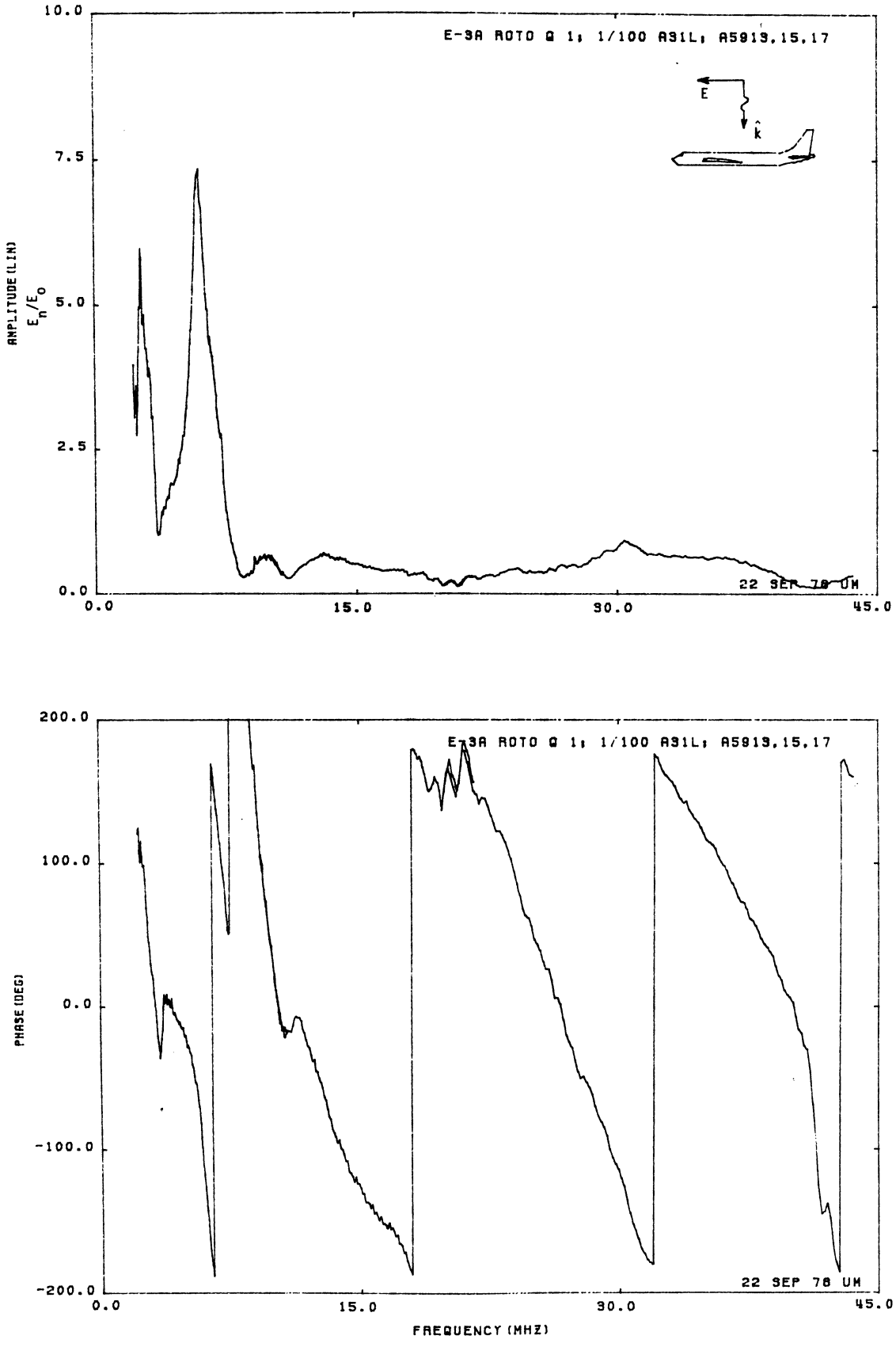

Figure 31L. Charge at STA:ROTO, Excitation 1, 1/100 Model.

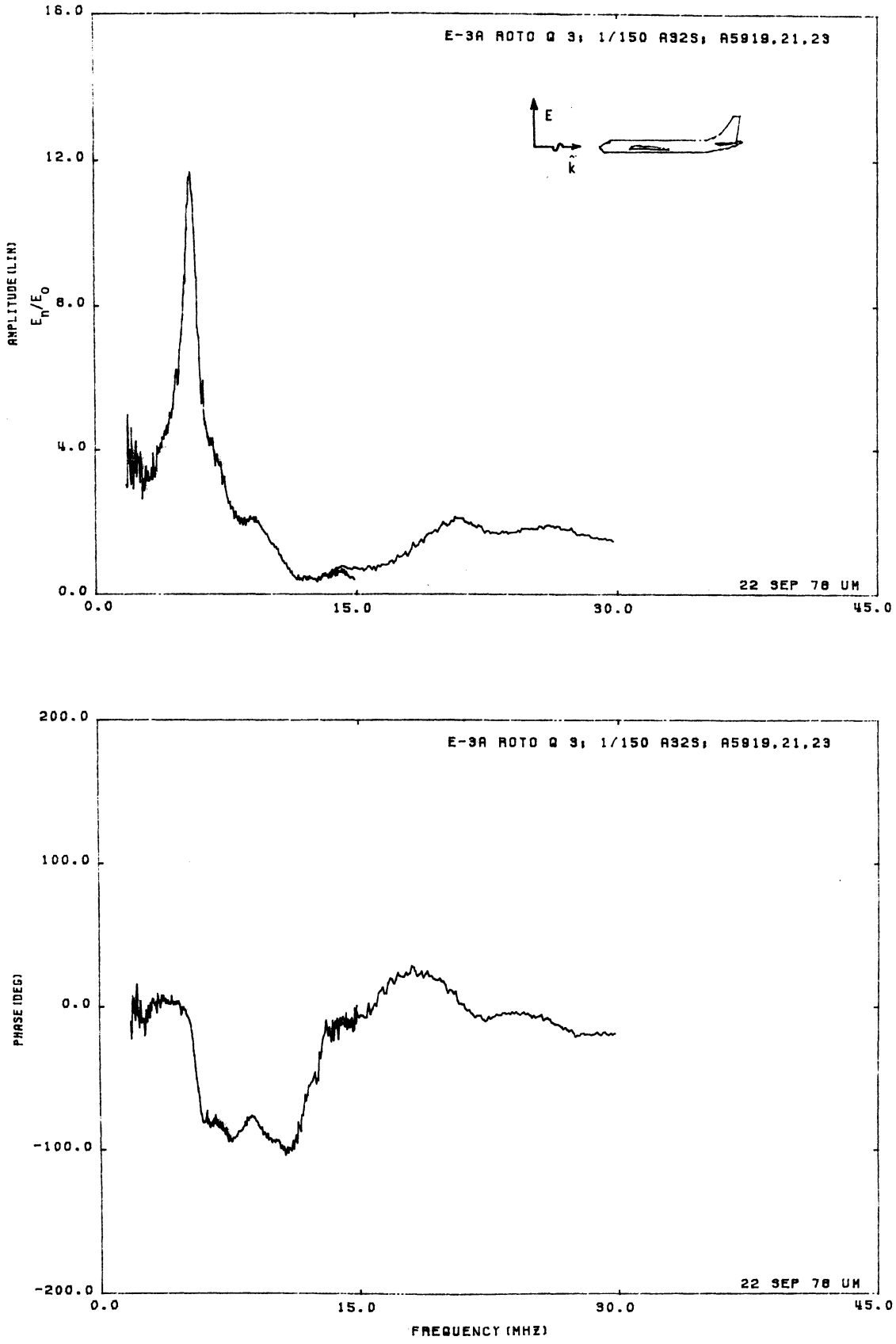

Figure 32S. Charge at STA:ROTO, Excitation 3, 1/150 Model.

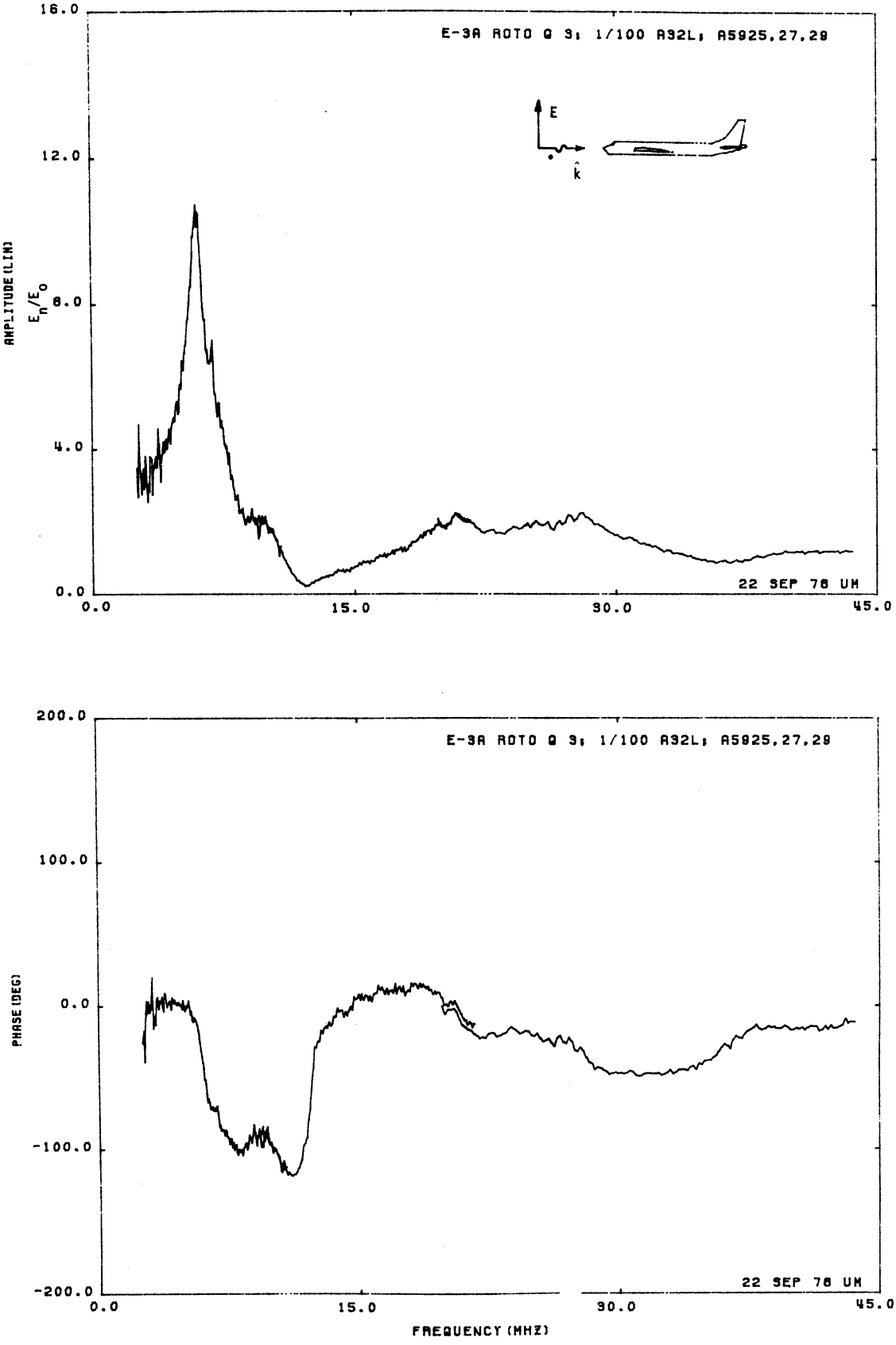

Figure 32L. Charge at STA:ROTO, Excitation 3, 1/100 Model.

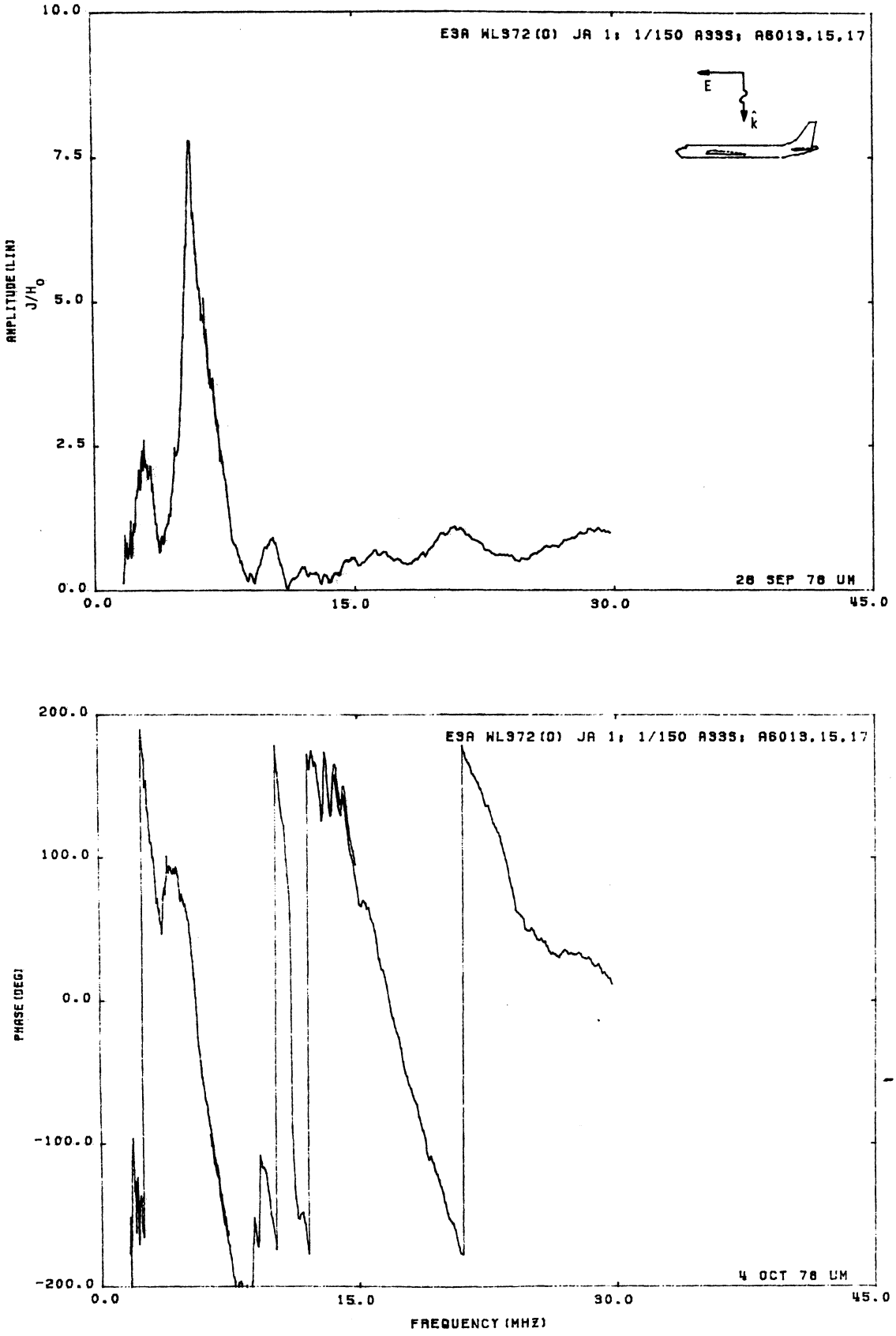

Figure 33S. Axial Current at STA:WL372(0), Excitation 1, 1/150 Model.

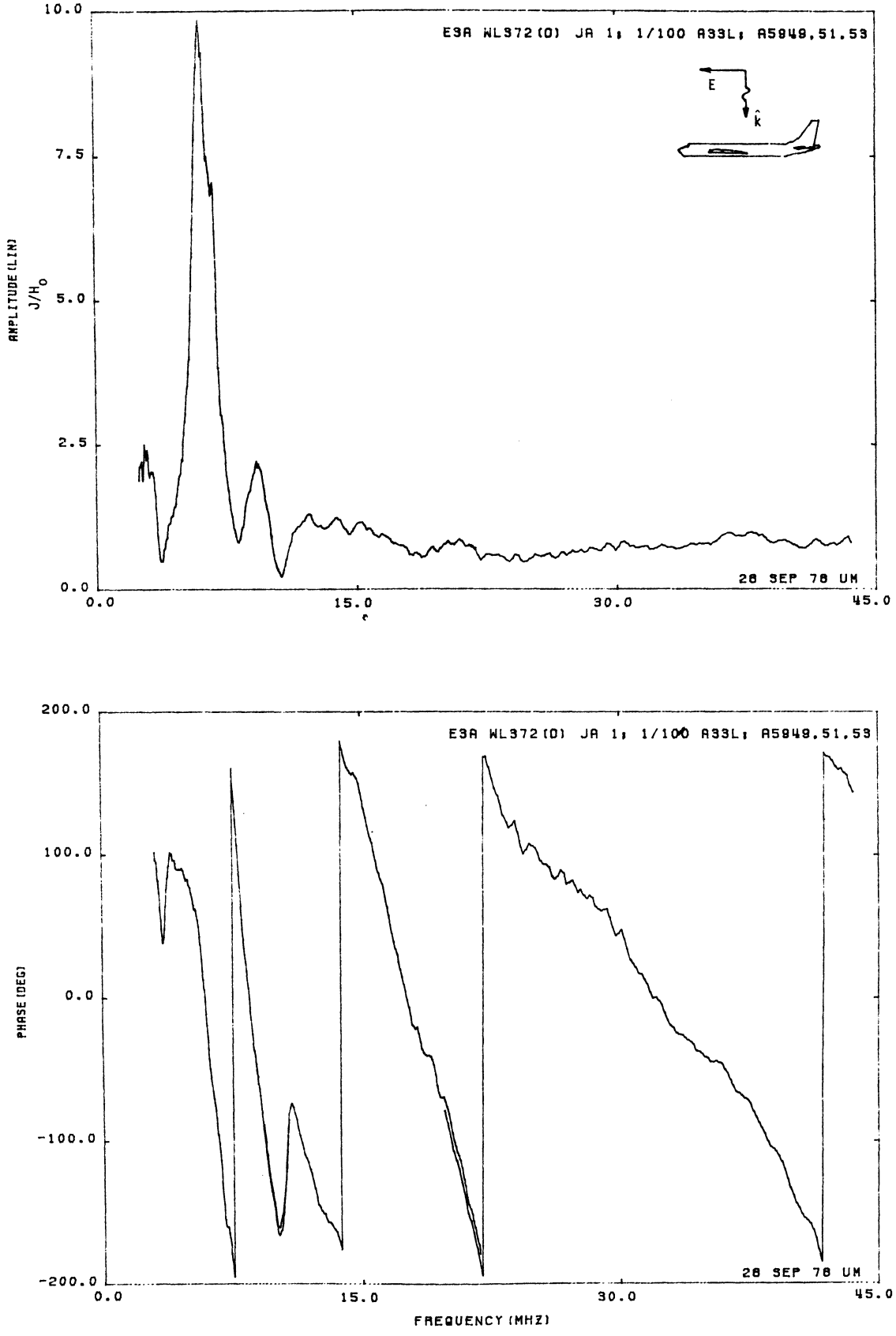

Figure 33L. Axial Current at STA:WL372(0), Excitation 1, 1/100 Model.

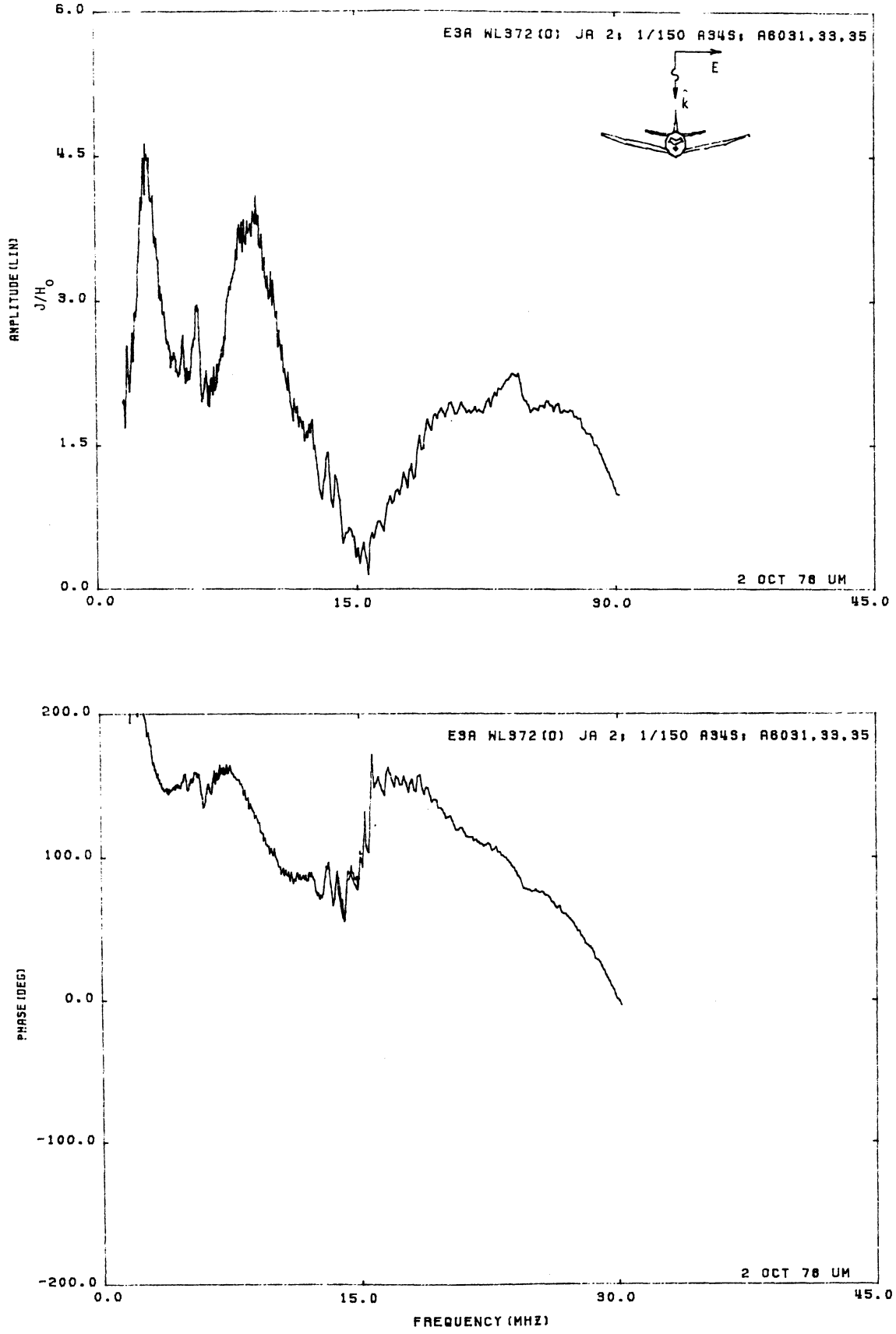

Figure 34S. Axial Current at STA:WL372(0), Excitation 2, 1/150 Model.

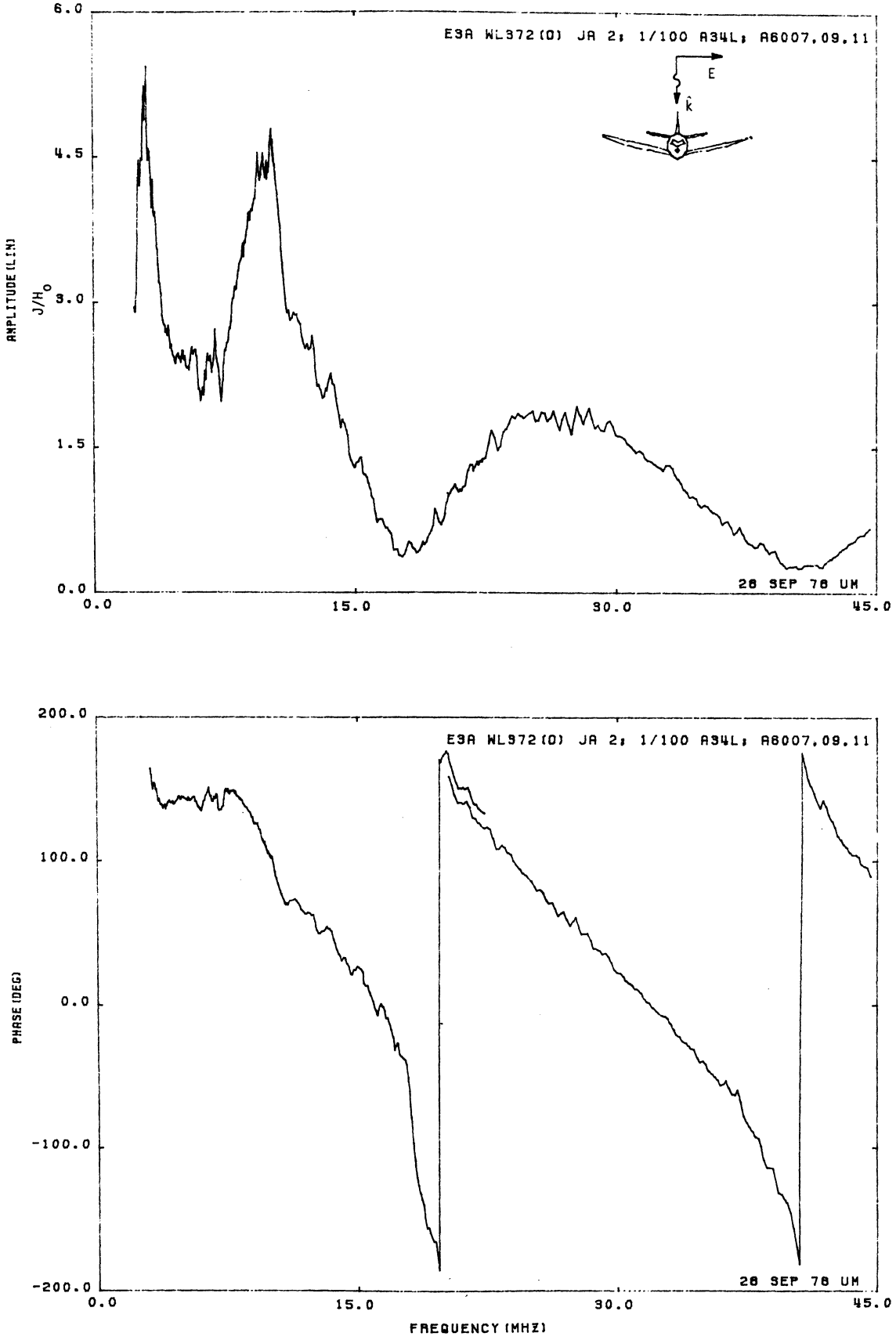

Figure 34L. Axial Current at STA:WL372(0), Excitation 2, 1/100 Model.

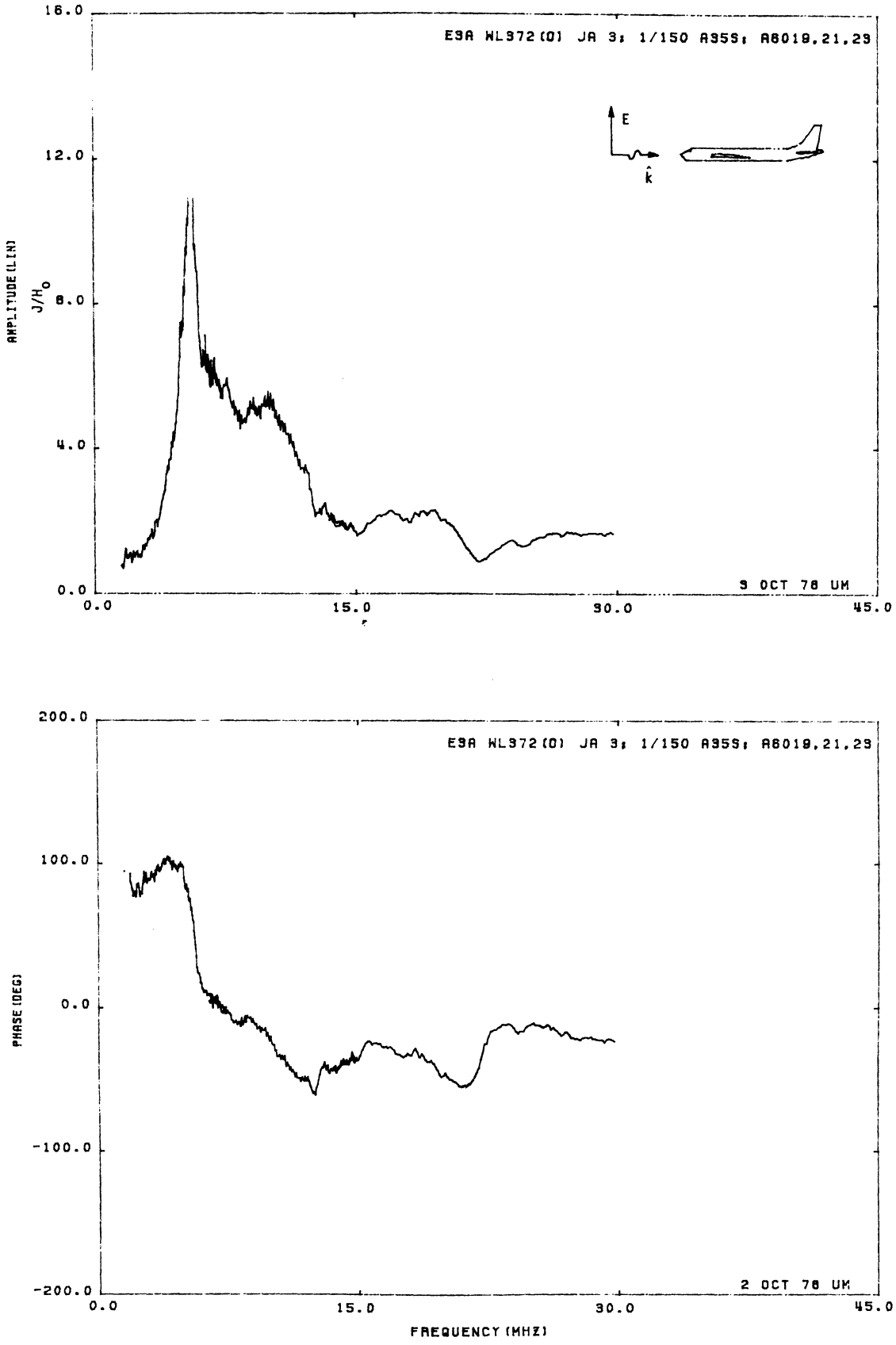

Figure 35S. Axial Current at STA:WL372(0), Excitation 3, 1/150 Model.

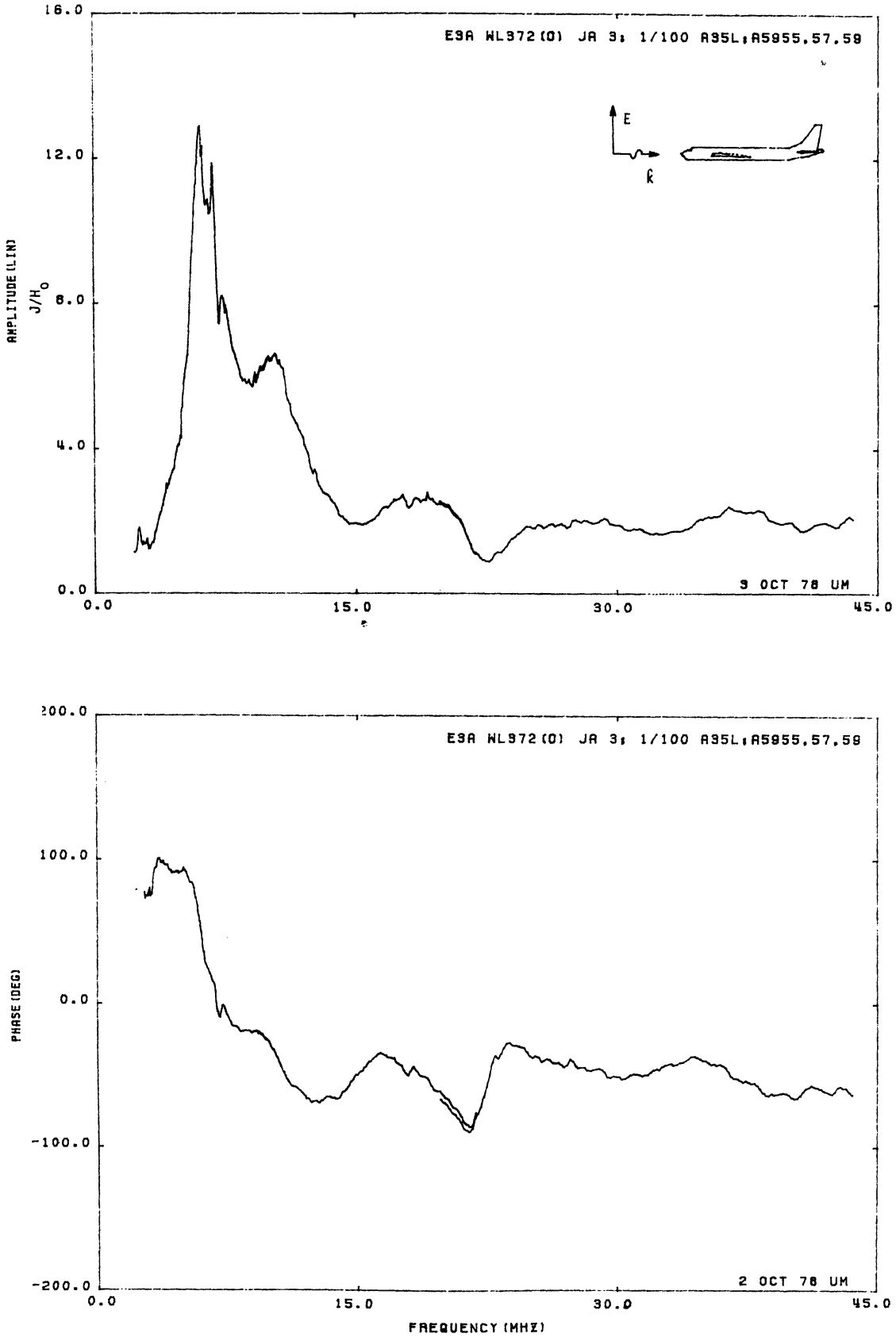

Figure 35L. Axial Current at STA:WL372(0), Excitation 3, 1/100 Model.

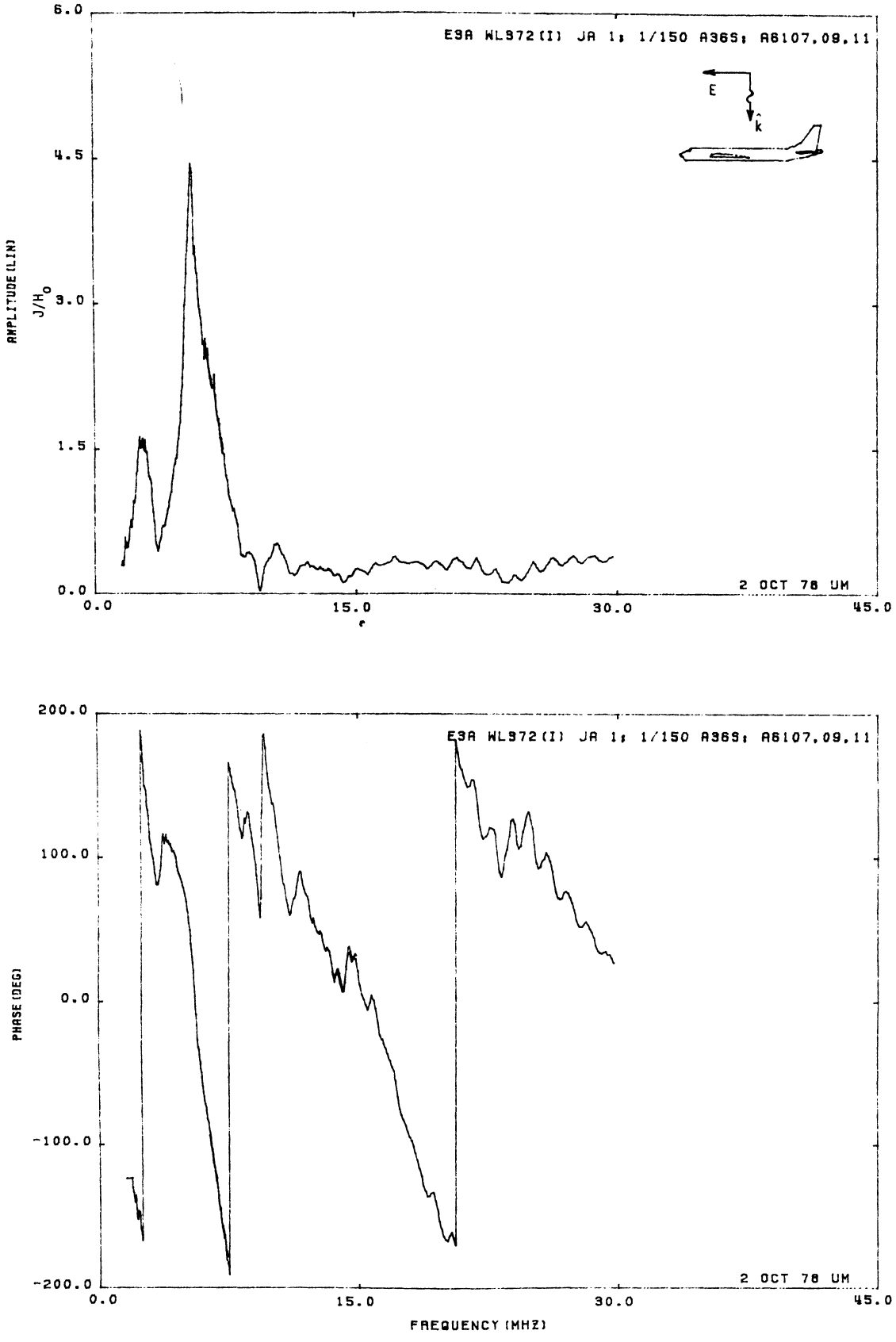

Figure 36S. Axial Current at STA:WL372(I), Excitation 1, 1/150 Model.

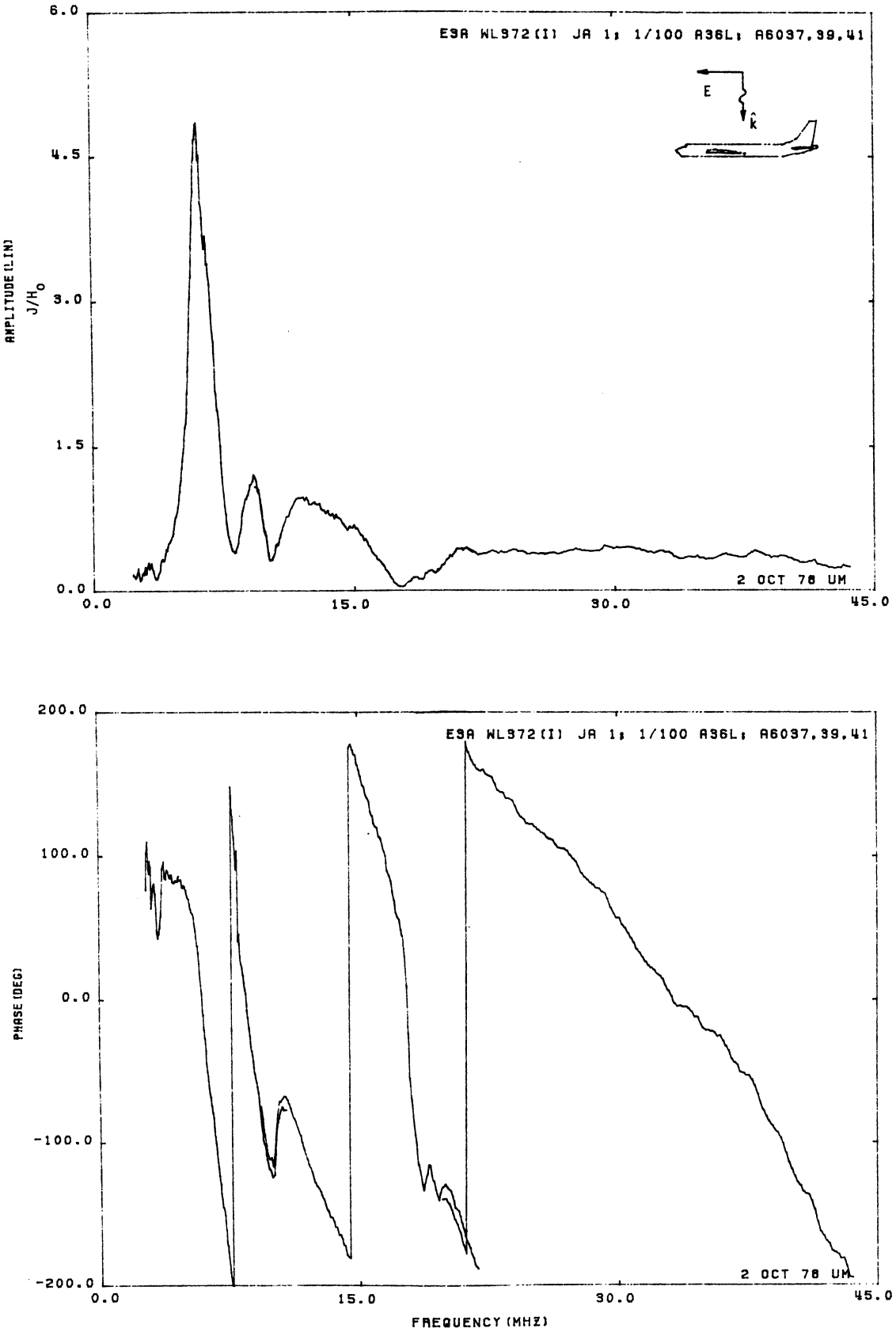

Figure 36L. Axial Current at STA:WL372(I), Excitation 1, 1/100 Model.

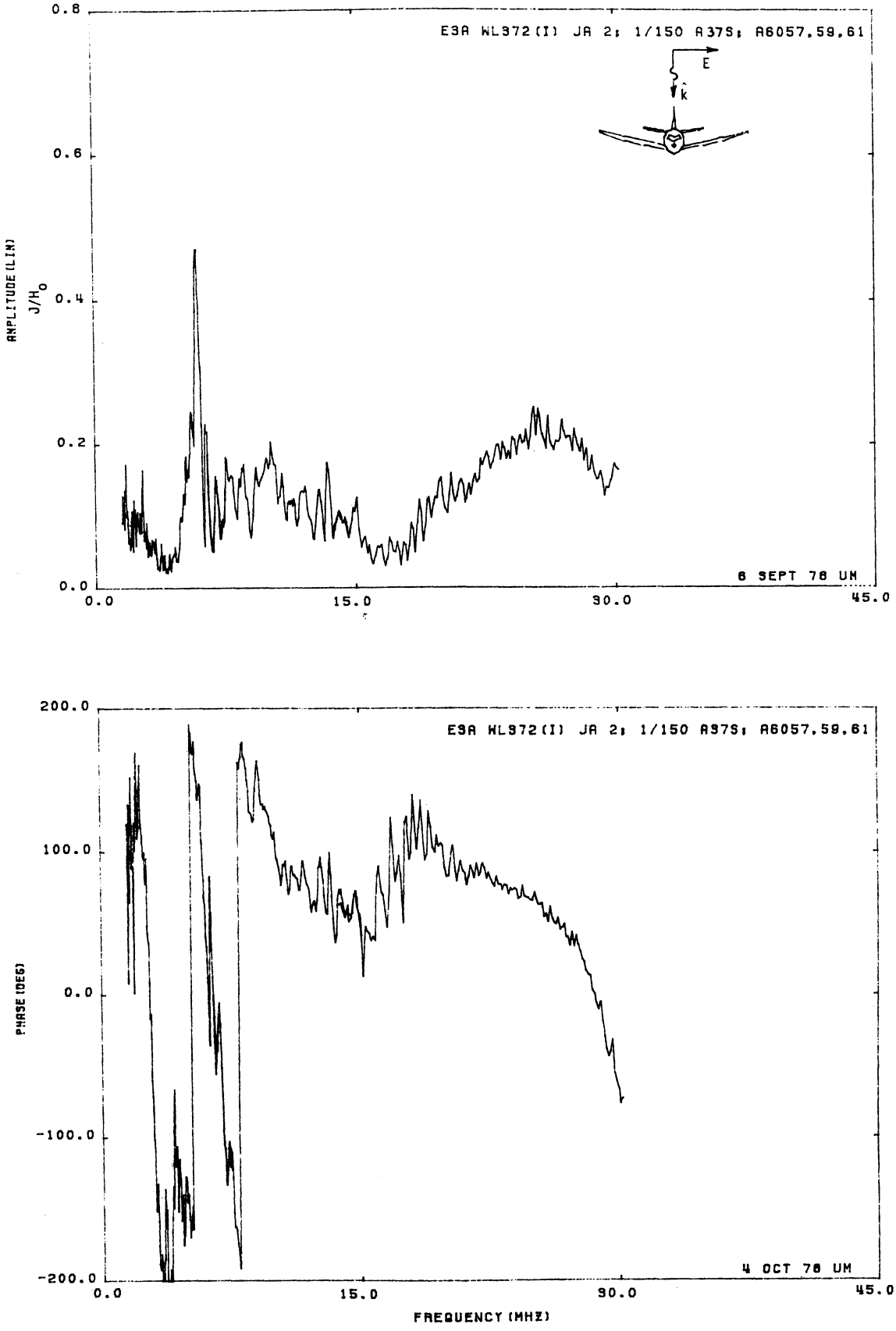

Figure 37S. Axial Current at STA:WL372(I), Excitation 2, 1/150 Model.

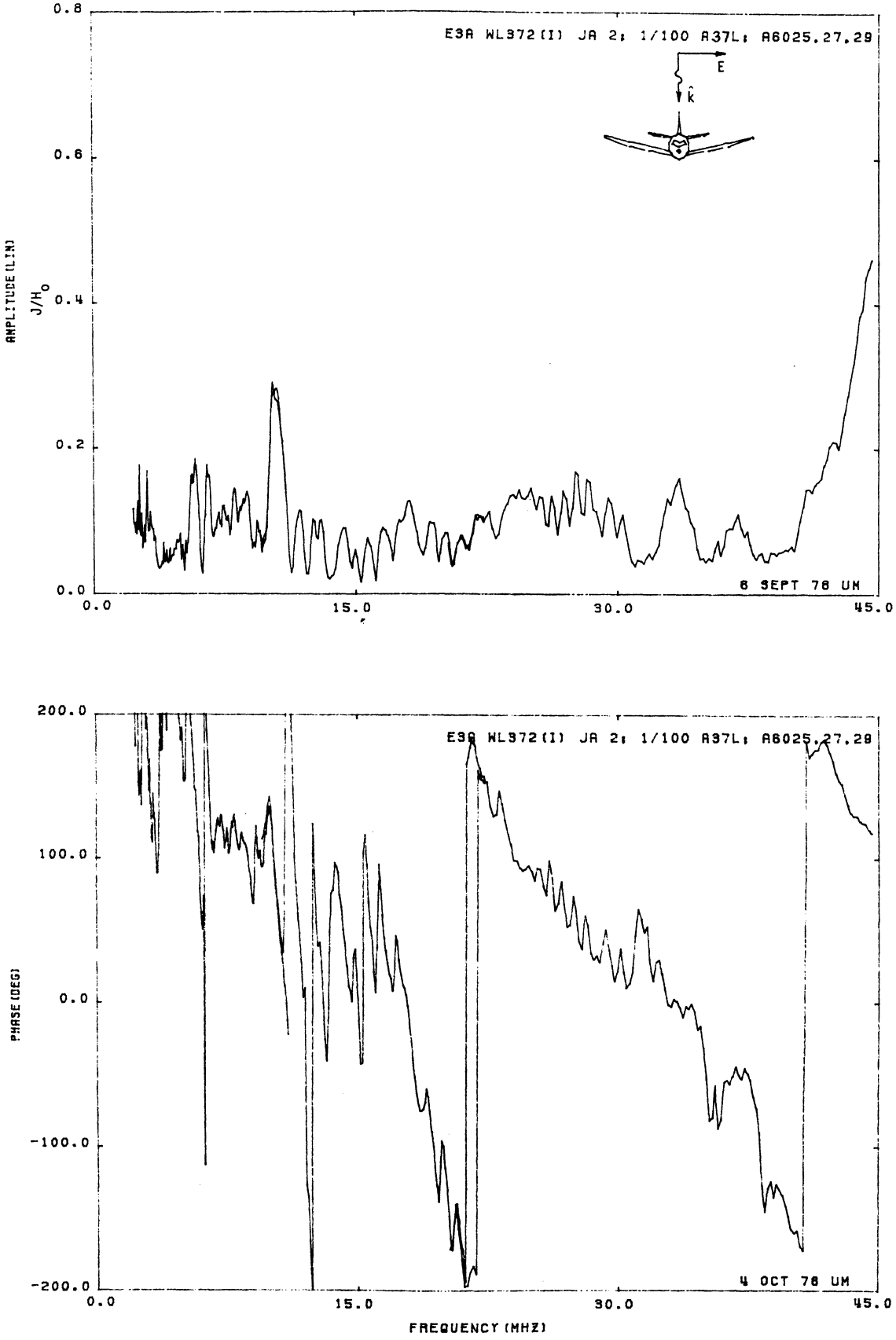

Figure 37L. Axial Current at STA:WL372(I), Excitation 2, 1/100 Model.

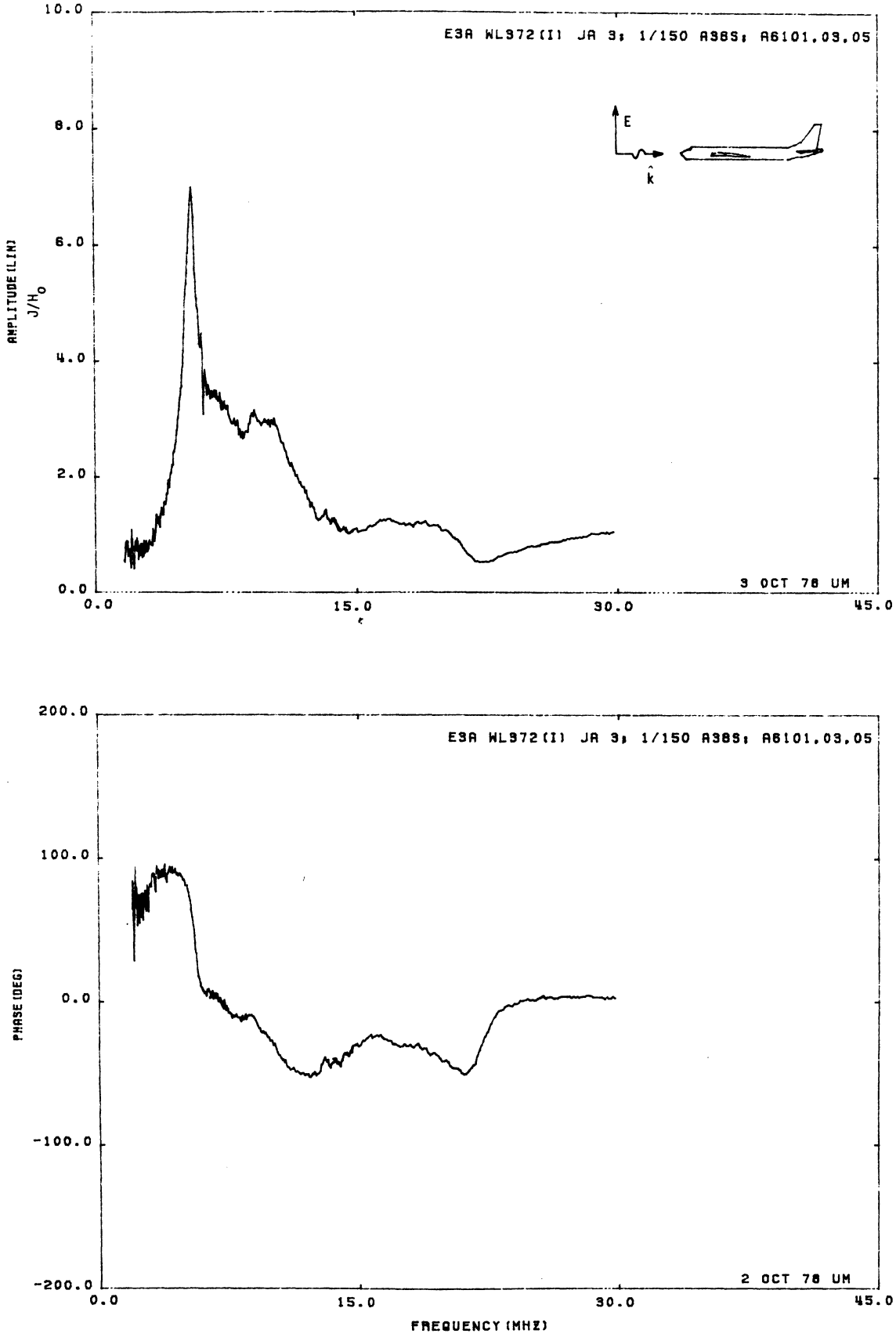

Figure 38S. Axial Current at STA:WL372(I), Excitation 3, 1/150 Model.

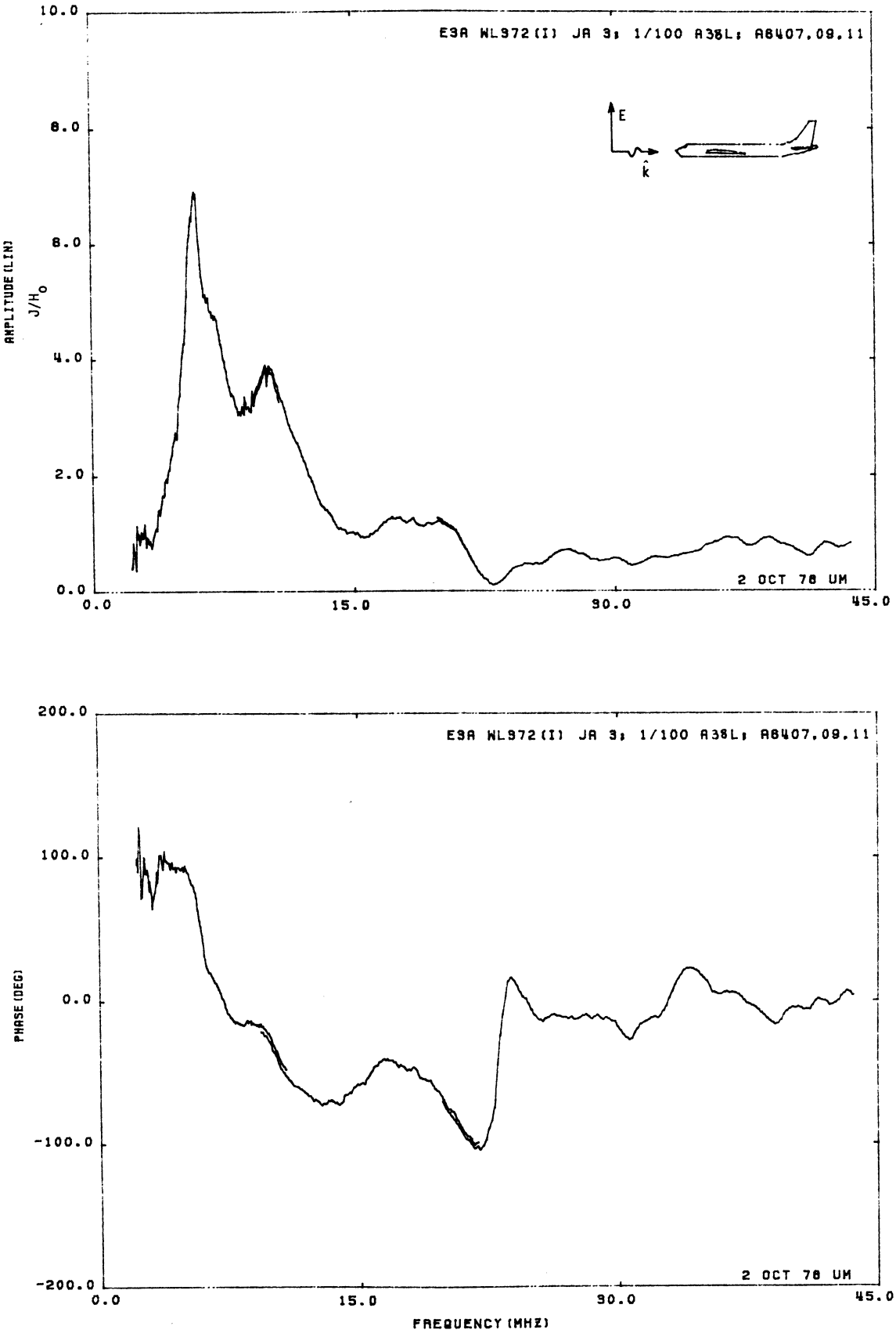

Figure 38L. Axial Current at STA:WL372(I), Excitation 3, 1/100 Model.

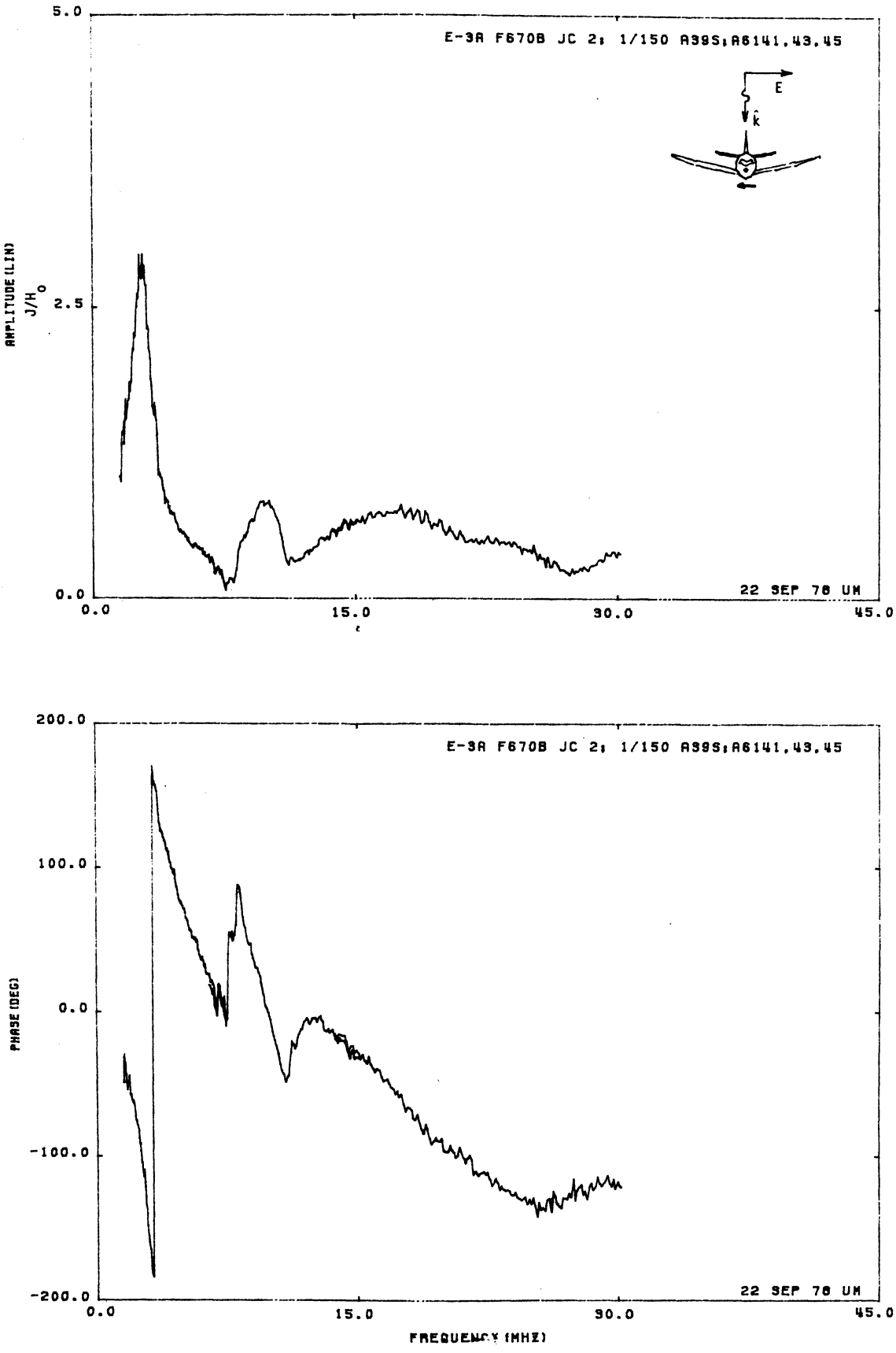

Figure 39S. Circumferential Current at STA:F670B, Excitation 2, 1/150 Model.

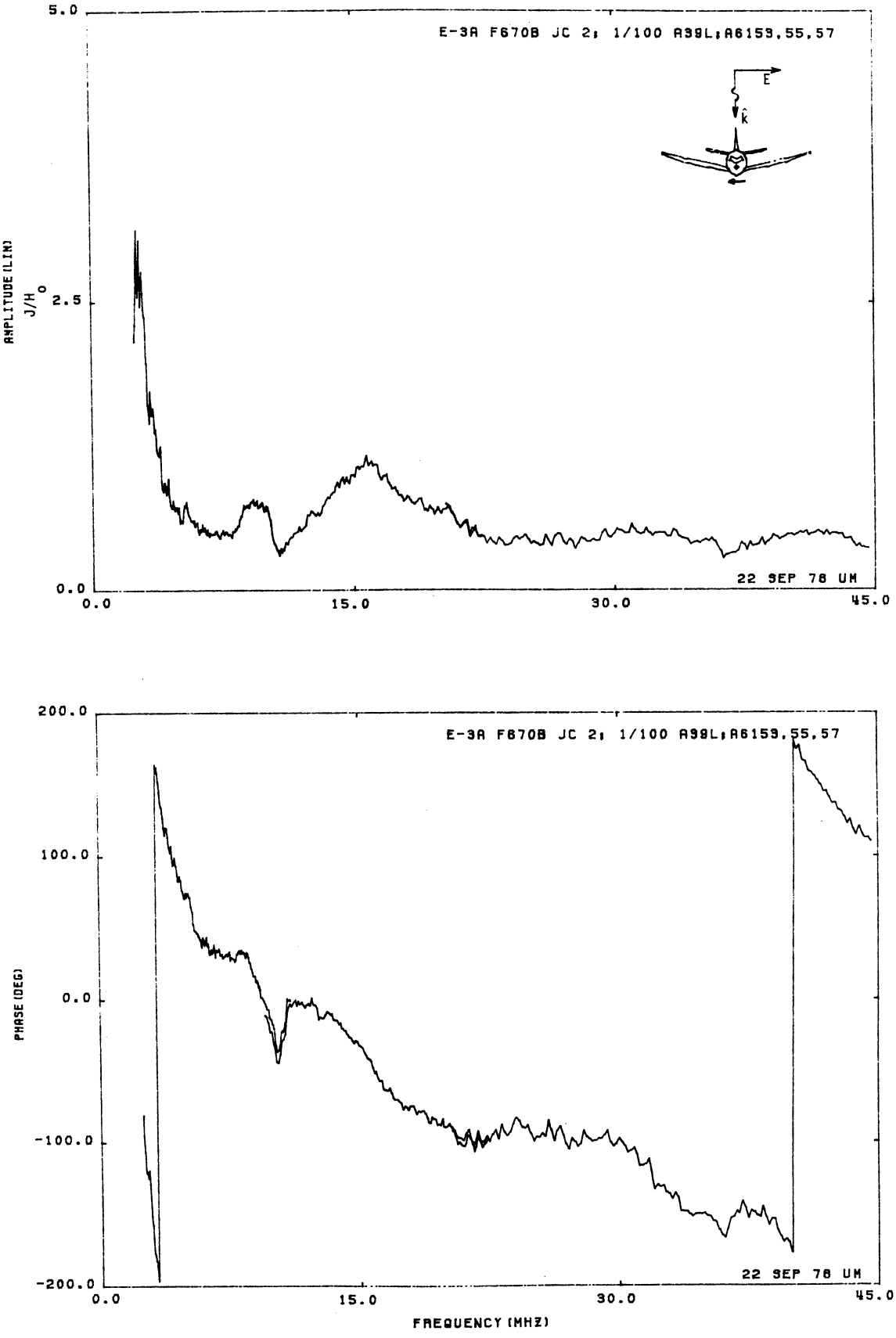

Figure 39L. Circumferential Current at STA:F670B, Excitation 2, 1/100 Model.

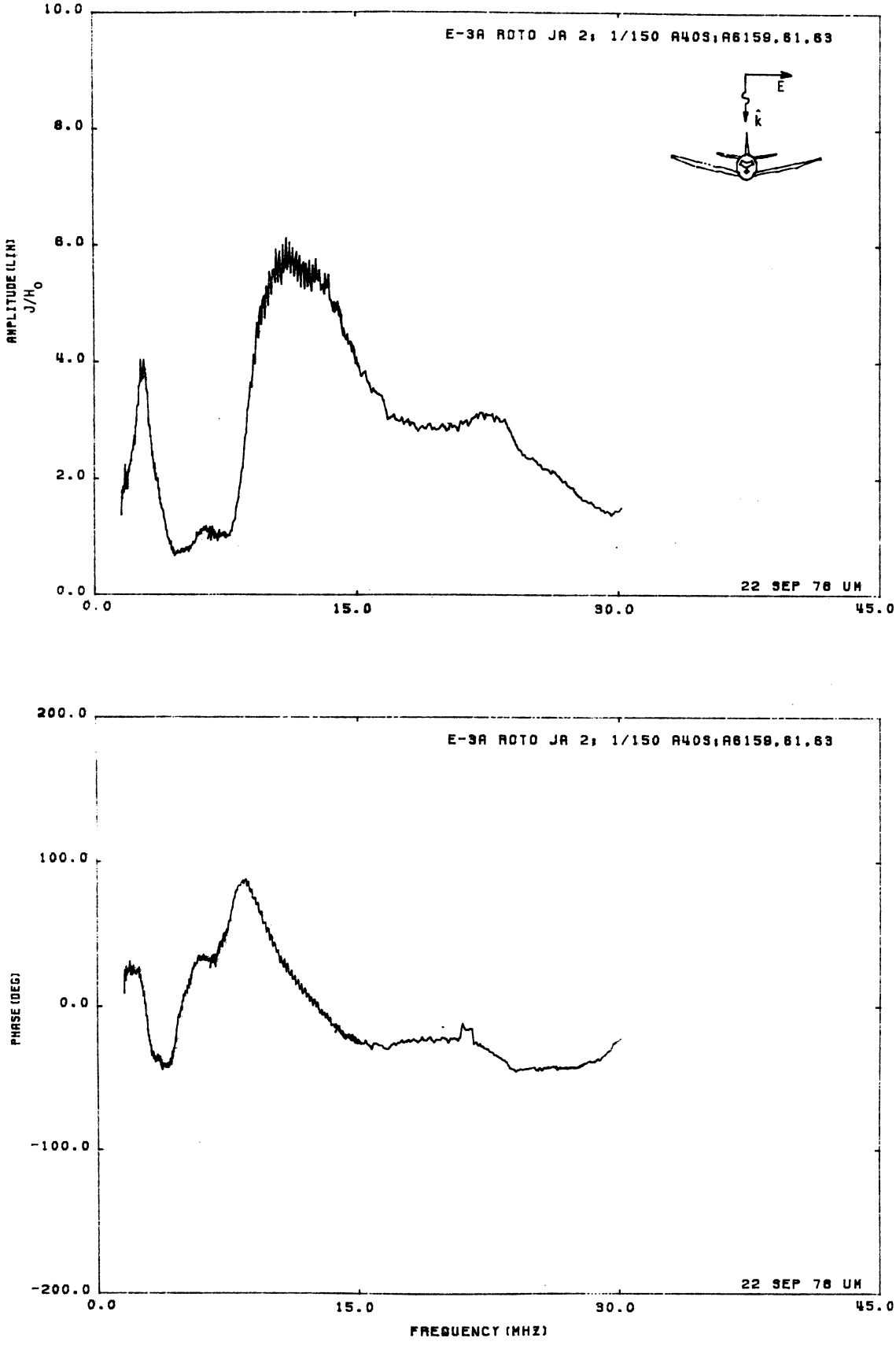

Figure 40S. Axial Current at STA:ROTO, Excitation 2, 1/150 Model.

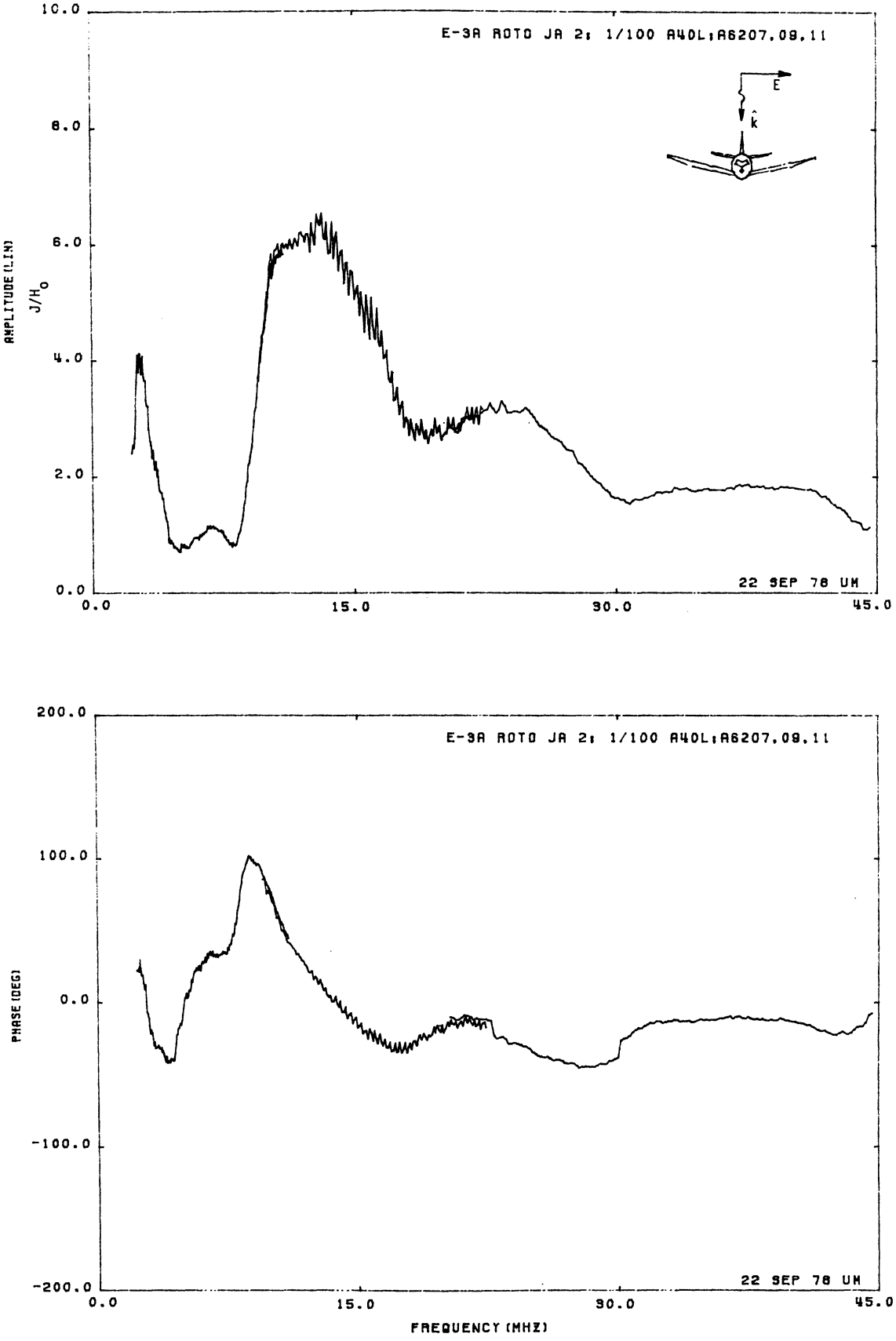

Figure 40L. Axial Current at STA:ROTO, Excitation 2, 1/100 Model.

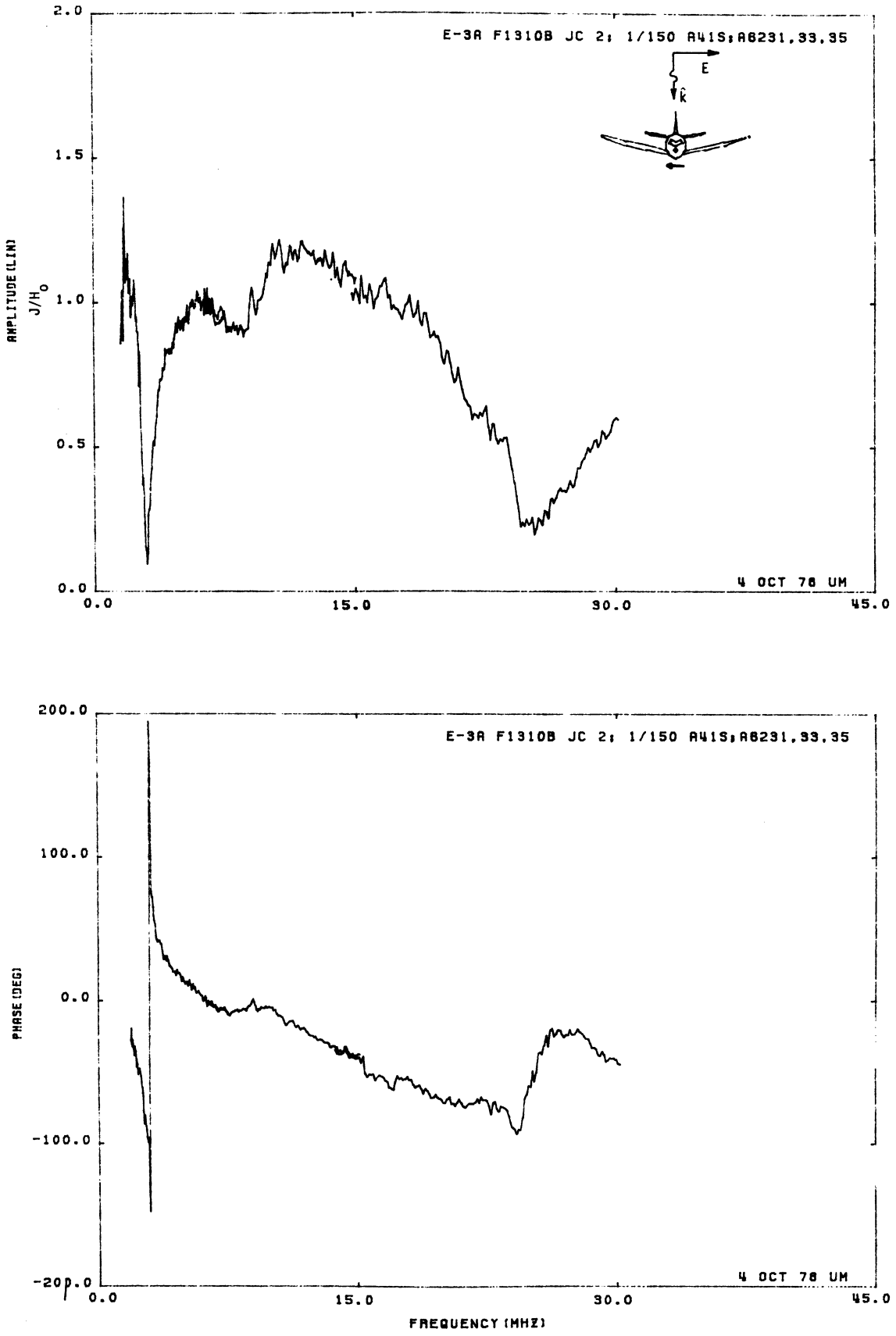

Figure 41S. Circumferential Current at STA:F1310B, Excitation 2, 1/150 Model.

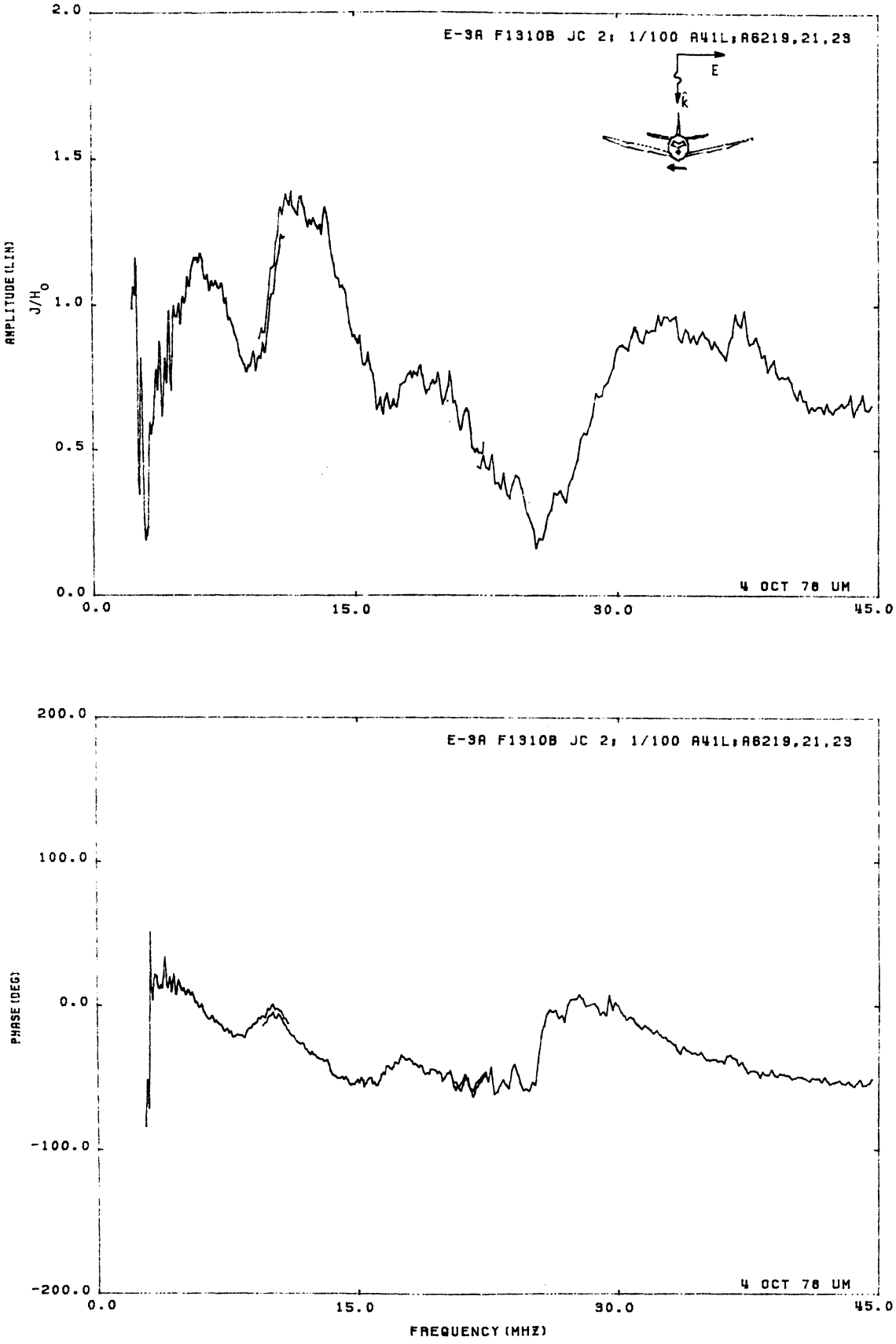

Figure 41L. Circumferential Current at STA:F1310B, Excitation 2, 1/100 Model.

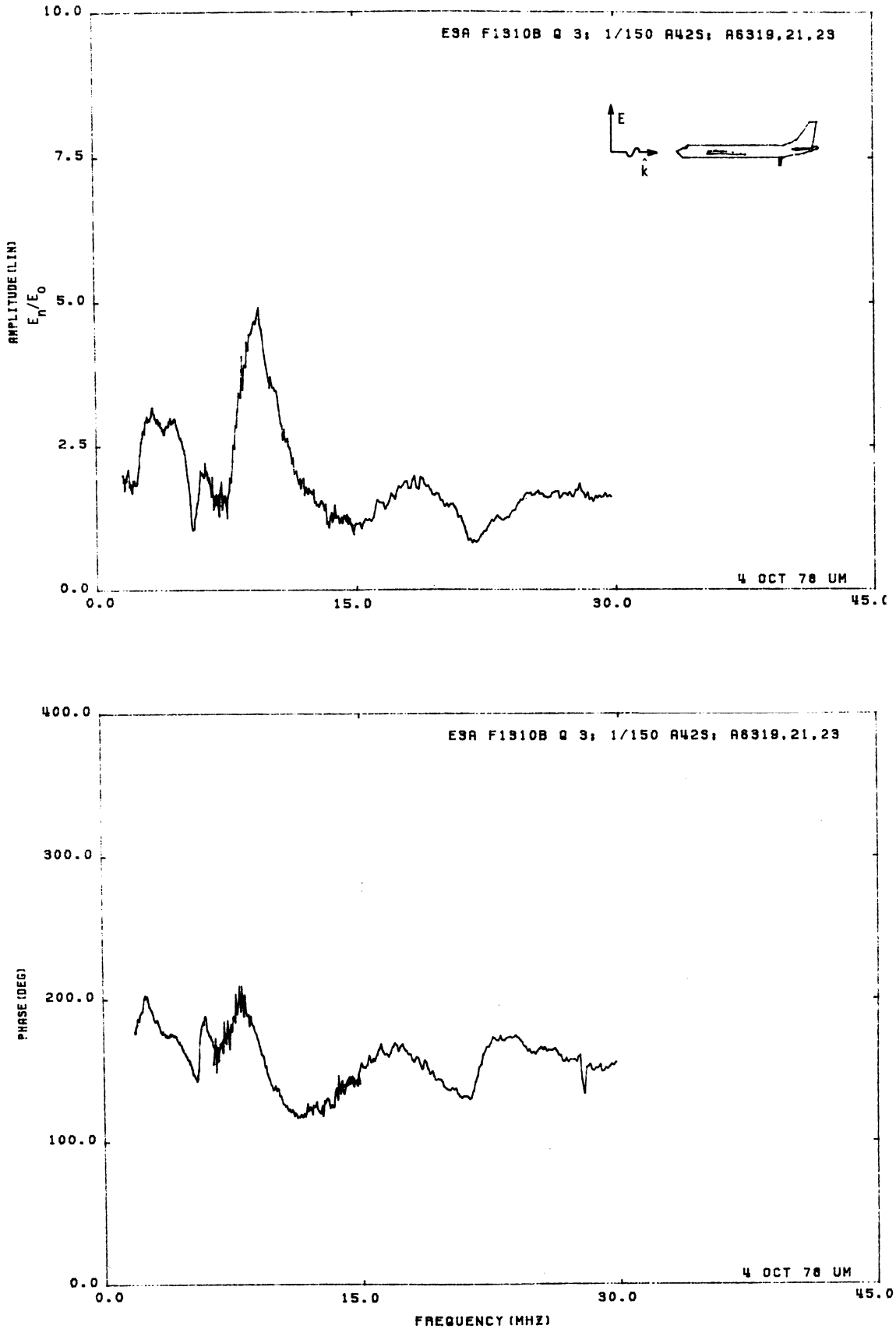

Figure 42S. Charge at STA:F1310B, Excitation 3, 1/150 Model.

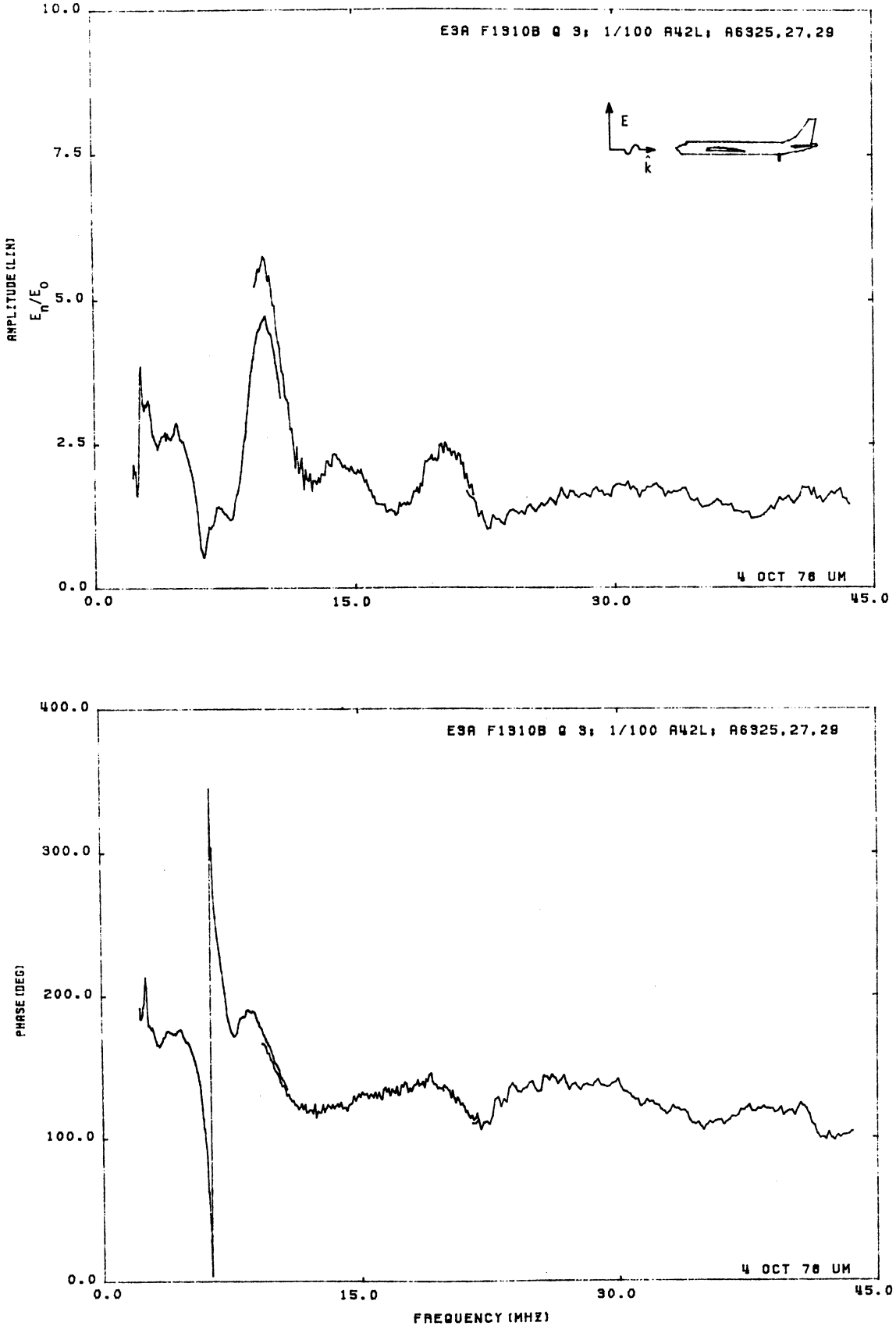

Figure 42L. Charge at STA:F1310B, Excitation 3, 1/100 Model.

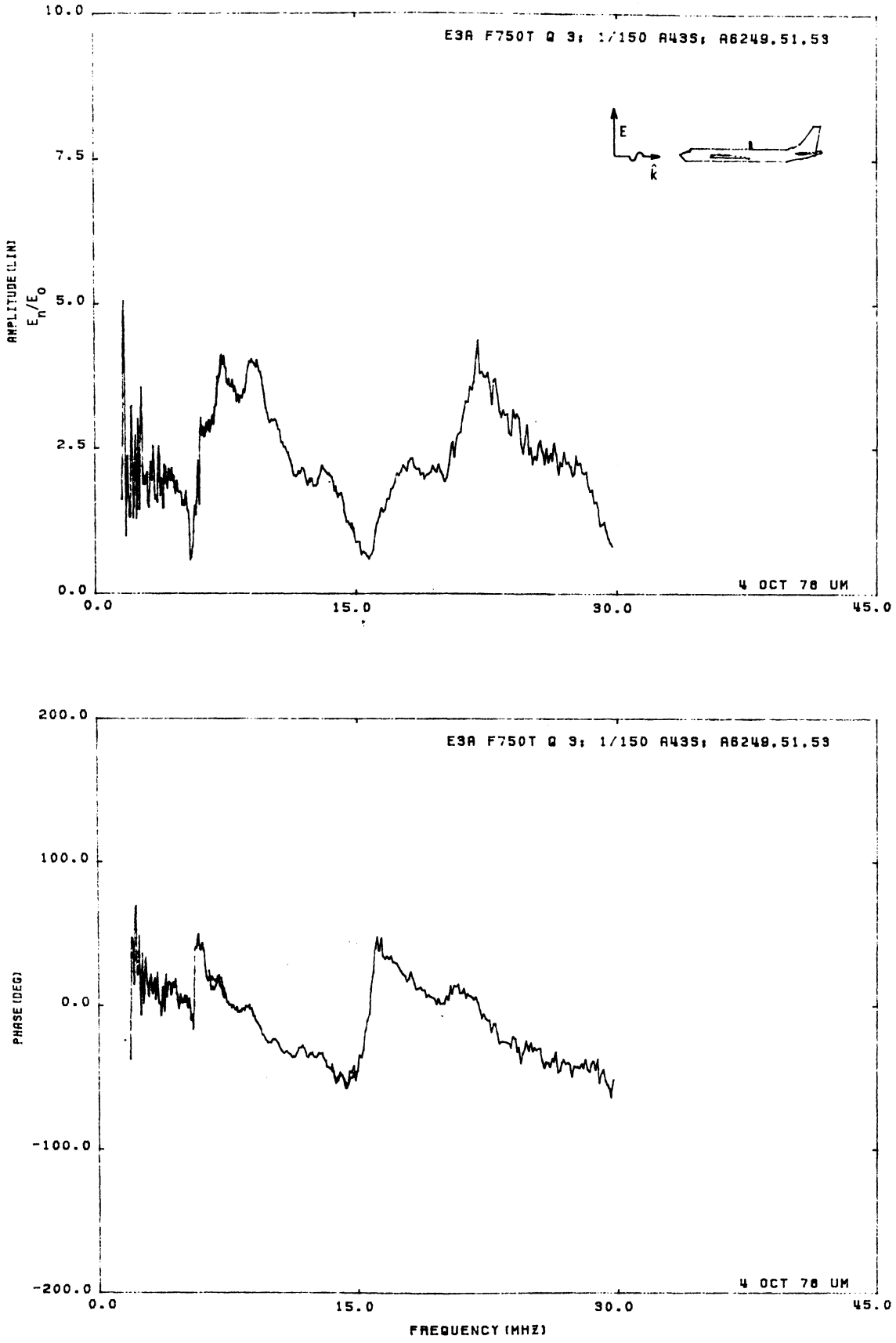

Figure 43S. Charge at STA:F750T, Excitation 3, 1/150 Model.

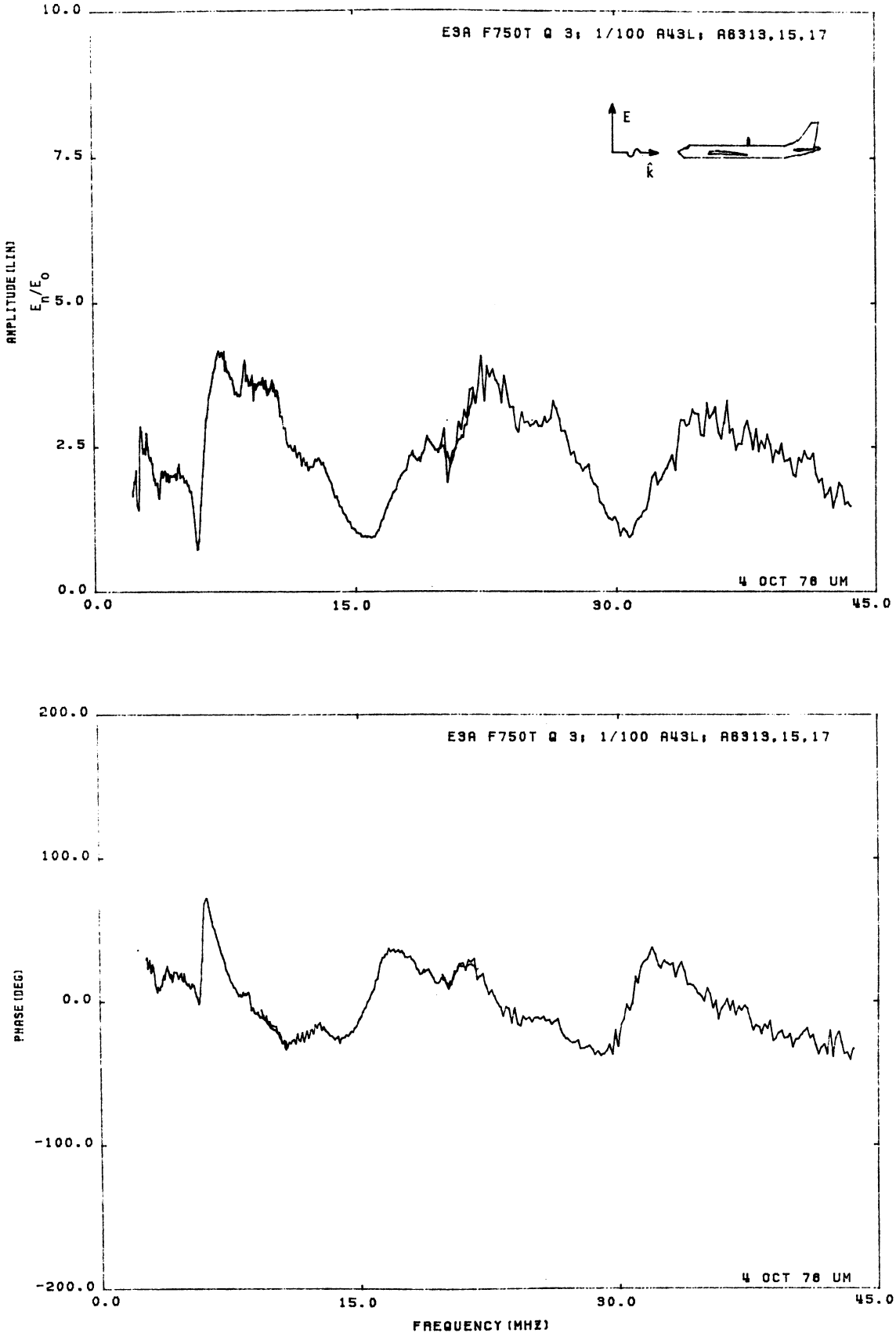

Figure 43L. Charge at STA:F750T, Excitation 3, 1/100 Model.

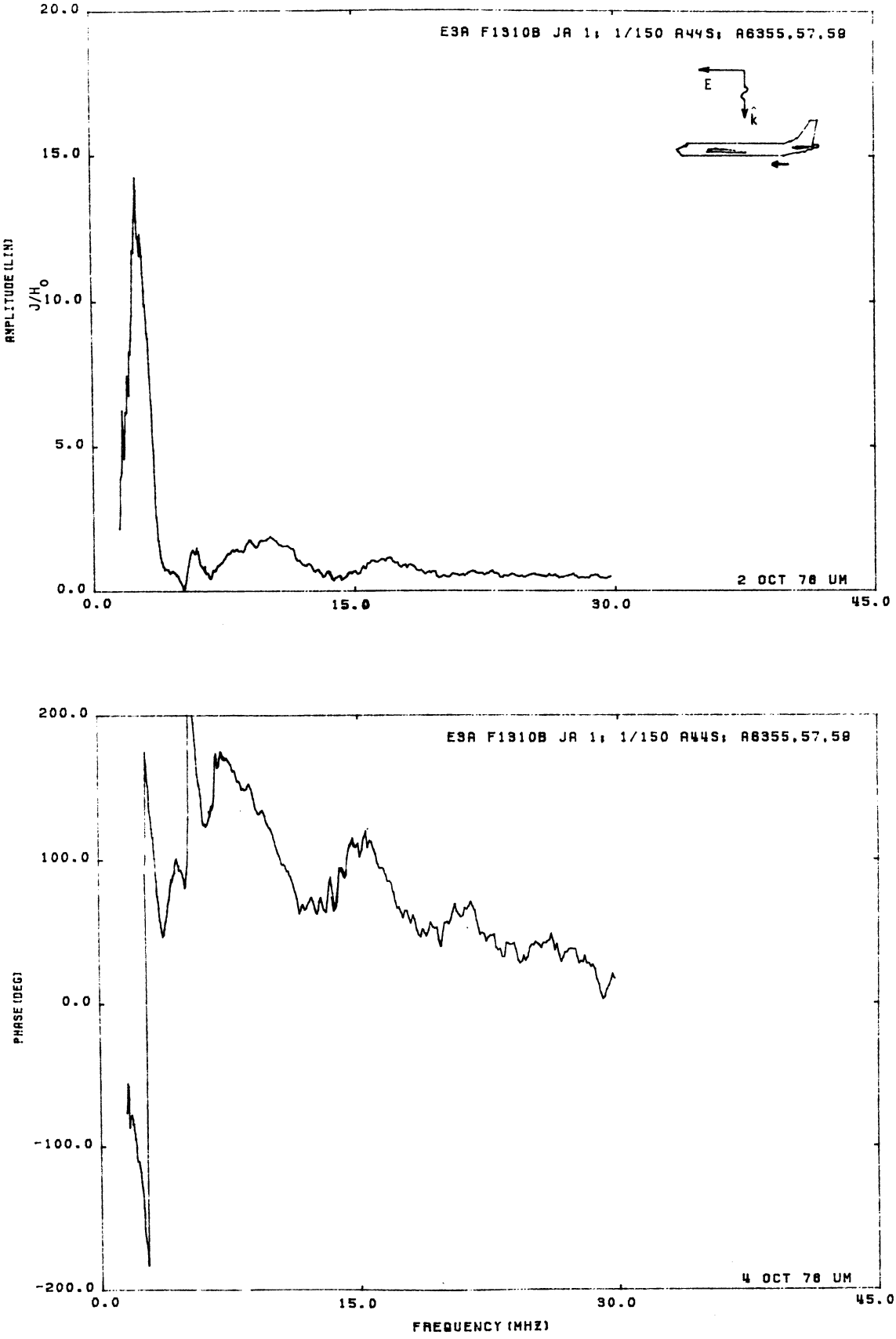

Figure 44S. Axial Current at STA:F1310B, Excitation 1, 1/150 Model.

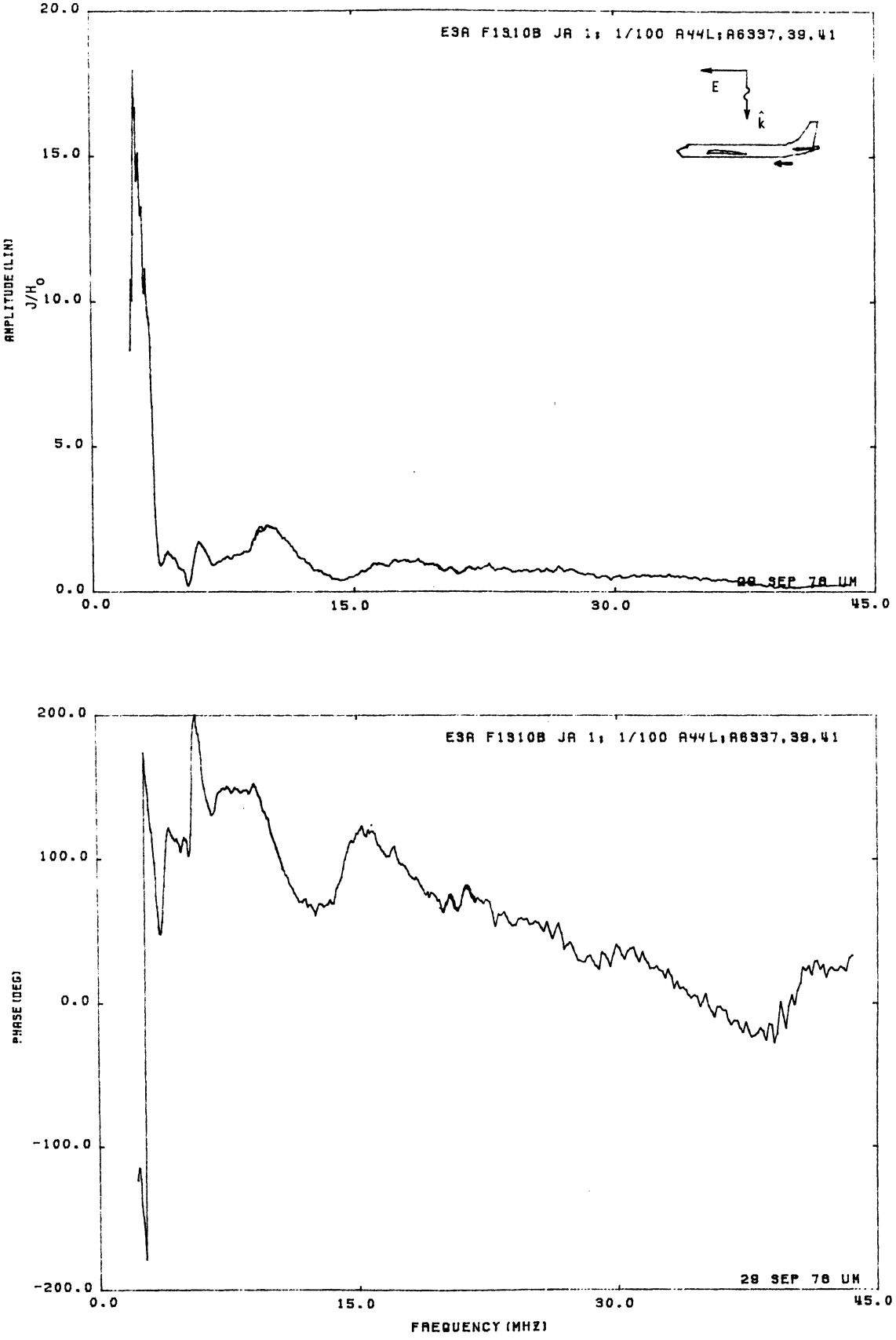

Figure 44L. Axial Current at STA:F1310B, Excitation 1, 1/100 Model.

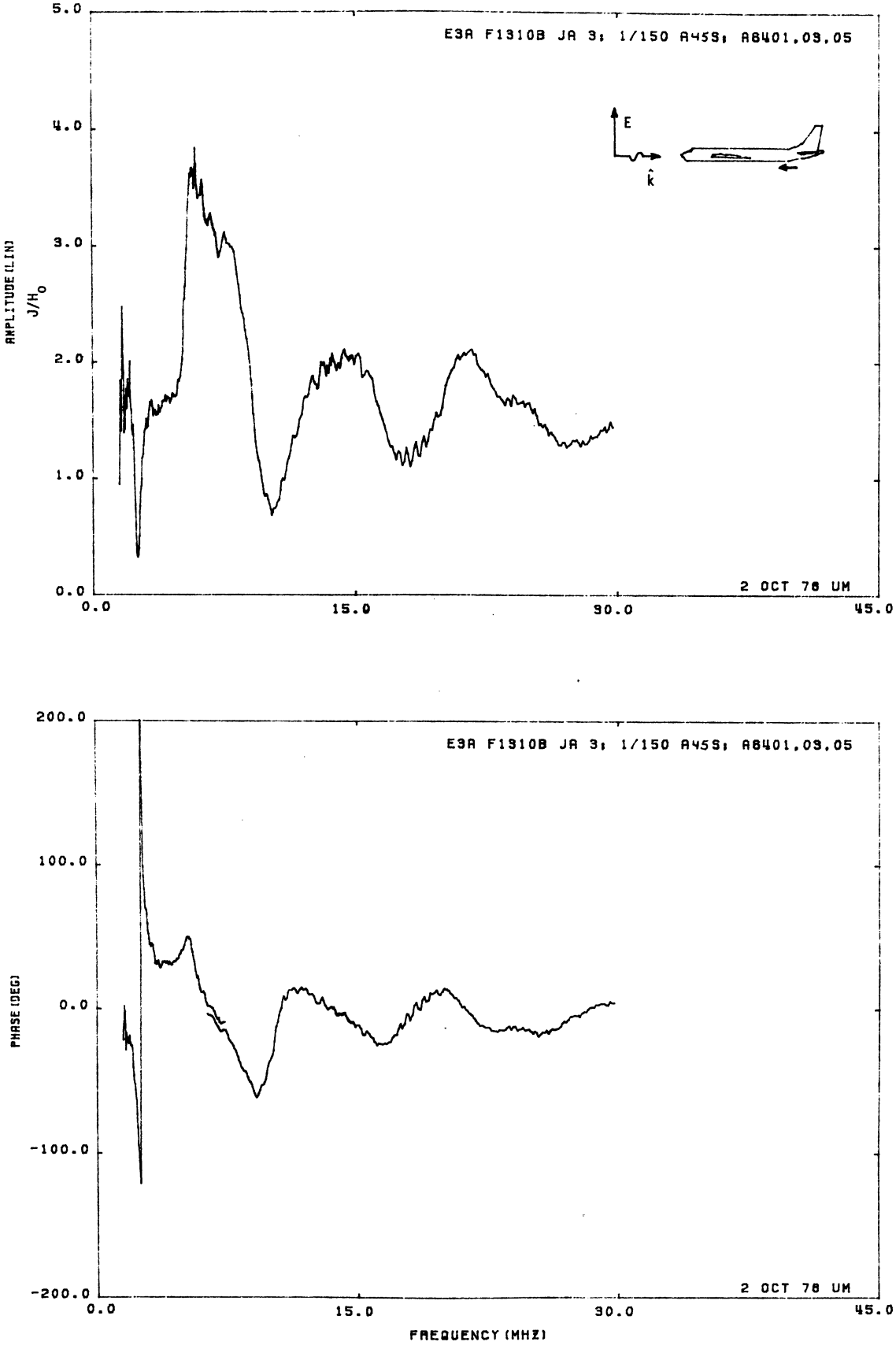

Figure 45S. Axial Current at STA:F1310B, Excitation 3, 1/150 Model.

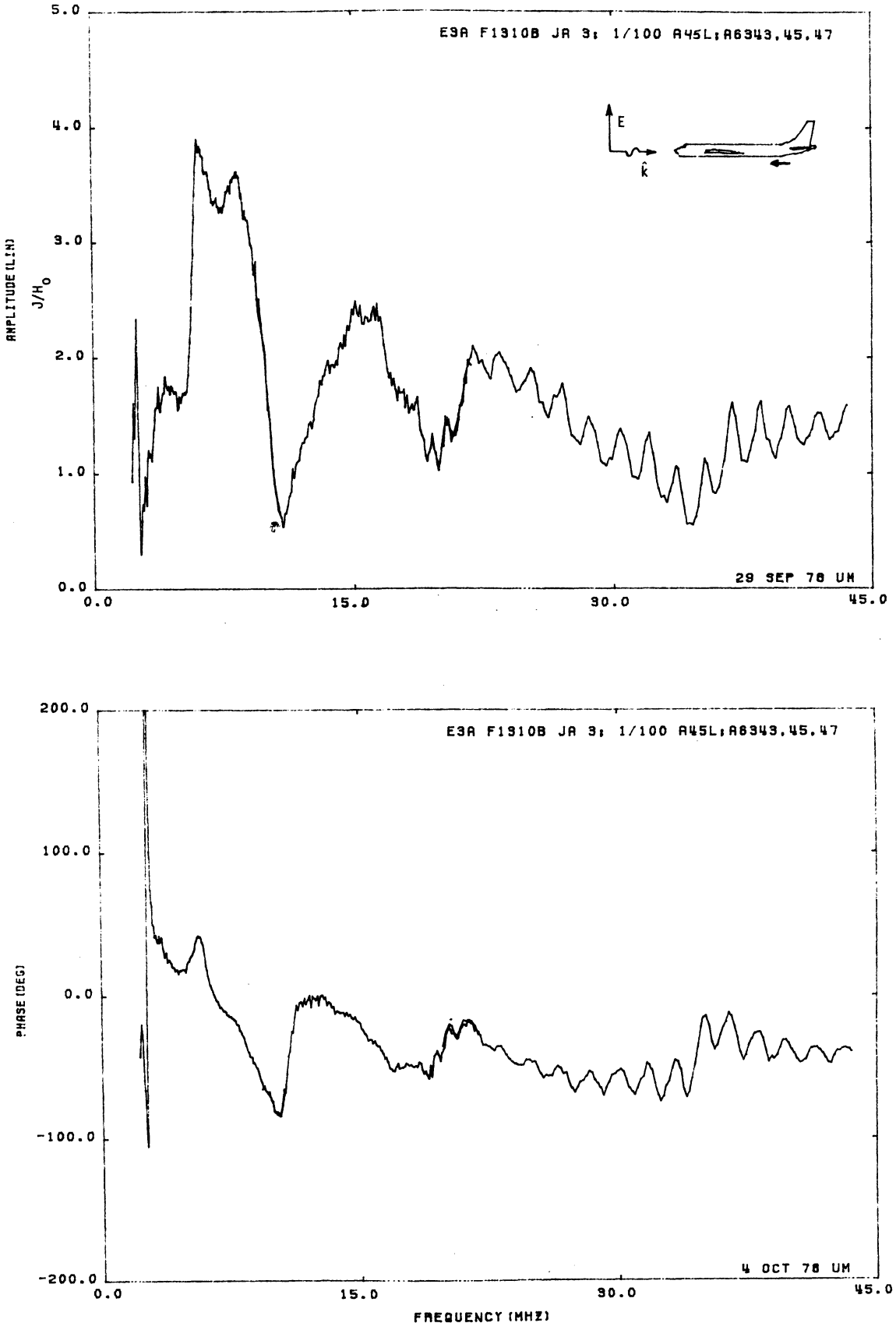

Figure 45L. Axial Current at STA:F1310B, Excitation 3, 1/100 Model.

UNIVERSITY OF MICHIGAN
3 9015 03483 1597